

FORAMINIFERAL INDICATORS OF PALEOCEANOGRAPHIC AND SEA-ICE
CONDITIONS IN THE AMUNDSEN GULF AND VISCOUNT MELVILLE SOUND,
CANADIAN ARCTIC

by

Olivia T. Gibb

Submitted in partial fulfillment of the requirements
for the degree of Master of Science

at

Dalhousie University
Halifax, Nova Scotia
September 2009

© Copyright by Olivia T. Gibb, 2009

DALHOUSIE UNIVERSITY

Department of Earth Sciences

The undersigned hereby certify that they have read and recommend to the Faculty of Graduate Studies for acceptance a thesis entitled "Foraminiferal indicators of paleoceanographic and sea-ice conditions in the Amundsen Gulf and Viscount Melville Sound, Canadian Arctic." by Olivia T. Gibb in partial fulfillment of the requirements for the degree of Master of Science.

Dated:

12/04/09

Supervisor:

Readers:

DALHOUSIE UNIVERSITY

DATE: September 14th, 2009

AUTHOR: Olivia T. Gibb

TITLE: FORAMINIFERAL INDICATORS OF PALEOCEANOGRAPHIC AND
SEA-ICE CONDITIONS IN THE AMUNDSEN GULF AND VISCOUNT
MELVILLE SOUND, CANADIAN ARCTIC

DEPARTMENT OR SCHOOL: Department of Earth Sciences

DEGREE: MSc CONVOCATION: May YEAR: 2010

Permission is herewith granted to Dalhousie University to circulate and to have copied for non-commercial purposes, at its discretion, the above title upon the request of individuals or institutions.

Signature of Author

The author reserves other publication rights, and neither the thesis nor extensive extracts from it may be printed or otherwise reproduced without the author's written permission.

The author attests that permission has been obtained for the use of any copyrighted material appearing in the thesis (other than the brief excerpts requiring only proper acknowledgement in scholarly writing), and that all such use is clearly acknowledged.

Table of Contents	Page
List of Tables.....	vii
List of Figures.....	viii
Abstract.....	x
List of Abbreviations Used.....	xi
Acknowledgements.....	xii
Chapter 1 Introduction.....	1
1.1 General Introduction.....	1
1.2 Amundsen Gulf.....	3
1.3 Viscount Melville Sound.....	5
Chapter 2 Background.....	9
2.1 Arctic Oceanography	9
2.2 Environmental Setting.....	10
2.2.1 Amundsen Gulf.....	10
2.2.2 Viscount Melville Sound.....	14
2.3 Paleoceanographic Proxies.....	16
2.4 Foraminifera in the Canadian Arctic.....	19
2.5 Paleoceanography and Paleoclimate in the Canadian Arctic.....	21
Chapter 3 Materials and Methods.....	27
3.1 Field Sampling.....	27
3.1.1 Amundsen Gulf.....	27
3.1.2 Viscount Melville Sound.....	28
3.2 Chronology.....	29

3.3 Foraminiferal Sampling and Processing.....	31
3.4 Foraminiferal Numerical Analyses.....	32
3.5 $\delta^{18}\text{O}$ and $\delta^{13}\text{C}$ of Foraminifera.....	32
Chapter 4 Results.....	34
4.1 Core Description.....	34
4.1.1 Amundsen Gulf.....	34
4.1.2 Viscount Melville Sound.....	34
4.2 Chronology – Amundsen Gulf.....	35
4.3 Foraminiferal assemblages.....	38
4.3.1 Amundsen Gulf.....	38
4.3.2 Viscount Melville Sound.....	44
4.4 Foraminiferal Assemblage Numerical Analyses – Amundsen Gulf.....	46
4.5 $\delta^{18}\text{O}$ and $\delta^{13}\text{C}$ of Foraminifera – Amundsen Gulf.....	50
Chapter 5 Discussion.....	52
5.1 Amundsen Gulf.....	52
5.1.1 Objective 1: Foraminiferal Species Assemblages Associated with Sea Ice Cover.....	52
5.1.2 Objective 2: Foraminiferal Assemblages Associated with Core Location...55	55
5.1.3 Objective 3: Chronology and Correlation among Cores.....	57
5.1.4 Objective 4: Correlation of Foraminiferal and Isotopic Events with External Factors.....	58
5.2 Viscount Melville Sound.....	64
Chapter 6 – Conclusion.....	72
References.....	75

Appendices.....	90
Appendix A - Boxcore and Sub-bottom Imaging.....	90
Appendix B - Abundance Data – Amundsen Gulf.....	97
Appendix C - Abundance Data – Viscount Melville Sound.....	123
Appendix D - Taxonomy.....	127

List of Tables

Page

Table 3.1 Physical properties recorded during the collection of cores 106, 109, 112, 118, and 124 of leg 8 of the CASES cruise 2004-804.....	27
Table 4.1 Radiocarbon ages for cores 109 and 124 in calibrated years BP (before present) and AD (Anno Domini).....	35
Table 4.2 ^{210}Pb and ^{226}Rn activities with 2σ error in boxcore 109.....	36
Table 4.3 Results of the SIMPER analysis listing the similarity within groups created by the Q-mode analysis. Dissimilarity is also shown between the (a) upper and lower sections, and (b) inner and outer Amundsen Gulf.....	49
Table 4.4 Stable oxygen and carbon isotope values in cores 106, 109, 112, 118, 124 for (a) <i>Neogloboquadrina pachyderma</i> (b) <i>Islandiella teretis</i>	51

List of Figures	Page
Figure 1.1 Map of the Arctic Ocean, with the Amundsen Gulf study area outlined in box (Fig 2.2).....	4
Figure 1.2 Map of the Canadian Arctic Archipelago, indicating the core location (*) within the Viscount Melville Sound.....	6
Figure 1.3 Map of the Amundsen Gulf region indicating the locations of five boxcore samples.....	7
Figure 2.1 Bathymetry of the Amundsen Gulf extending from approximately core 118 to core 106, was produced by Jason Bartlett at the University of New Brunswick Ocean Mapping Group.....	11
Figure 2.2 A conductivity-temperature-depth (CTD) device recorded the temperature and salinity during prior to sediment sampling from each of the five locations in the Amundsen Gulf in July-August (CASES2004, Leg 8 (0305) CCGS Amundsen Cruise & Preliminary Data Report).....	13
Figure 2.3 Yearly average summer sea ice concentration of the Amundsen Gulf from 1980 to 2004, is the sum of old, first-year, young and new sea ice concentrations (Galley et al., 2008).....	14
Figure 4.1 ²¹⁰ Pb activities plotted against depth of core 109. Analyses performed at GEOTOP (Université du Québec à Montréal).....	37
Figure 4.2 The total number of species, specimens and tintinnids per 10 cm ² , relative fractional abundances (% of the total) for abundant or indicator species and total calcareous species, and values for δ ¹³ C and δ ¹⁸ O for planktic <i>Neogloboquadrina pachyderma</i> (Npl) as functions of depth from boxcore 106.....	39
Figure 4.3 The total number of species, specimens and tintinnids per 10 cm ² , relative fractional abundances (% of the total) for abundant or indicator species and total calcareous species, and values for δ ¹³ C and δ ¹⁸ O for planktic <i>Neogloboquadrina pachyderma</i> (Npl) as functions of depth from boxcore 109.....	40
Figure 4.4 The total number of species, specimens and tintinnids per 10 cm ² , relative fractional abundances (% of the total) for abundant or indicator species and total calcareous species, and values for δ ¹³ C and δ ¹⁸ O for planktic <i>Neogloboquadrina pachyderma</i> (Npl) and benthic <i>Islandiella teretis</i> as functions of depth from boxcore 112.....	41

Figure 4.5 The total number of species, specimens and tintinnids per 10 cm², relative fractional abundances (% of the total) for abundant or indicator species and total calcareous species, and values for δ¹³C and δ¹⁸O for planktic *Neogloboquadrina pachyderma* (Npl) and benthic *Islandiella teretis* as functions of depth from boxcore 118.....42

Figure 4.6 The total number of species, specimens and tintinnids per 10 cm², relative fractional abundances (% of the total) for abundant or indicator species and total calcareous species, and values for δ¹³C and δ¹⁸O for planktic *Neogloboquadrina pachyderma* (Npl) and benthic *Islandiella teretis* as functions of depth from boxcore 124.....43

Figure 4.7 The total number of species, specimens and tintinnids per 10 cm³, and relative fractional abundances (% of the total) for abundant or indicator species and total calcareous species as a function of depth for boxcore 012.....45

Figure 4.8 Dendrogram produced by the Q-mode cluster analysis based on 60 species and 85 specimens. Four distinct clusters are identified as upper and lower sections of each core, and inner and outer Amundsen Gulf within the ice cover clusters.....47

Figure 5.1 The foraminiferal and isotopic profiles for all five cores as displayed in Figs. 3.2-3.6, with a visual representation of the two groups (upper and lower sections of each core) produced by the hierarchical clustering. Also plotted are the dates produced by the radiometric analyses in cores 109 and 124.....53

Abstract

Sediment cores were collected from the Canadian Arctic Archipelago to reconstruct the region's oceanographic and sea ice history via foraminiferal proxies. Foraminiferal species assemblages reflect changes in sea ice cover due to the dissolution of calcareous foraminifera during increased productivity in ice-free waters. The upper five cm of sediment of the core located in the Amundsen Gulf is characterized by a predominantly agglutinated foraminiferal assemblage that spanned the last century, indicative of a seasonally ice-free Amundsen Gulf. In contrast to the recent assemblage, a predominantly calcareous assemblage indicated carbonate preservation within the Amundsen Gulf during a period of perennial ice extending back to the 9th century AD. During the Medieval Warm Period and the Anthropocene, two recent periods of warmer climate, foraminiferal proxies indicated different sea ice regimes. These results suggest that the factors forcing sea ice extent have changed in recent decades.

List of Abbreviations Used

AG	Amundsen Gulf
AO	Arctic Oscillation
BG	Beaufort Gyre
CAA	Canadian Arctic Archipelago
CASES	Canadian Arctic Shelf Exchange Study
DIC	dissolved organic carbon
LIA	Little Ice Age
MWP	Medieval Warm Period
MYI	Multi-year ice
NAO	North Atlantic Oscillation
NWP	Northwest Passage
TPD	Transpolar drift
VMS	Viscount Melville Sound

Acknowledgements

I would like to express my gratitude towards those who have helped fund this project. Thanks especially to the Cushman Foundation for Foraminiferal Research for providing me with a 2008 Joseph A Cushman Student Research Award. That award funded my stable isotope analyses. Various stages of this project were presented at the 2008 Geological Society of America Annual Meeting and the 2009 American Geophysical Union Joint Assembly, and I would like to thank both the GSA and the AGU for contributing toward my travel expenses. I would also like to thank the Dalhousie Association of Graduate Students and the Department of Graduate Studies for covering some of my conference traveling expenses. Finally, I would like to thank NSERC for providing student support through their contributions to the International Polar Year program.

For outstanding guidance and support, and for his enthusiasm for Arctic research involving foraminifera, I thank my supervisor Dave Scott. Also within the Dalhousie community, I would also like to thank my supervisory committee members, Martin Gibling and Markus Kienast for offering their time and valuable comments as my research progressed. I express my gratitude to Chloe Younger (Dalhousie Centre for Marine Geology) and Kate Jarrett (Geological Survey of Canada – Atlantic) for their instruction and help with core and sample processing. I would also like to thank all my peers in the Department of Earth Sciences, including Julie Griffiths, Pete van Hengstum, and Gwen Williams for their comments and willingness to share ideas. Thanks also to

Franco Medioli for external examination of my thesis. André Rochon, a co-author on the forthcoming draft manuscript based on Chapter 2, also provided his valuable comments.

My thesis is, in part, a contribution to the Canadian Arctic Shelf Exchange Study (CASES) and Network of Centres of Excellence ArcticNet, and I wish to thank the Canadian Coast Guard officers and crew of the CCGS Amundsen and all those who carefully collected the cores.

Last but certainly not least, I thank my husband Jon, for his continuous love, support, and patience.

Chapter 1 - Introduction

1.1 General Introduction

Arctic paleoceanographic records assist in quantifying long-term variability in atmospheric and oceanographic Arctic regimes and place current climate conditions into a long-term context. Satellite records and ocean moorings have produced the highest resolution records of Arctic sea ice and water mass variability over the last 30 years (Serreze et al., 2003; Swift et al., 2005; Dickson et al., 2007; Comiso et al., 2008; Stroeve et al., 2008). The recent decline in Arctic sea ice extent is related to Arctic warming within recent decades, resulting in increased thermodynamic and sea ice-albedo feedback melting (Lindsay and Zhang, 2005). However, without paleoceanographic records, scientists would be unable to determine changes in Arctic sea ice extent and oceanographic circulation on time scales longer than decades. Therefore, the recent decline has not only increased the amount of research performed at high latitudes, but has also allowed research to be conducted in areas previously inaccessible for the collection of marine sediment samples. Proxies found within sediment cores, including foraminifera, are used as paleoceanographic indicators on longer time scales and are useful for relating Holocene oceanographic changes to changes within recent decades. These marine records can also be compared to terrestrial paleoclimate records across the northern hemisphere (e.g., Jones et al., 2001). Detailed histories of paleoceanographic research performed in these regions are presented in the background chapter (Chapter 2). Also within that chapter, I describe the mechanisms by which foraminiferal species assemblages change and are useful as paleoceanographic proxies. Because their tests are

preserved in marine sediments, foraminifera are used globally as environmental indicators, and as proxies for demonstrating long-term changes in their habitats. In my thesis, foraminifera are used as paleo-sea ice indicators in Arctic environments. Other indicators of past sea ice conditions, which are also discussed in the background and discussion chapters, include bowhead whale bones, diatom biomarkers, and even the extent and limits of historical Arctic voyages. Dinoflagellate cyst assemblages also provide proxies for sea surface temperature and salinity. However, benthic foraminifera are a reliable proxy for bottom water conditions because they live at the water-sediment interface. Stable isotope values from calcareous foraminifera are also used globally for reconstructions of temperature, salinity, sea ice and water mass provenance. Unlike larger shells (e.g., molluscs, ostracods), large numbers of foraminiferal characteristics (individuals, species, relative abundances) can be analysed at relatively high resolution from small sediment samples collected from cores in order to obtain paleo-environmental chronosequences.

The Canadian Arctic Shelf Exchange Study (CASES, 2002-2004) and the Network of Centres of Excellence, ArcticNet (2005-2009) have been studying the Canadian Arctic with expeditions via the icebreaker *CCGS Amundsen*. These research programs have mainly focused on recent changes in sea ice type, extent, and thickness, benthic and pelagic biological activity, and nutrients (Fortier et al., 2008). There are, however, few studies investigating the long term variability of these physical and biological features using established proxies such as foraminifera, dinoflagellate cysts, and biomarkers. In the context of these successful Arctic research programs, my

examinations of foraminifera as paleo-sea ice proxies provide analyses of long term changes in marine environments.

1.2 Amundsen Gulf

The Amundsen Gulf and Beaufort Sea (Figs. 1.1-1.3) were extensively investigated during the 2003-2004 CASES sampling campaign. The focus area of a large portion of the CASES and ArcticNet research is the western Canadian Arctic Cape Bathurst Polynya and flaw lead extending along the Beaufort Shelf, into the Amundsen Gulf, and along the western coast of Banks Island (Fig. 1.3). Since polynyas are areas of open water and thin ice that can occur at any time during the year due to their wind-generated nature, they are of great interest to researchers who study benthic and planktic communities, as well as local water circulation and chemistry. Satellites have revealed the spatial and temporal variability of the Cape Bathurst Polynya, but those data span only the last 30 years. Determining the long term variability of the polynya and its contribution to the ecology and oceanography of the Amundsen Gulf requires using proxies derived from sediment cores sampled below the polynya. Dinoflagellate cyst and foraminiferal species assemblages are now being implemented as proxies for past conditions within the Amundsen Gulf and Beaufort Sea regions due to the collection of cores by the CASES program (Scott et al., 2009; Fortier et al., 2008; Richerol et al., 2008; Schell et al., 2008). The original proposal for my thesis research was written prior to radiometric dating of the core samples, and the assumption was initially made that the cores extended back to the deglaciation of the Amundsen Gulf (i.e. >1000 years). My original hypothesis stated that a transect of cores would resolve the timing of the retreat

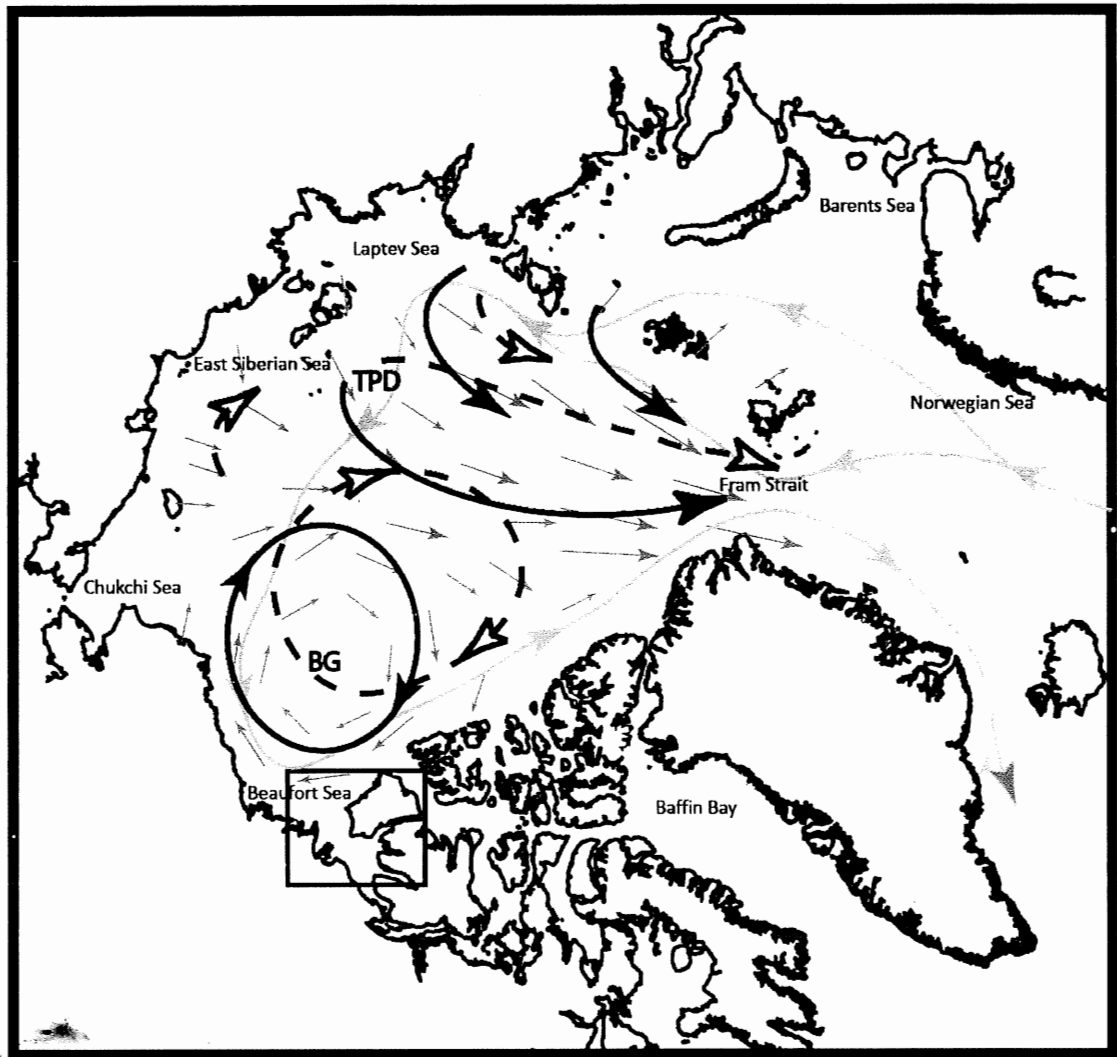


Fig. 1.1. Map of the Arctic Ocean, with the Amundsen Gulf study area outlined in box (Fig 2.2). North Atlantic water circulation within the Arctic Ocean is indicated using large grey arrows (c.f. Jones, 2001). General sea ice movement is directed by the Beaufort Gyre (BG) and the Transpolar Drift (TPD) and shown with small grey arrows. The large black arrows indicate shifts in the BG and TPD during strong shifts in the Arctic atmospheric regime. During years of persistently positive Arctic Oscillations (+AO), sea ice and surface waters follow the solid line, and follow the dashed line during negative Arctic Oscillations (-AO) (Rigor et al., 2002).

of the Laurentide Ice Sheet. However, since radiometric dating revealed that the records are only 1000 years old, instead my focus has shifted towards recreating the recent oceanographic and sea-ice history of the Amundsen Gulf.

In this thesis, I interpret the sea-ice and oceanographic history of the Amundsen Gulf spanning the last millennium, using data derived from a series of boxcores collected during CASES. My objectives are to: (1) determine the foraminiferal species assemblages associated with seasonal and perennial ice cover within this area of the Arctic; (2) associate differences among foraminiferal assemblages with their collection locations in the Amundsen Gulf; (3) align cores temporally based on similarities in foraminiferal species assemblages and determine core chronology based on radiocarbon and ^{210}Pb dating, and; (4) interpret the local variability in foraminiferal assemblages and their stable isotopes in the context of known regional oceanographic changes and climate oscillations.

1.3 Viscount Melville Sound

Within the Canadian Arctic Archipelago (CAA), the Northwest Passage (NWP) is a network of waterways connecting the North Atlantic and North Pacific Oceans and was the focus of explorations during the 19th century (Pharand, 1984). The CAA (Fig. 1.2) has a relatively limited recorded history of sea ice extent, mainly produced by European explorers starting in the 18th century. However, observations of ice free conditions in both Lancaster Sound and Jones Sound were documented by William Baffin from within Baffin Bay in 1616 (Serreze and Barry, 2005). There are several possible passages through the CAA that have been described as the Northwest Passage. The most common

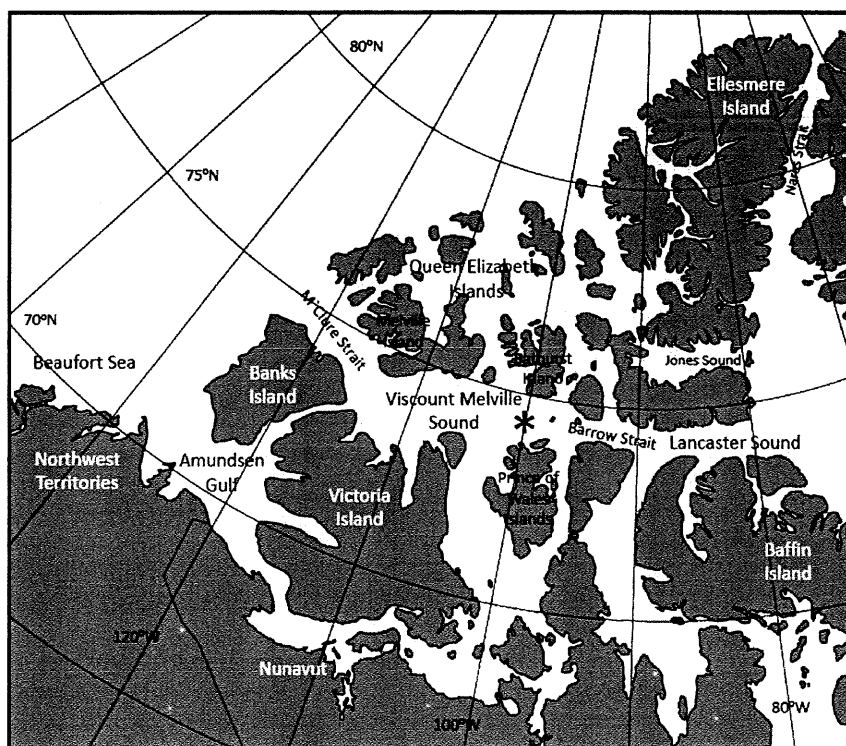


Fig. 1.2. Map of the Canadian Arctic Archipelago, indicating the core location (*) within the Viscount Melville Sound.

recently used passage begins in Lancaster Sound in the east, travels west through Barrow Strait and Viscount Melville Sound until M'Clintock Channel, heads south around the east coast of Victoria Island through Victoria Strait, Queen Maud Gulf, Coronation Gulf, Dolphin and Union Strait, then out into the Beaufort Sea through the Amundsen Gulf (Fig. 1.2). The ideal Northwest Passage would be a route bearing west directly from Lancaster Sound, through Barrow Strait and Viscount Melville Sound, and finally to the Arctic Ocean and Beaufort Sea through M'Clure Strait (Fig. 1.2). This second route had been impassable without an icebreaker until M'Clure Strait and the northern coast of Banks Island became ice free during the summer of 2007, and will be the route described in this thesis as NWP.

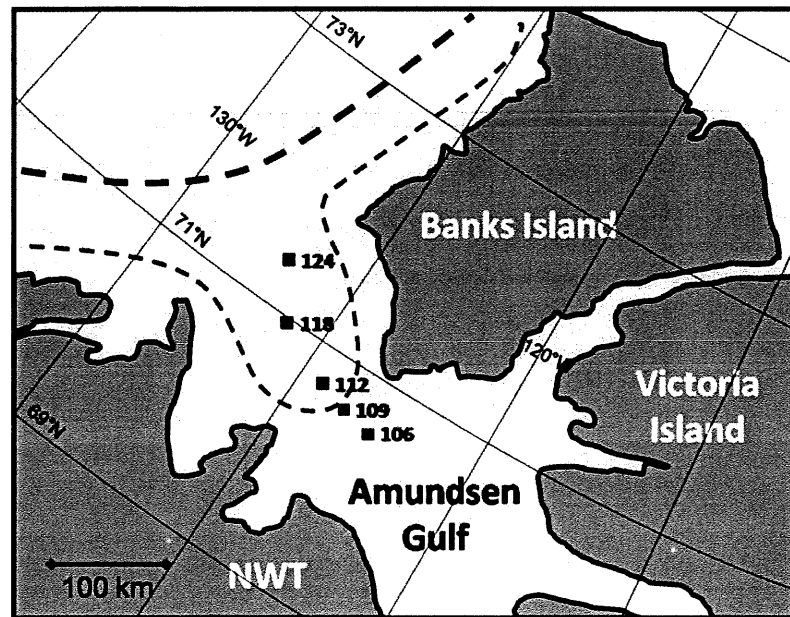


Fig. 1.3. Map of the Amundsen Gulf region indicating the locations of five boxcore samples. The thick dashed line represents the approximate extent of the polar pack ice, and the thin dashed line represents the approximate extent of the Cape Bathurst Polynya (Barber and Hanesiak, 2002).

Since the passage has been increasingly navigable during ice free or first year ice summers over the past 40 years, issues of sovereignty, climate change and environmental change have created a renewed focus on NWP research, particularly on seasonal sea-ice coverage. For example, as mentioned above, for the first time in recent history, during the summer of 2007 the NWP was ice free from Lancaster Sound through M'Clure Strait to the Arctic Ocean (National Snow and Ice Data Centre, [www://nsidc.org](http://www.nsidc.org)). Such an ice-free NWP also potentially provides a much deeper route for commercial shipping. Additionally, due to increased open water access, M'Clure Strait and the Viscount Melville Sound are now accessible for scientific study, to explore their oceanographic and sea-ice history and variability.

ArcticNet has sampled areas within the NWP during these recent, ice-free summers and the Viscount Melville Sound site 307 is the farthest west that they sampled (Fig. 1.2). Using a sediment core collected from site 307, the main objective of my analyses of these Viscount Melville Sound data is to use foraminiferal assemblages and abundances to document the recent oceanographic and sea-ice history of the Viscount Melville Sound. These records will also be compared to a few other paleoceanographic records within the CAA to establish similarities and differences among locations. Unfortunately, the Viscount Melville Sound (VMS) core could not be radiocarbon dated due to insufficient amounts of carbonate within the sampled increments. This renders the task of interpreting foraminiferal species assemblages quite difficult due to the lack of a defined chronological control. In the discussion chapter (Chapter 5), I therefore suggest a few scenarios for the recent sea ice history of the VMS, based on oceanographic records derived from foraminifera and other proxies sampled within the CAA.

Chapter 2 – Background

2.1 Arctic Oceanography

The stratigraphic profile of the Arctic Ocean has been well described by Serreze and Barry (2005). They characterized a profile that consists of three layers as follows. The surface layer (few 10s of metres) consists of cold fresh water, produced by the influx of Pacific water, riverine water, and the formation and melting of sea ice. These surface freshwaters exit the Arctic through Fram Strait and the Canadian Arctic Archipelago, assisting in Atlantic deep-water formation. Waters below the surface waters down to 200-300 m consist of a layer of increasing temperature and salinity. This halocline is a product of cooler less saline Pacific-derived water through Bering Strait, and warmer more saline Atlantic-derived waters through Fram Strait and the Barents Sea.

The Arctic Ocean is covered with a layer of sea ice, whose thickness and extent are variable. Due to wind stress on the top surface and ocean currents on the bottom surface, sea ice is always in motion, where divergent ice motion causes flaw leads (areas of open water) and convergent ice motion causes rafting (Serreze and Barry, 2005). The movement of the polar pack ice covering the central Arctic is coupled to atmospheric circulation (Serreze and Barry, 2005). The Beaufort Gyre (BG) (Fig. 1.1) drives the sea ice and surface waters from the land-fast ice in a dominantly clockwise (anticyclonic) direction during winter, which slows dramatically or can reverse during summers (Carmack and Macdonald, 2002; Lukovich and Barber, 2006). Sea ice can circulate within the BG or be exported from the Arctic into the North Atlantic through Fram Strait by the Transpolar Drift (TPD) (Fig. 1.1). The TPD can alter its path: coupled with a

strong BG to direct flow from the Eastern Arctic to Fram Strait creating a clockwise (anticyclonic) motion, or it can diverge toward the Beaufort Sea converging with a weakened BG to produce anticlockwise (cyclonic) flow of sea ice (Rigor et al., 2002). These sea ice and water mass circulation regimes can vary spatially and temporally, and have been correlated with the atmospheric circulation regimes of the Arctic Oscillation (AO) and North Atlantic Oscillation (NAO) on multiyear to multi-decadal time scales (Mysak, 2001; Protushinsky et al., 2002; Rigor et al., 2002; Lukovich and Barber, 2006). Persistently positive AO/NAO produce counterclockwise (cyclonic), divergent sea ice and surface water motion in the Eurasian Basin. They also produce a weakened BG and divergent TPD, which increases the flux of freshwater and sea ice out of the Arctic and flux of Atlantic water into the Arctic (Mysak, 2001). On a longer time scale, the different modes of the AO and NAO have shown long-term persistence during the last millennium, where positive anomalies dominated during the Anthropocene and the Medieval Warm Period (MWP), and negative anomalies persisted through the Little Ice Age (LIA) (Trouet et al., 2009).

2.2 Environmental Setting

2.2.1 Amundsen Gulf

The Amundsen Gulf is a 100 km wide and 400 km long inlet that lies within the southwestern region of the Canadian Arctic Archipelago, north of the mainland Northwest Territories (Fig. 1.1-1.3). In the centre of the Gulf the water reaches 600 m in depth, to an ocean bottom that was scoured by the Laurentide Ice Sheet (Fig. 2.1). The water column stratifies into three layers as shown in temperature and salinity profiles

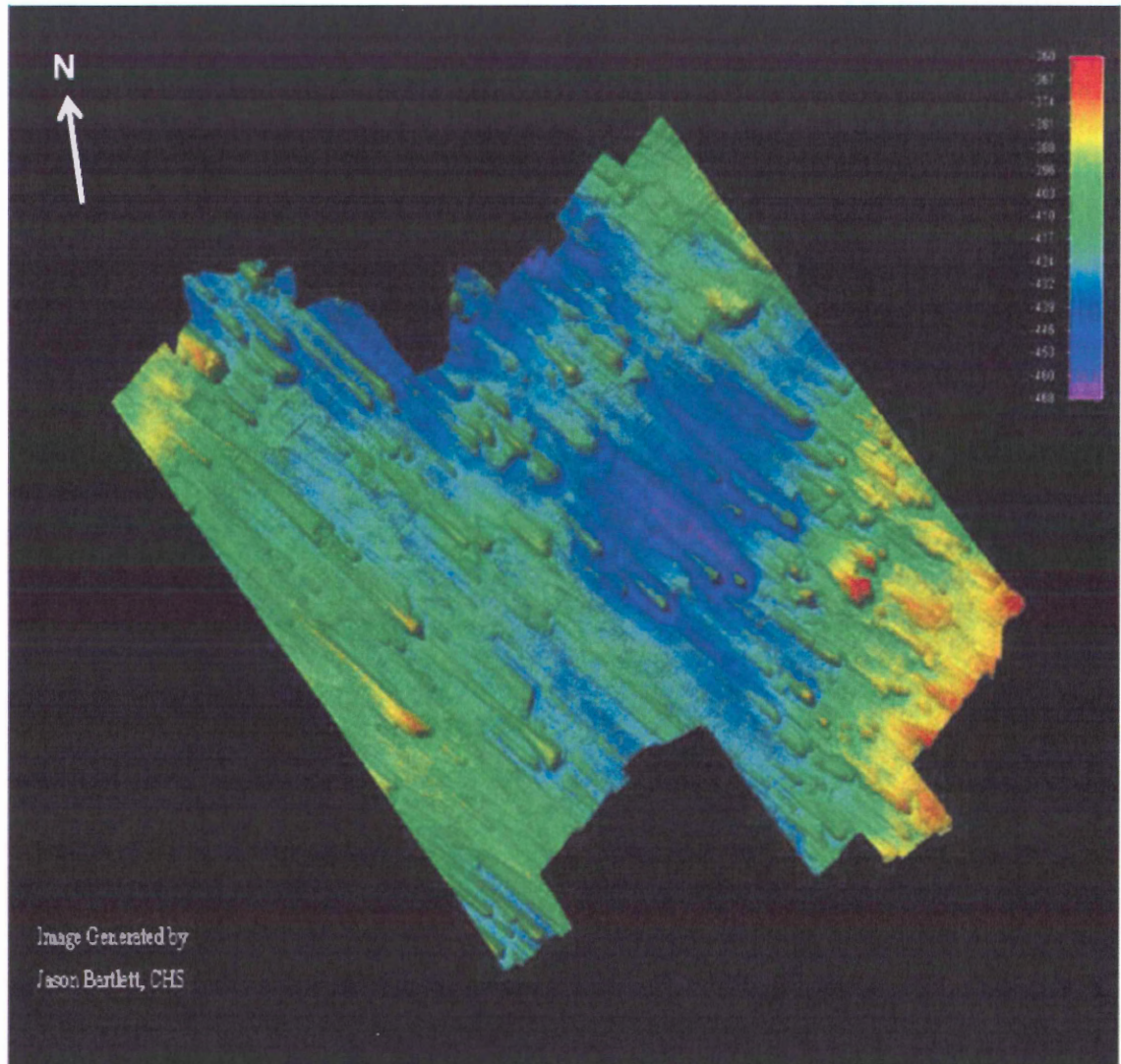


Fig. 2.1. Bathymetry of the Amundsen Gulf extending from approximately core 118 to core 106, was produced by Jason Bartlett at the University of New Brunswick Ocean Mapping Group. Glacial features produced by the Laurentide Ice Sheet toward the NW, observed at ~ 400 km depth that can measure up to 300 m wide, 4 km long, and 40 m high (<http://www.arcticnet.ulaval.ca/pdf/ASMTalks/Bennet.pdf>).

collected during the CASES sampling expedition (Fig. 2.2). The surface waters (< 20 m) are a seasonal mixed layer, that is cold and saline in winter due to the formation of sea-ice and decreased freshwater influx, and becomes warmer and fresher during the summer months due to sea ice melt and input of freshwater from land (Vilks, 1989). The layer between the surface waters and 200 m consists of cold, low salinity nutrient-rich Pacific water. The waters below 200 m are modified Atlantic waters entering through Fram Strait, that are warmer and more saline than the layers above, creating a halocline and reversed thermocline (Macdonald et al., 1989; Steele et al., 2004; Ingram et al., 2005). The deeper Pacific and Atlantic waters are brought into the Amundsen Gulf along the Beaufort Shelf by the counterclockwise (cyclonic) movement of the Beaufort undercurrent (Carmack and Macdonald, 2002).

Since the beginning of satellite observations in 1979, the Amundsen Gulf has been completely ice covered from mid-January to mid-April, and ice free from mid-July to mid-October, with some variation in extent (Fig. 2.3) (Galley et al., 2008; Ingram et al., 2008). The Cape Bathurst flaw lead system extends along the coast of the Yukon and Northwest Territories, across the opening to the Amundsen Gulf, and along Banks Island's west coast (Fig. 1.3). The Cape Bathurst Polynya is the section of the flaw lead where an area of open water forms when high easterly winds push the annual and multiyear ice away from the landfast ice (Carmack and Macdonald, 2002). Vertical mixing and upwelling can occur within the polynya via sustained winds and by sinking brines during sea-ice formation (Carmack and Macdonald, 2002; Williams and Carmack, 2008). Arrigo and van Dijken (2004) documented plankton blooms within the Amundsen Gulf using satellite images from 1998-2002. Two plankton blooms occur every summer:

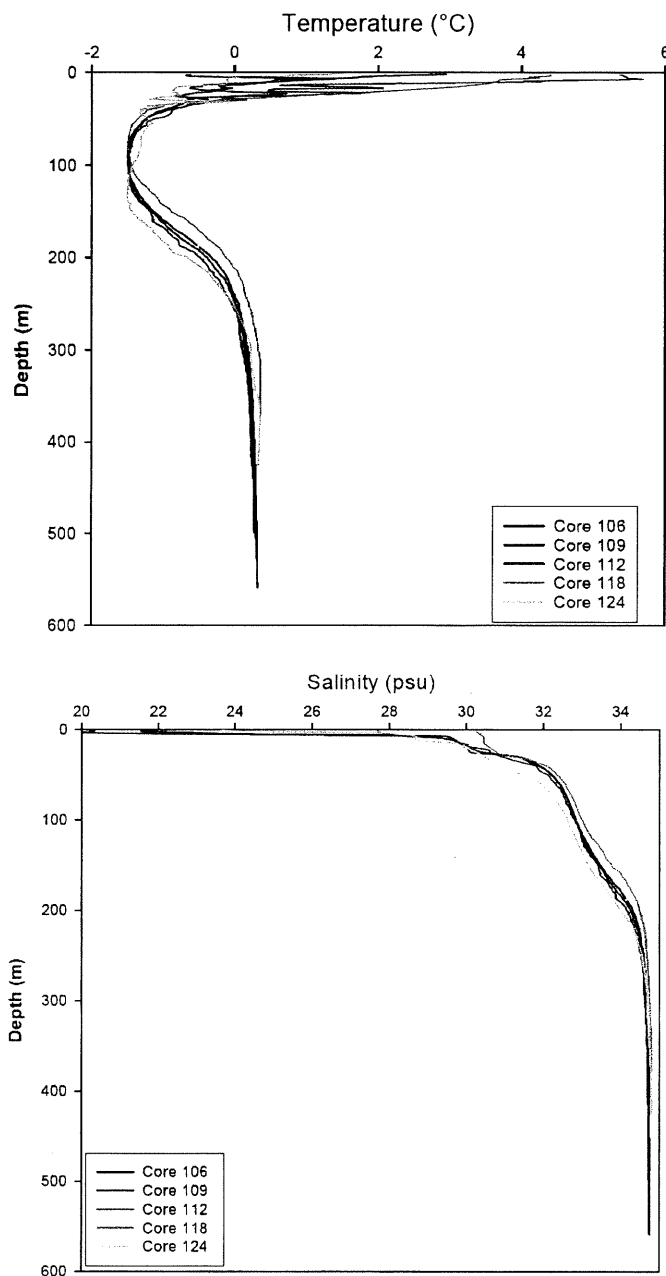


Fig. 2.2. A conductivity-temperature-depth (CTD) device recorded the temperature and salinity during prior to sediment sampling from each of the five locations in the Amundsen Gulf in July-August (CASES2004, Leg 8 (0305) CCGS Amundsen Cruise & Preliminary Data Report). Three distinctive layers are visible: the warm, fresh seasonal surface layer, the cold, saline Pacific layer, and the warmer, more saline Atlantic layer.

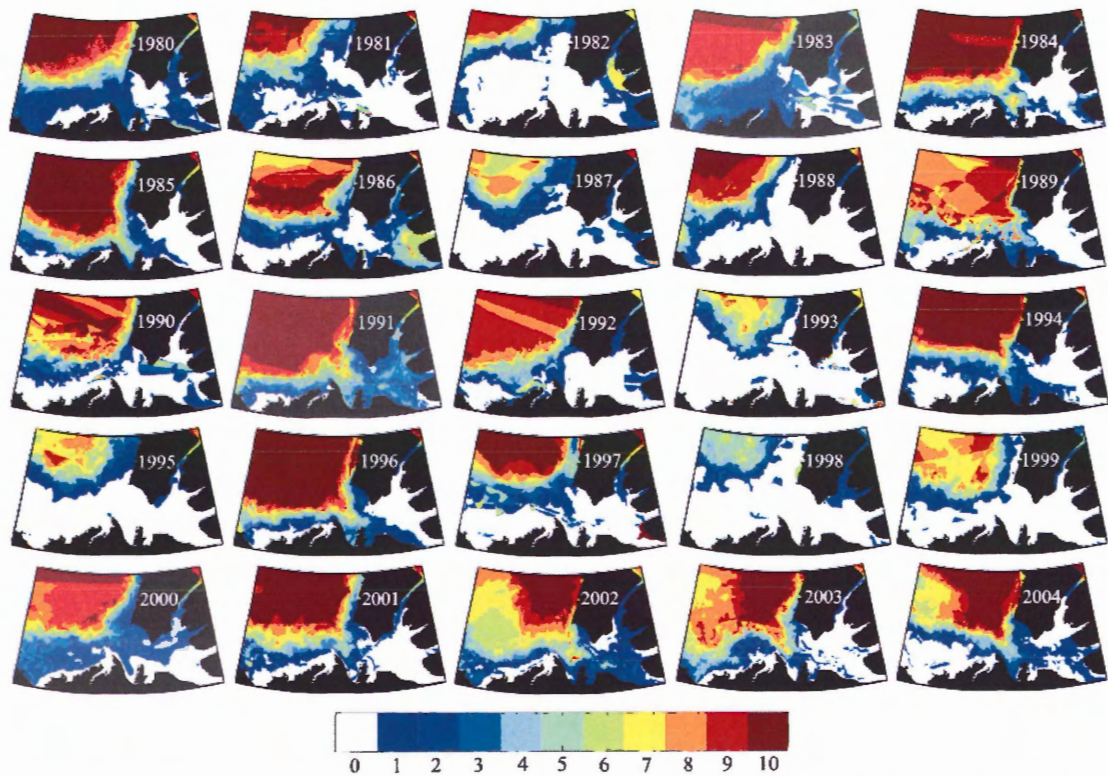


Fig. 2.3. Yearly average summer sea ice concentration of the Amundsen Gulf from 1980 to 2004, is the sum of old, first-year, young and new sea ice concentrations (Galley et al., 2008).

the first during initial melting of sea ice within the polynya, the second much larger bloom occurs once the waters have stratified due to sustained open waters (Arrigo and van Dijken, 2004). These plankton blooms vary in strength and timing since they are dependent on sea ice cover.

2.2.2 *Viscount Melville Sound*

Viscount Melville Sound (VMS) lies within the southwestern region of the CAA, north of Victoria and Prince of Wales Islands and south of Melville and Bathurst Islands (Fig. 1.2). The VMS waterway is 400 km long and 100 km wide, connecting Barrow Strait and Lancaster Sound to the east, with M'Clure Strait to the west. VMS is stratified

vertically into three layers: cold, dilute Arctic surface water within approximately the upper 20 m; cold, saline Pacific waters from 20 to 200 m; and warm, saline Atlantic waters below 200 m (Vilks, 1989; Jones et al., 2003). The deeper Pacific and Atlantic waters are brought into the CAA by the counterclockwise (cyclonic) movement of the Beaufort undercurrent (Carmack and Macdonald, 2002). Sills within the CAA, specifically those across Barrow Strait, control the displacement of those deeper waters (Prinsenbergh and Bennett, 1987; Vilks, 1989).

Historically, during the winter season (November to May) VMS waters are covered with multi-year and young sea ice (Howell et al., 2008). A large portion of the multiyear sea ice is formed in situ as land-fast ice and the rest enters through M'Clure Strait from cyclonic movement of the Beaufort Gyre, or from the Queen Elizabeth Islands in the North (Howell et al., 2008). The multi-year sea ice breaks up in the summer from east to west, leading to a September minimum coverage (Vilks, 1989), which then gets in-filled with first year ice in the fall. Barber and Massom (2007) documented polynyas within the CAA that can occur any time of year, mainly caused by tidal enhanced vertical mixing, or restrictions creating a plug of sea ice that allows winds to push other sea ice away from the plug. Vilks (1989) also described open water along the north shore of the VMS with mobile fractured ice within the Sound in July. In 2007, the VMS was ice free for the first time since continuous satellite observation began approximately 40 years ago (National Snow and Ice Data Centre, [www://nsidc.org](http://www.nsidc.org)), and multi-year ice ceased its movement into M'Clure Strait due to the northward movement of the polar pack ice (Howell et al., 2008). With a very long melting season coupled with less multi-year ice,

the 2008 summer season produced continued decreases in sea ice extent (Howell et al., 2008).

2.3 Paleooceanographic Proxies

Foraminifera are single-celled organisms that live in the water column or on the ocean floor, and foraminifera tests are preserved within ocean sediments. Foraminiferal species abundances and assemblages are used as paleoceanographic proxies in the Arctic because certain species have been shown to be responsive to various oceanographic conditions including nutrient and oxygen concentrations, temperature, salinity, sea-ice cover, primary production, and low pH in the sediments (Wollenburg and Mackensen, 1998). In polar settings, one consistent indicator of seasonal (perennial) sea-ice cover is the absence (presence) of calcareous foraminifera within cold, saline water (Hald and Steinsund, 1996; Wollenburg et al., 2001, 2004; Seidenkrantz et al., 2007). The solubility of calcium carbonate is dependent on temperature, salinity, partial pressure of dissolved CO₂, and hydrostatic pressure (the latter was not a factor for this study due to depths < 600 m). Following the equation $\text{CaCO}_3 + \text{CO}_2 + \text{H}_2\text{O} \leftrightarrow \text{Ca}^{+2}_{(\text{aq})} + 2\text{HCO}_3^{-}_{(\text{aq})}$, dissolution occurs within cold Arctic waters with increased salinity, high pressures (increased depths), and with increased amounts of dissolved CO₂ (Hald and Steinsund, 1996). Hald and Steinsund (1996) observed that open water during seasonally sea ice-covered (warmer climate) conditions promotes the production of abundant organic matter due to increased primary productivity that sinks and oxidizes, producing increasing amounts of CO₂ which causes carbonate dissolution and prevents carbonate formation on the sea floor. CO₂ continues to form, and therefore calcareous foraminifera continue to

dissolve, until all of the organic matter and/or oxygen have been depleted, or until the conditions of solubility have changed (Hald and Steinsund, 1996). As a result of these different processes, agglutinated foraminifera are found in Arctic shelf areas that have high sedimentation rates, high freshwater runoff, and higher surface productivity, all of which result from seasonally open water (Hald and Steinsund, 1996; Schröder-Adams et al., 1990; Wollenburg et al., 2001, 2004). However, such conditions cause the dissolution or prevention of formation of calcareous fauna. In contrast, calcareous foraminifera may be preserved under perennial ice-cover, which is associated with low organic flux, sedimentation rates, and meltwater flux (Hald and Steinsund, 1996; Schröder-Adams et al., 1990; Wollenburg et al., 2001, 2004). Therefore, the abundances and species assemblages of benthic foraminifera in different layers in marine sediments may reflect changes in water circulation, temperature and salinity at the surface (planktic foraminifera) and sea floor (benthic foraminifera), reflect changes in ice cover, freshwater influx, and sedimentation rates. The presence and abundance of cysts of different dinoflagellate species also reflect paleo-sea ice cover and freshwater influx (Ledu et al., 2008; Richerol et al., 2008). The abundance of tintinnids (*Tintinnopsis rioplatensis*), a ciliate present in Arctic waters, also reflects the incursion of freshwater and high concentrations of suspended particulate matter (SPM), and this species is also found within samples processed for foraminifera (Scott et al., 1995; Schell et al., 2008).

Other useful proxies that can be derived from calcareous foraminifera are oxygen and carbon stable isotopes obtained from planktic and benthic species. These values can be analytically correlated to other areas of the Arctic. Changes in $\delta^{18}\text{O}$ of benthic and planktic calcareous foraminiferal tests reflect changes in temperature, salinity and source

water where they formed. Recently, Hillaire-Marcel and de Vernal (2008) discussed two scenarios to achieve lighter $\delta^{18}\text{O}$ values in the Arctic. Firstly, decreases in $\delta^{18}\text{O}$ are due to warmer water temperatures and/or lower salinity due to freshwater input and increased atmospheric temperatures. Secondly, when freshwater is used during the formation of sea ice, the isotopically light brines are released by fractionation. Both scenarios would have an immediate impact on the planktic foraminifera. As for the benthic foraminifera however, the bottom waters would require time to warm or freshen in the first scenario, but could become immediately lighter due to the second scenario due to the sinking of the dense, yet isotopically light brines. Although intriguing, these two potential mechanisms remain unresolved and would require ancillary data for interpretation.

Changes in the carbon stable isotope values of benthic and planktic calcareous foraminifera reflect the values of the dissolved inorganic carbon (DIC) in the water where they form. Primary productivity negatively fractionates CO_2 (DIC) during respiration at the sediment surface, which will cause a decrease of the $\delta^{13}\text{C}$ of benthic foraminifera (Hald and Steinsund, 1996). Increased photosynthesis within surface waters sequesters isotopically depleted CO_2 , which increases DIC and planktic foraminiferal $\delta^{13}\text{C}$. Enriched planktic and depleted benthic foraminiferal $\delta^{13}\text{C}$ values can therefore reflect increased primary productivity during seasonally ice-covered conditions. Increase in freshwater influx through rivers during warmer climate periods boosts the influx of depleted, terrestrially-derived DIC (Ravelo and Hillaire-Marcel, 2007). Changes in water stratification and circulation will also produce shifts in the isotopic composition of planktic and benthic foraminifera depending on the isotope values of the various sources.

Stable isotopic shifts of carbon and oxygen occurring in both planktic and benthic foraminifera indicate hydrographic changes throughout the water column.

2.4 Foraminifera in the Canadian Arctic

Due to the increasing interest and accessibility in the Arctic, research implementing foraminiferal species assemblages has become more frequent. The earliest Arctic sampling expeditions by Cushman (1948) and Loeblich and Tappan (1953) created the Arctic's first foraminiferal taxonomy. Phleger (1952) was the first to examine distributions of foraminifera along the Canadian Arctic shelf, specifically the surficial distributions of Lancaster Sound and Viscount Melville Sound within the Northwest Passage (NWP). Phleger (1952) described these as very cold, less saline environments which prevent the formation of calcareous foraminifera, and result in a predominantly agglutinated foraminiferal assemblage. Schröder-Adams et al. (1990) re-examined Lancaster Sound in 1981, and also described the association of agglutinated fauna with high sedimentation, and low salinity due to increased freshwater runoff and melting sea ice during seasonally ice covered conditions. In 1973, Iqbal sampled M'Clure Strait and documented a transition from a dominantly calcareous foraminiferal assemblage in the outer M'Clure Strait to an agglutinated one progressing west into the NWP (Vilks, 1989). Marlowe and Vilks (1963) expanded the sampling of the NWP and Canadian Arctic Archipelago (CAA) into the Queen Elizabeth Islands. Vilks (1989) summarised these sampling expeditions and described a relationship between the source of bottom water and foraminiferal species assemblage. Calcareous foraminifera are found in the deeper areas of the CAA such as the Beaufort Sea, below the surface waters and within the

Atlantic and Arctic waters. Vilks (1989) also demonstrated that agglutinated foraminifera thrive within the surface sediments and were found within the lower salinity surface layer of the CAA. Their species assemblages are correlated to their provenance of bottom water with an Arctic Ocean influenced Atlantic water to the west, and a Baffin Bay influenced Atlantic water to the east where their extent depends on sills and water depth. During the Ice Island Project located on the northwest shelf of Axel Heiberg, Schröder-Adams et al. (1990) were able to study the foraminiferal species assemblage within surface sediments beneath permanent ice cover. They described this environment as low sedimentation, and high salinity due to reduced freshwater influx.

Researchers associated with the Canadian Arctic Shelf Exchange Study (CASES) and ArcticNet have begun to extensively re-examine foraminiferal assemblages in sediments from the Beaufort Sea, Amundsen Gulf and CAA during summer expeditions from 2002 to 2006. In addition to surface samples, boxcores and piston cores were also collected for paleoceanographic interpretations, using improved concepts and equipment of foraminiferal assemblage assessment. Scott et al. (2008) re-examined foraminifera from sites initially sampled by Vilks (1989), given the recently highlighted importance of smaller foraminifera ($< 45 \mu\text{m}$) as significant contributors to the total abundance in Arctic waters. They found a similar species assemblage, however due to the reduction in sieve size also found a larger number of smaller foraminifera. Scott et al. (2008) attributed their reported higher numbers in agglutinated species to the fact that their samples were preserved wet, while the Vilks (1989) samples were dried, which can disintegrate the tests. Scott et al. (2008) also presented the modern foraminiferal distributions of the Amundsen Gulf and Beaufort Sea surface sediments. Those distributions were used to

construct the paleoceanographic records from sediment cores such as those analysed by Schell et al. (2008) which reconstructed Late Holocene histories from shallow areas of the Amundsen Gulf. The shallower sites in the Amundsen Gulf contain warmer waters conducive to calcareous foraminiferal production. A reduction in Arctic Bottom waters coupled with the presence of seasonal sea ice decreased the calcareous fauna and increased the agglutinated fauna, all a result of the increase in recent climate warming (Schell et al., 2008). Scott et al. (2009) reconstructed paleoceanographic conditions since the late glacial using data from a piston core collected in both the Amundsen Gulf and Beaufort Sea. The foraminiferal species assemblages indicated seasonal sea ice during the most of the Holocene, and permanent ice cover during the late glacial period.

2.5 Paleoceanography and Paleoclimate in the Canadian Arctic

There are relatively few paleoceanographic records that have been reconstructed from the Eastern CAA by utilizing foraminifera or other proxy methods from within sediment cores. However, another record produced from CASES boxcores from the Beaufort Sea was reconstructed from dinoflagellate cyst assemblages due to their ability to resist dissolution (Richerol et al., 2008). Their 600 year reconstructions indicate an increase in productivity, sea-surface temperature and ice cover, and a decrease in salinity in recent centuries, parameters that were heavily influenced by increases in the Mackenzie River outflow (Richerol et al., 2008).

In the Western CAA, few multi-proxy records consisting of dinoflagellate cyst assemblages, foraminiferal species assemblages, sedimentology and stable isotopes have been developed. Mudie et al. (2006) analysed a piston core at the entrance to Jones

Sound. This record contained one of the first foraminiferal assemblages sieved at 45 μm and produced a calcareous assemblage that would not have been observed otherwise using coarse mesh sieves. These very small calcareous species also indicated the influence of deep Arctic water through Baffin Bay since the mid-Holocene (4 ka BP) until approximately the last millennium (Mudie et al., 2006). At the surface however, dinocysts indicated a change in water mass from mainly Atlantic to Atlantic and Arctic at 4 ka BP. This change was also coupled to fluctuations and a slight increase in sea ice cover and sea surface salinity, and a decrease in sea surface temperature. A similar record from a 12 cal ka BP piston core from Lancaster Sound was constructed by Ledu et al. (2008). This reconstruction includes the deglaciation of the Canadian Arctic, gradual warming conditions associated with increased Arctic and Atlantic water flux into Baffin Bay until the Late Holocene, in which cooling occurred until present. Ledu et al. (2008) have positively correlated their record with terrestrially derived climate records including pollen and diatoms and the Arctic Oscillation atmospheric regime. A paleo-spring-sea ice record from a piston core in Barrow Strait has been constructed using the sea-ice diatom biomarker IP_{25} by Vare et al. (2009). This record indicates an increase in sea ice since the Holocene Optimum (6 ka BP). These paleorecords of varying timescales and locations will subsequently be discussed comparatively with the cores from this study, which will provide high temporal resolution records and the first stable isotope values of the last millennium from multiple sites in the Amundsen Gulf.

Other non-sedimentological records of paleoceanography and more specifically paleo-sea ice cover include archaeological evidence from beached whale bones, human settlement, and historical records of recent Arctic expeditions. Radiocarbon dated

bowhead whale bones from raised beaches within the CAA provides a timeline for the presence of these whales. Dyke et al. (1996) and Dyke and Savelle (2001) have produced a record of sea ice during the Holocene with these bones because the whales were only present with summer sea ice breakup. The dating of whale bones collected from past Thule Inuit settlements has been correlated to the availability of food (Dyke et al., 1996; Dyke and Savelle, 2001), which would be available during summer sea ice breakup. These records of seasonal sea ice cover consist of discrete measurements, and therefore do not provide a continuous record of sea ice cover in a specific area.

Since there exists a coupling between the ocean and the atmosphere (Serreze and Barry, 2005), and due to the limited number of paleoceanographic records within the Canadian Arctic, we can compare paleoceanographic records with terrestrially derived paleoclimate records. Climate proxies have been used within the Canadian Arctic to recreate past climate, with the various climate proxies providing different temporal resolution ranging from decades to millennia. For example, varved sediments, tree ring, and ice core records provide annual resolution, but diatom, pollen, foraminifera, and dinoflagellate indicators are dependent on the sedimentation rates in which they were deposited. Canadian Arctic climate throughout the Holocene (11.5 ka), as reconstructed by the aforementioned proxies, has reflected continued warming since the deglaciation of the Laurentide and Innuitian Ice Sheets, with some variability. Following the Holocene Thermal Maximum (HTM) (Holocene Climatic Optimum) ~9.5 to 3 ka (Serreze and Barry, 2005), which consisted of higher temperatures than those of recent warming, cooler climates have persisted through the neoglacial cooling. The cooler late Holocene consisted of three climate oscillations: the warming through the Medieval Warm Period

(MWP, 900-1200 AD, Jones et al., 2001), the cooling through the Little Ice Age (LIA, 1550-1900 AD, Jones et al., 2001), and the recent warming due to human industrialisation called the Anthropocene (~ 1800 AD to present, Smol et al., 2005; Crutzen, 2002). Several global late-Holocene climate reconstructions have been created using multi-proxy data (Jones et al., 2001), or in combination with modeling programs (Mann et al., 2009), which identify the recent warming as unprecedented. Models also show that this warming is not only due to the natural forcing of solar and volcanic activity, but also due to the increasing greenhouse gases (Mann, 2007; Bertrand et al., 2002). Because these global climate reconstructions consist of few Arctic proxy records relative to the remaining latitudes, the resolution of the high latitude reconstructions is poor. However, the late-Holocene climatic oscillations have been documented in climate records created by several different proxies from high latitude environments and are discussed below.

The closest paleoclimate records to the Amundsen Gulf and Viscount Melville Sound utilize proxies from lakes on Victoria, Banks, and Melville Islands (Fig. 1.2). A Victoria Island diatom record produced by Prodritske and Gajewski (2007) reconstructs several changes in the diatom community during the Holocene. A warming during the MWP and during the recent warming period (Anthropocene) were inferred using increased warmer water species, increased diatom concentrations, and increased organic matter, whereas a cooling during the LIA is evident in decreases in diatom concentration and diversity (Prodritske and Gajewski, 2007). Diatom records from Melville and Banks Islands span recent centuries, and document a change in species composition due to recent climate warming at approximately 1950 AD (Keatley et al., 2006) and 1850 AD

(Lim et al., 2008), respectively. There are several other diatom records from the CAA that demonstrate changes in fauna due to recent climate oscillations. Some records show evidence of the MWP, LIA and Anthropocene including records from Boothia Peninsula (LeBlanc et al., 2004) and Baffin Island (Joynt and Wolfe, 2001). However, some records may only indicate the LIA and Anthropocene, such as the record from Prince of Wales Island produced by Finkelstein and Gajewski (2007), or only the recent warming of the Anthropocene as recorded on Banks Island (Lim et al., 2008). Banks Island also contains a record of pollen assemblages though the Holocene, however the resolution is too poor to decipher oscillations within the last millennium (Gajewski et al., 2000). Due to their annual resolution, varved sediments have become useful in recreating past climate. Varved sediments from Baffin Island (Thomas and Briner, 2009; Moore et al., 2001) and Ellesmere Island (Besonen et al., 2008) have revealed the temperatures of the recent warming, LIA cooling, and pre LIA warmer period (MWP), that indicate a warmer recent climate than during the pre LIA period. Ice core records are another reliable indicator of warming that document periods of ice melting and subsequent changes to the $\delta^{18}\text{O}$ signal within the ice. Ice cores from Agassiz Ice Cap (Ellesmere Island, Bourgeois et al., 2000) and Devon Ice Cap (Devon Island, Koerner and Fisher, 1990) have similarly recorded post glacial warming, gradual cooling since the Holocene Optimum, that the lowest temperatures of the Holocene occurred during the LIA, and recent warming of the Anthropocene.

Smol et al. (2005) constructed a compilation of 55 paleolimnological (diatom) records from the circumpolar Arctic. Most records indicate a shift in diatom ecology ~1850 AD, the Holocene-Anthropocene boundary, and that the shift can only be

explained by warmer and longer summers due to anthropogenic influences. A similar compilation was constructed from sites within the Canadian Central Arctic treeline region, and it also demonstrated a shift ~1850 AD (Rühland et al., 2003). Multi-proxy climate reconstructions of the Northern Hemisphere of the last millennium demonstrate the three climate anomalies (Osborn and Briffa, 2006).

Chapter 3 - Materials and Methods

3.1 Field Sampling

3.1.1 Amundsen Gulf

The *CCGS Amundsen* was re-outfitted with sediment sampling equipment for the CASES programme to sample the Beaufort Sea and Amundsen Gulf from 2003-2004. Boxcoreing was performed at each location, which provided one cubic metre of undisturbed sediment per sample. The surface water was slowly siphoned off by gravity revealing any organisms on the sediment surface, and then a plastic tube was inserted under slight vacuum to retrieve an uncompressed sediment core (Murdoch and MacKnight, 1994). The samples analysed in this study were taken from five 30-40 cm pushcores removed from boxcores collected from the Amundsen Gulf during leg 8 of the 2004 summer season (Table 3.1). Sites 106, 109, 112, 118, and 124 completed the 180

Table 3.1. Physical properties recorded during the collection of cores 106, 109, 112, 118, and 124 of leg 8 of the CASES cruise 2004-804.

2004-804 - CASES 2004 Leg 8							
Collection Date	CASES Sample ID	Latitude (°N)	Longitude (°W)	Water Depth (m)	Core Length (cm)	Bottom Temperature (°C)	Bottom Salinity (psu)
10-Aug-04	2004-804-106A	70.5850	122.6300	544	37	0.32	34.75
30-Jul-04	2004-804-109A	70.6600	123.4304	569	34	0.33	34.75
09-Aug-04	2004-804-112A	70.7533	124.2317	511	35	0.29	34.73
18-Jul-04	2004-804-118A	70.9940	125.8503	388	30	0.36	34.80
28-Jul-04	2004-804-124B	71.3895	126.7185	442	33.5	0.34	34.81

km long transect of 5 short sediment cores, from the northwestern edge of the Amundsen Gulf to its deepest area in the southeast. This transect was used to identify differences in benthic conditions between the opening and deeper reaches of the Gulf (Fig. 1.3). The cored sites were chosen based on the undisturbed stratigraphy of the seafloor as shown by profiles from multibeam sonar and sub-bottom profiler (3.5 kHz) as provided by the University of New Brunswick Ocean Mapping Group (Appendix A). The pushcores ranged from 30 to 37 cm in length and were collected from waters 388 to 569 m deep (Table 3.1). Temperature and salinity measurements were obtained during sediment collection at each core location with a conductivity-temperature-depth (CTD) meter. The CTD profiles reveal bottom water conditions of 0.3 °C averaged temperature and 35 psu averaged salinity (Fig. 2.2). Immediately after collection, the push cores were sealed, refrigerated at 4 °C and archived in the National Core Repository at the Geological Survey of Canada – Atlantic in Dartmouth, NS. Each core was later split longitudinally, described lithologically, photographed and X-rayed.

3.1.2 *Viscount Melville Sound*

Marine sediments from within the Northwest Passage, the Beaufort Sea, the Amundsen Gulf, and other interstitial waters of the Canadian Arctic Archipelago, were sampled in 2006 by the icebreaker *CCGS Amundsen*, which was commissioned by ArcticNet (<http://www.arcticnet.ulaval.ca/>). One push core (labelled 012) was collected (following the same method in section 3.1.1) from a boxcore collected at site 307 within the Viscount Melville Sound (74°24'001" N, 100°34'991" W) during leg 1 of the ArcticNet cruise on September 24th, 2006 (Fig. 1.3). The bathymetry, backscatter and

sub-bottom profile of the seafloor at the cored site (Appendix A) indicated ice scours and disturbed stratigraphy as shown by onboard profiles from multibeam sonar and a 3.5 kHz sub-bottom profiler from the University of New Brunswick Ocean Mapping Group. Core 012 was collected in 172 m of water and measured 22 cm in length at the time of collection, but appears to measure 24 cm due to separation at bottom (Appendix A). Upon collection, the push core was sealed, refrigerated at 4 °C and archived in the National Core Repository at the Geological Survey of Canada – Atlantic (GSC-A) in Dartmouth, Nova Scotia. The core was split longitudinally, photographed and X-rayed, and described lithologically (Appendix A).

3.2 Chronology

In order to establish the timing of the oceanographic changes shown within the cores, radiocarbon (^{14}C) and ^{210}Pb measurements were carried out on the marine sediments. Unfortunately, due to limited funding and the limited amount of available calcareous foraminifera, I was only able to perform those measurements on two of the cores from the Amundsen Gulf. The core from the Viscount Melville Sound was also characterized by a limited amount of calcareous material, which prevented us carrying out ^{14}C measurements. Thus, foraminiferal species abundances were used to chronologically correlate the 5 boxcores.

Bulk calcareous foraminifera samples were analysed from cores 109 and 124 for ^{14}C activity using accelerator mass spectrometry (AMS) at the National Ocean Sciences Accelerator Mass Spectrometry Facility (NOSAMS) at the Woods Hole Oceanographic Institution. The radiocarbon ages were then converted to calibrated years using CALIB

version 5.0 (Stuiver and Reimer 1993). Calibrated ages were then corrected for marine reservoir effect with a $\Delta R = 430 \pm 50$ measured on mollusc shells (McNeely et al. 2006). The calibrated dates are reported as age \pm error in years (2σ) *Anno Domini* (AD) and Before Present (BP).

Lead-210 geochronology is based on the ^{238}U decay series. Due to the short half life ($t_{1/2}$) of ^{210}Pb of 22.6 years (decay constant $\lambda=0.03114 \text{ y}^{-1}$), one can calculate the accumulation of ^{210}Pb in sediments as they undergo decay over 100 years. The total activity of ^{210}Pb down-core represents both the unsupported and supported components of ^{210}Pb . The unsupported component of ^{210}Pb is the decay product of ^{222}Rn which is formed in the atmosphere. The supported component of ^{210}Pb originates from the in situ decay of ^{222}Rn and ^{226}Ra (^{238}U series) in rocks (sediment). Under the assumption that unsupported ^{210}Pb activity is directly related to the flux of ^{210}Pb from the water column (which, in turn, came from the atmosphere) that reaches the seafloor, its exponential decay down-core can be used to estimate the sedimentation rate over those last ~110 years (5 half lives). Total (supported and unsupported) activities of ^{210}Pb were measured by α counting of the activity of ^{210}Po , the daughter of ^{210}Pb , following the extraction procedures of Baskaran and Naidu (1995). The ^{210}Pb values are reported in dpm/g with a counting error reported as 1σ standard deviation. Since the radioisotopes between ^{226}Ra and supported ^{210}Pb have very short half-lives, their activities are assumed to be in secular radioactive equilibrium. Therefore the supported fraction of ^{210}Pb is determined by calculating the activity of ^{226}Ra from the measurement of ^{214}Pb and ^{210}Bi by gamma spectroscopy (Ghaleb, 2009). Analyses were performed at GEOTOP (Université du Québec à Montréal) on dried and ground bulk sediment samples from boxcore 109. ^{210}Po

analyses were measured by α counting every cm from 0-11 cm, and every second cm from 12-33 cm. ^{226}Rn analyses were measured by gamma counting a composite sample of 8-11 cm.

3.3 Foraminiferal Sampling and Processing

A ten cubic centimetre (10 cm^3) volume was subsampled from every other centimetre along each core from the Amundsen Gulf and Viscount Melville Sound for foraminiferal species identification and enumeration and isotopic analyses. Each 10 cm^3 sample was initially rinsed with cold tap water through a $500\text{ }\mu\text{m}$ sieve to remove the debris and break up the sediment lumps, and the sample was collected on a $45\text{ }\mu\text{m}$ sieve. The sample was washed with dish soap and water to separate the silt and clay from the foraminifera. The samples were transferred and stored in sample cups with 20 mL of ethanol and 1 mL of borax before and after analysis to preserve and buffer the specimens to prevent organic decay and carbonate dissolution. Each species was visually identified using published species descriptions from the Amundsen Gulf and Beaufort Sea (Scott et al., 1991; Scott et al., 2008), and other studies conducted in the Western Canadian Arctic (Phleger, 1952; Iqbal, 1973; Lagoe, 1980; Vilks, 1989). Counts of 250 to 300 individual foraminifera were obtained from each sample for a representative number of species (Patterson and Fishbein, 1989), using a 20-80x microscope. Samples with high abundances were wet-split down to 300 specimens, to facilitate counting, following methods outlined by Scott and Hermelin (1993). The total number of foraminifera for each sample was recorded as total foraminifera per 10 cm^3 of sediment. Relative fractional abundances were calculated for each species of the total number of specimens

for each sample, and were presented as species percent of the total abundance. Also recorded per 10 cm³ was the total number of species, and the total number of tintinnids (*Tintinnopsis rioplatensis*), a ciliate that is abundant in brackish water and/or indicative of increased suspended particulate matter (Scott et al., 1995).

3.4 Foraminiferal Numerical Analyses

The following numerical analyses were performed on the cores from the Amundsen Gulf, in order to statistically identify any correlation of foraminiferal species assemblage among and within cores. Relative fractional abundance data were used to calculate the standard error for each taxonomic unit (Patterson and Fishbein, 1989). Taxonomic units whose standard errors were greater than their fractional abundance were removed for subsequent statistical analyses. Q-mode agglomerative hierarchical cluster analysis was performed in the Palaeontological Statistics (PAST) program (<http://folk.uio.no/ohammer/past/>) using Euclidean distance dissimilarity and a constrained Ward's method linkage type on square-root transformed data (Prodritske and Gajewski, 2007). SIMPER (similarity percentages) was used to quantify the species-specific contributions to the differences between the groups designated via cluster analysis (Clarke, 1993).

3.5 $\delta^{18}\text{O}$ and $\delta^{13}\text{C}$ of Foraminifera

To determine variation in water temperature and salinity, and primary productivity, oxygen and carbon isotopic analyses were performed on the benthic species *Islandiella teretis* and the planktic species *Neogloboquadrina pachyderma* sinistral.

Islandiella teretis (*I. teretis*) was the most abundant (> 63 µm) calcareous benthic foraminiferal species common to all Amundsen Gulf cores, and was collected from all size fractions when present. *Neogloboquadrina pachyderma* (Npl) was the only planktic species found in the Amundsen Gulf, and was collected from the 150-210 µm size fraction, producing values from a consistent water depth since planktics stratify with size within the water column (Hillaire-Marcel et al., 2004). The organic material within the benthic foraminiferal shells was removed by combustion in a 400 °C oven for one hour under vacuum, to remove any potentially contaminating organic carbon. The foraminiferal stable isotopic analyses were performed at GEOTOP (Université du Québec à Montréal) by acidification with 100 % orthophosphoric acid in a MulticarbTM preparation device coupled to an IsoPrimeTM isotope ratio mass spectrometer. The isotopic composition for each sample was measured relative to the international reference VPDB (Vienna Peedee Belemnite) using permil notation. Reference (NBS 19, IAEA) and working (UQ6 carbonate, GEOTOP, Hillaire-Marcel et al., 2004) standards were used as a check of accuracy. The reproducibility of UQ6 has determined the analytical 1-σ error to be 0.05‰ (Hillaire-Marcel et al., 2004).

Chapter 4 - Results

4.1 Core Description

4.1.1 *Amundsen Gulf*

All five cores (106, 109, 112, 118, 124) from the transect through the Amundsen Gulf (Fig. 1.3) were described lithologically based on visual inspection of split cores and their X-rays (Appendix A). The sediments of all five cores are similar in colour, texture and composition, and consist of two distinct, upper and lower sections (or units) separated by mottling of the two sediments. The upper sections consist of very soft massive dark-brown silty clay which are an average of 9.2 cm thick (range 4.0-16.5 cm). The bottom sections consist of soft massive dark- to olive-grey silty clay to clayey silt. Cores 112 and 118 contain open burrows, and core 118 contains fine to coarse sand within the bottom 4 cm.

4.1.2 *Viscount Melville Sound*

Core 012 consists of massive yellowish-grey muddy silt throughout (Appendix A). A crack at 8 cm and a void from 19 to 23 cm are visible in both the photograph and the X-ray (Appendix A). The X-ray also reveals some ice-rafted debris (IRD), ranging from a millimetre to nearly two centimetres in diameter throughout the core. The bathymetry of the sea floor at the cored site (Appendix A) shows evidence of ice scours by the jagged appearance of the sediment.

4.2 Chronology – Amundsen Gulf

The chronology for cores 109 and 124 indicate that the ~ 34 cm long sediment cores represent sediment and foraminiferal accumulation over approximately the last millennium. The radiocarbon and calibration results for cores 109 and 124 are listed in Table 4.1. If one could assume constant sedimentation, the rate produced in core 109 is 0.23 mm/yr and in core 124 is 0.27 mm/yr.

The results of the ^{210}Pb and ^{226}Ra analyses are listed in Table 4.2, and plotted as total ^{210}Pb in dpm/g in Fig. 4.1. The 2- σ errors of the ^{210}Pb activities from intervals 0-2 cm, 2-5 cm, 5-15 cm, 16-23 cm, and 24-33 cm indicate that the values within these intervals are not statistically different from one another. The sediment sample is at secular radioactive equilibrium if the ratio of ^{210}Pb (avg. activity = 5.014 ± 0.382 dpm/g) to ^{226}Ra (avg. activity = 4.359 ± 0.224 dpm/g) is equal to one. The ratio is 1.150 ± 0.109 , which is very close to being 1.0 considering errors of 2σ , indicating that the ^{210}Pb activities from 5 to 15 cm represent supported lead, and sediment older than 110 years (5

Table 4.1. Radiocarbon ages for cores 109 and 124 in calibrated years BP (before present) and AD (Anno Domini).

Radiocarbon ages and related data					
NOSAMS ID	Sample ID	Interval	Conventional radiocarbon age (yr BP)	2- σ calibrated age range (cal yr BP) (cal yr AD)	Median calibrated age (cal yr BP) (cal yr AD)
OS-69272	2004-804-109A	30-32 cm	2020 \pm 40	996-1275 675-954	1135.5 814.5
OS-69097	2004-804-124B	24-25 cm	1930 \pm 30	919-1186 764-1031	1052.5 897.5

Table 4.2. ^{210}Pb and ^{226}Rn activities with 2σ error in boxcore 109.

Boxcore 109 – ^{210}Pb Profile			
Interval (cm)	Midpoint (cm)	^{210}Pb activity (dpm/g)	error (2σ)
0-1	0.5	11.563	0.882
1-2	1.5	11.195	1.208
2-3	2.5	6.899	0.526
3-4	3.5	6.236	0.476
4-5	4.5	6.620	0.505
5-6	5.5	5.237	0.399
6-7	6.5	5.380	0.410
7-8	7.5	5.293	0.404
8-9	8.5	4.817	0.367
9-10	9.5	5.202	0.397
10-11	10.5	5.023	0.383
12-13	12.5	5.177	0.395
14-15	14.5	5.031	0.543
16-17	16.5	6.681	0.883
18-19	18.5	6.278	0.678
20-21	20.5	6.197	0.669
22-23	22.5	6.497	0.702
24-25	24.5	4.012	0.433
26-27	26.5	3.756	0.287
28-29	28.5	3.342	0.361
30-31	30.5	3.617	0.276
32-33	32.5	3.830	0.413

Interval (cm)	Midpoint (cm)	^{226}Ra activity (dpm/g)	error (2σ)
8-11	9.5	4.359	0.224

half lives). Therefore the sediment above 5 cm is younger than 110 years. Considering there are statistically only two samples above 5 cm, it is difficult to assume constant sedimentation, and therefore a sedimentation rate can not be calculated from the decay of ^{210}Pb activity. There is a shift in the averaged activities of intervals 16-23 cm relative to 5-15 cm, and then of intervals 24-33 cm relative to 16-23 cm (Fig. 4.1). Since interval 5-15 cm consists of supported ^{210}Pb , then the lower intervals also consist of supported lead, and are older than 110 years.

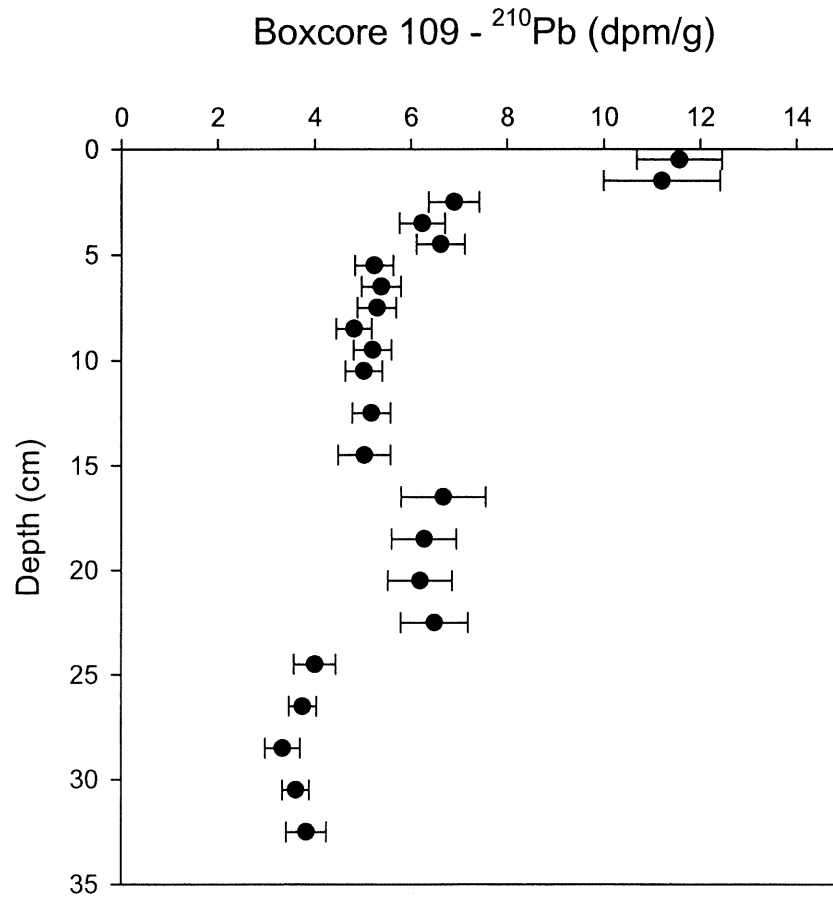


Fig. 4.1. ^{210}Pb activities plotted against depth of core 109. Analyses performed at GEOTOP (Université du Québec à Montréal).

The radiocarbon dates provided by cores 124 and 109 suggest millennium-scale interpretations and an approximate age for the changes in foraminiferal assemblages and isotopic values down-core. The ^{210}Pb dating indicates that the upper 5 cm of core 109 is less than 110 years old.

4.3 Foraminiferal Assemblages

4.3.1 Amundsen Gulf

Total numbers of species, specimens, tintinnids, and relative fractional abundance data with standard error are listed for all species in Appendix B for all even intervals of each core. For each core along the transect, total numbers of species, specimens and tintinnids are illustrated as functions of depth in Figs. 4.2-4.6. Also illustrated are the relative fractional abundance data (percent of the total) with depth for several abundant or indicative species or genera, as well as percent total calcareous foraminifera. The total number of species remains fairly constant within each except for core 118. The total number of species is on average lower in cores 106 and 109 which are located toward the inner part of the Gulf, than in cores 112 and 124 which are located towards the mouth of the Gulf. The total number of specimens per 10 cm³ per sample varies within each core. Total foraminiferal counts from samples in cores 106 and 109 (inner Gulf) average 1000 specimens, and are only two thirds the average total numbers of specimens of samples from cores 112, 118 and 124 (outer Gulf) (Fig. 1.3). The total number of species and specimens decreases significantly in core 118, which is a characteristic not shared by the other cores. Total numbers of tintinnids are variable within each core and among all cores, with counts reaching 300 specimens. There are spikes of tintinnids within each core. *Trochammina* spp. and *Bathysiphon rufus* are the most abundant agglutinated species (Figs. 4.2-4.6). Their relative fractional abundance data exhibits no clear trend within and among cores, except for core 118 (Fig. 4.5) where abundances decrease with depth, similar to the number of specimens per 10 cm³. The percent totals of minor agglutinated species including *Saccammina* spp. follow decreasing trends with depth in

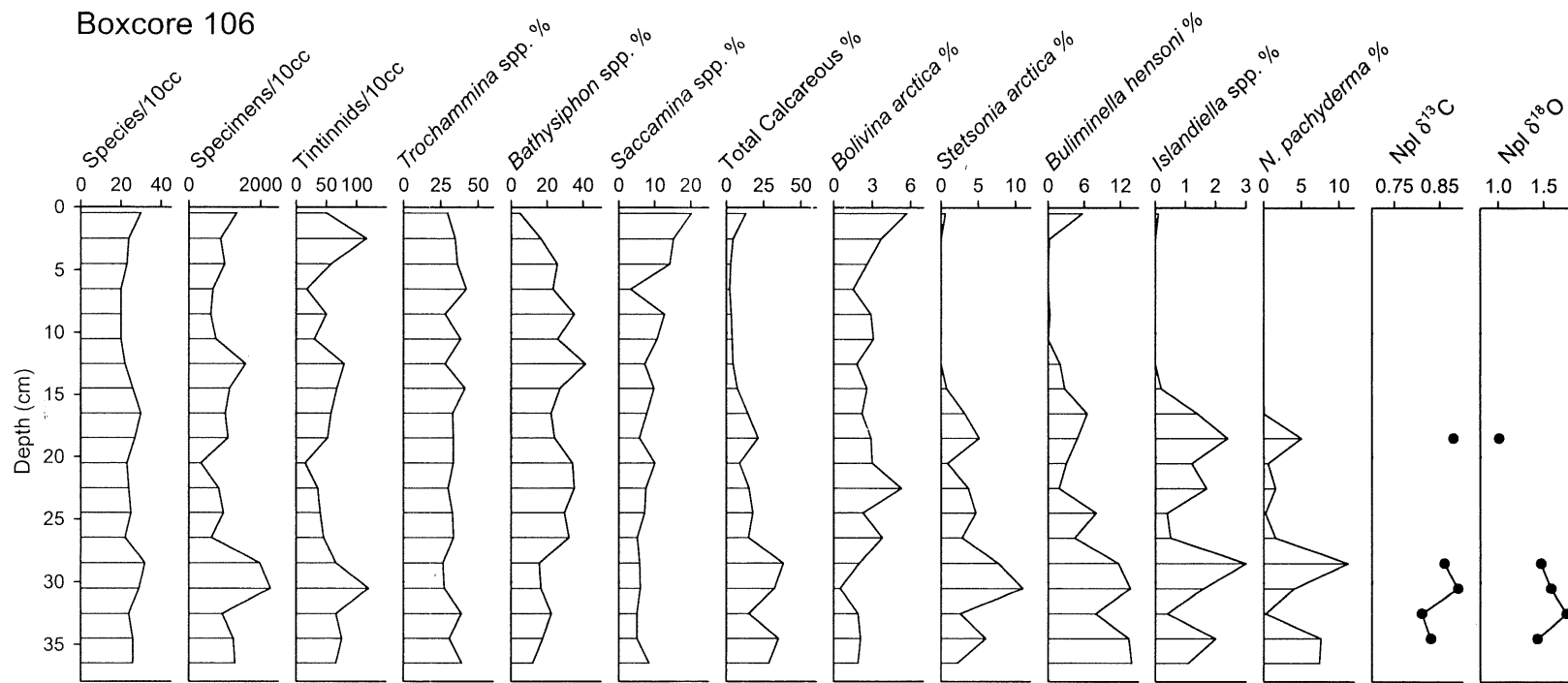


Fig. 4.2. The total number of species, specimens and tintinnids per 10 cm², relative fractional abundances (% of the total) for abundant or indicator species and total calcareous species, and values for $\delta^{13}\text{C}$ and $\delta^{18}\text{O}$ for planktic *Neogloboquadrina pachyderma* (Npl) as functions of depth from boxcore 106.

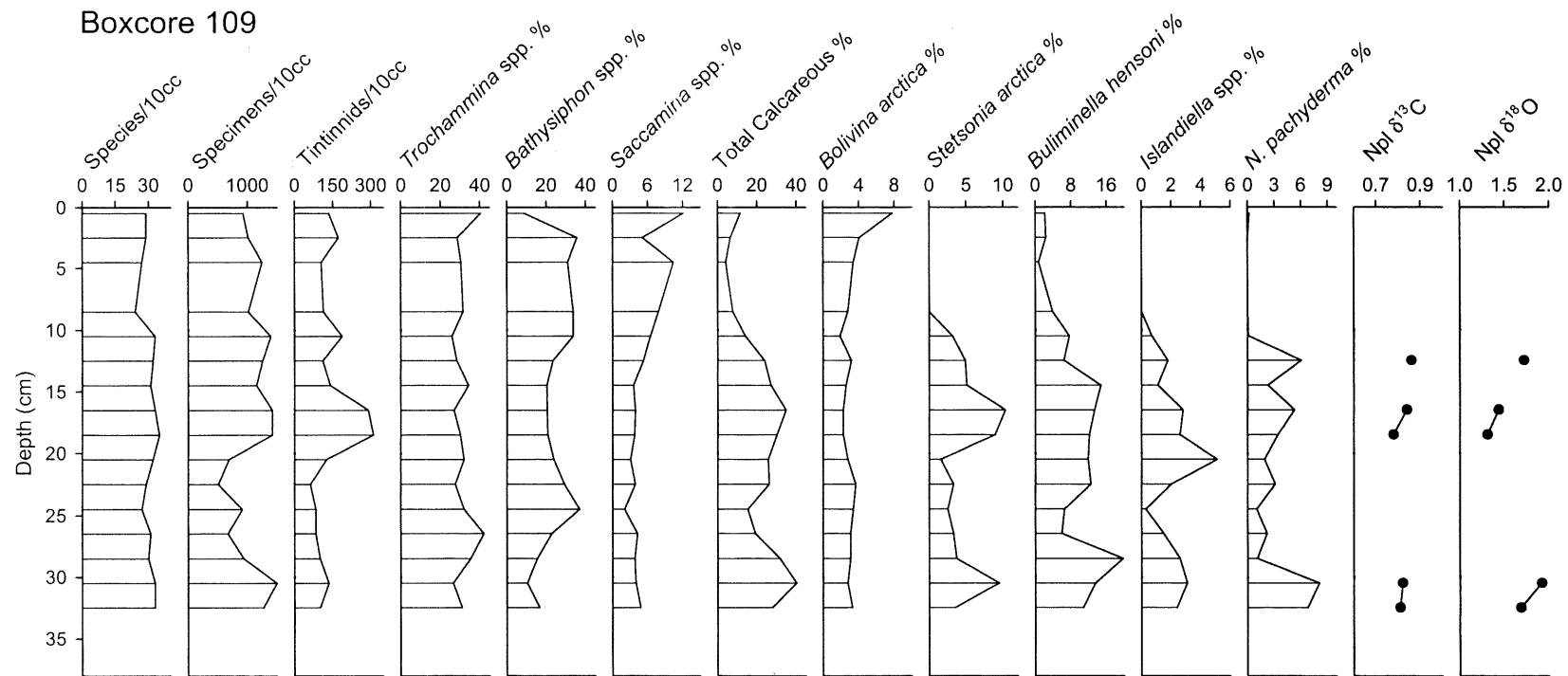


Fig. 4.3. The total number of species, specimens and tintinnids per 10 cm², relative fractional abundances (% of the total) for abundant or indicator species and total calcareous species, and values for $\delta^{13}\text{C}$ and $\delta^{18}\text{O}$ for planktic *Neogloboquadrina pachyderma* (Npl) as functions of depth from boxcore 109.

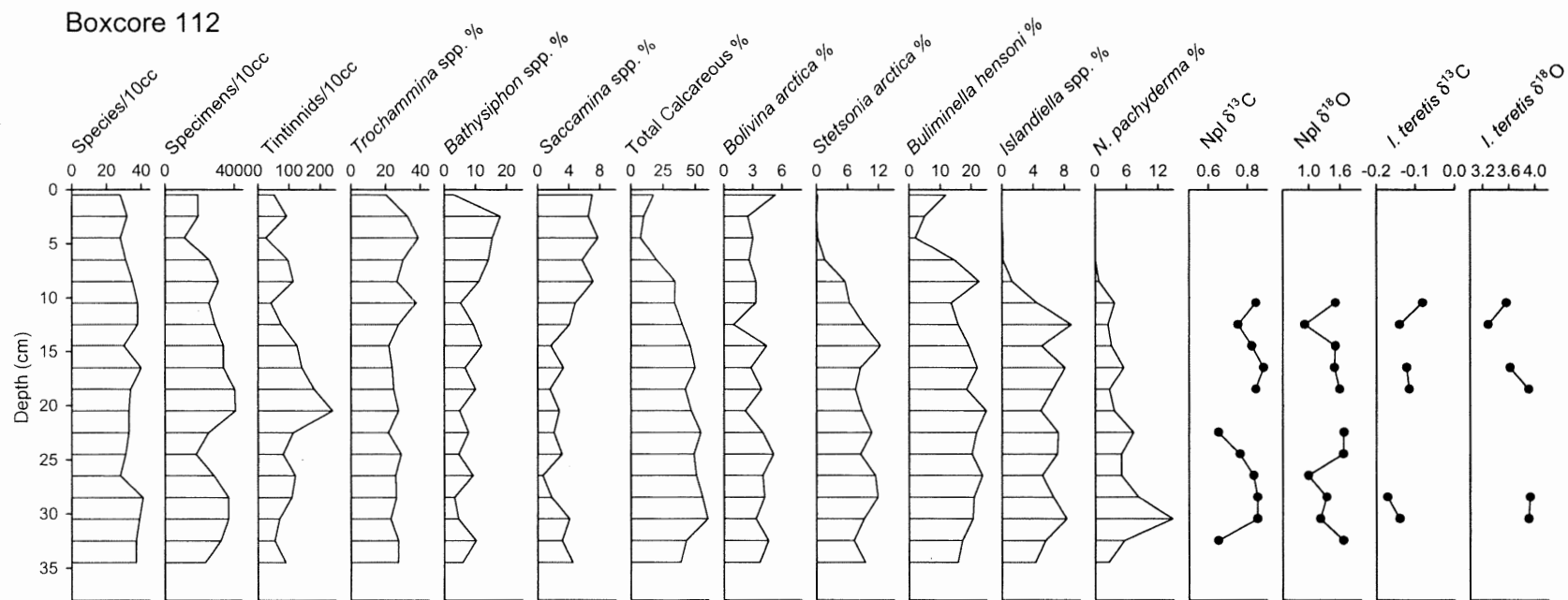


Fig. 4.4. The total number of species, specimens and tintinnids per 10 cm², relative fractional abundances (% of the total) for abundant or indicator species and total calcareous species, and values for $\delta^{13}\text{C}$ and $\delta^{18}\text{O}$ for planktic *Neogloboquadrina pachyderma* (Npl) and benthic *Islandiella teretis* as functions of depth from boxcore 112.

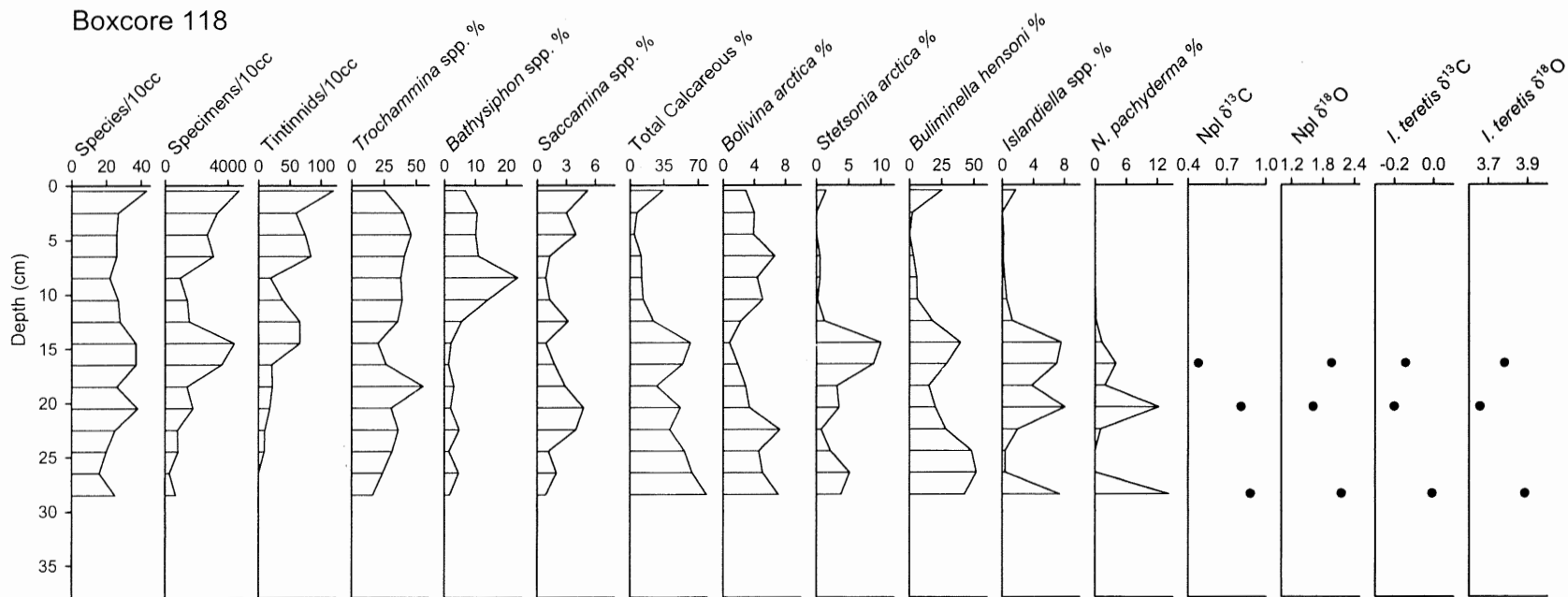


Fig. 4.5. The total number of species, specimens and tintinnids per 10 cm², relative fractional abundances (% of the total) for abundant or indicator species and total calcareous species, and values for $\delta^{13}\text{C}$ and $\delta^{18}\text{O}$ for planktic *Neogloboquadrina pachyderma* (Npl) and benthic *Islandiella teretis* as functions of depth from boxcore 118.

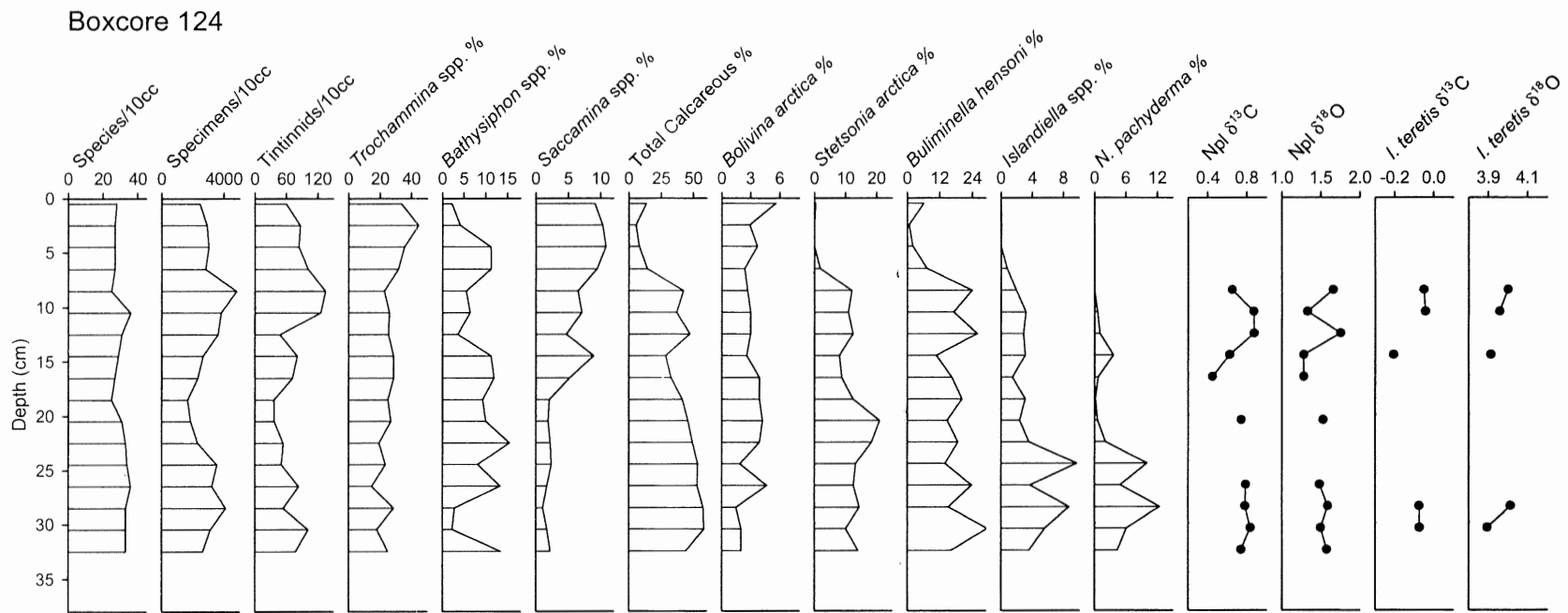


Fig. 4.6. The total number of species, specimens and tintinnids per 10 cm², relative fractional abundances (% of the total) for abundant or indicator species and total calcareous species, and values for $\delta^{13}\text{C}$ and $\delta^{18}\text{O}$ for planktic *Neogloboquadrina pachyderma* (Npl) and benthic *Islandiella teretis* as functions of depth from boxcore 124.

all cores, in contrast to the percent total calcareous specimens which increase with depth. The increase of abundant calcareous species, except for *Bolivina arctica*, is variable with a transition that occurs over 1 to 3 samples (2 to 6 cm). Notably, calcareous species are nearly absent from the upper section of each core, except for *Bolivina arctica*. In contrast, calcareous specimens reach up to 75 % of the total abundance of foraminifera in the lower sections. The percent total of calcareous species are primarily represented by *Buliminella hensoni*, followed by *Bolivia arctica*, *Stetsonia arctica*, *Islandiella* spp., and the planktic species *Neogloboquadrina pachyderma*. Also listed in Appendix B are the percent calcareous foraminifera in each sample that were partially dissolved rendering species identification impossible. Samples containing dissolving calcareous foraminifera also contained specimens that were beginning to dissolve, however their species was identifiable.

4.3.2 *Viscount Melville Sound*

Total numbers of species, specimens, tintinnids, and relative fractional abundance data with standard errors are listed for all species in Appendix B for all even intervals of each core. For each core along the transect, total numbers of species, specimens and tintinnids are illustrated as functions of depth in Fig. 4.7. Also illustrated are the relative fractional abundance data (percent of the total) with depth for several abundant or indicative species or genera, as well as percent total calcareous foraminifera. The number of species remains fairly consistent with only a slight decrease towards the bottom of the core (Fig. 4.7). The total number of species averages 29, and ranges from 16 to 36. The core top contains ~3000 specimens per 10 cm³, increases to ~5000 by 10.5 cm, then

Boxcore 012

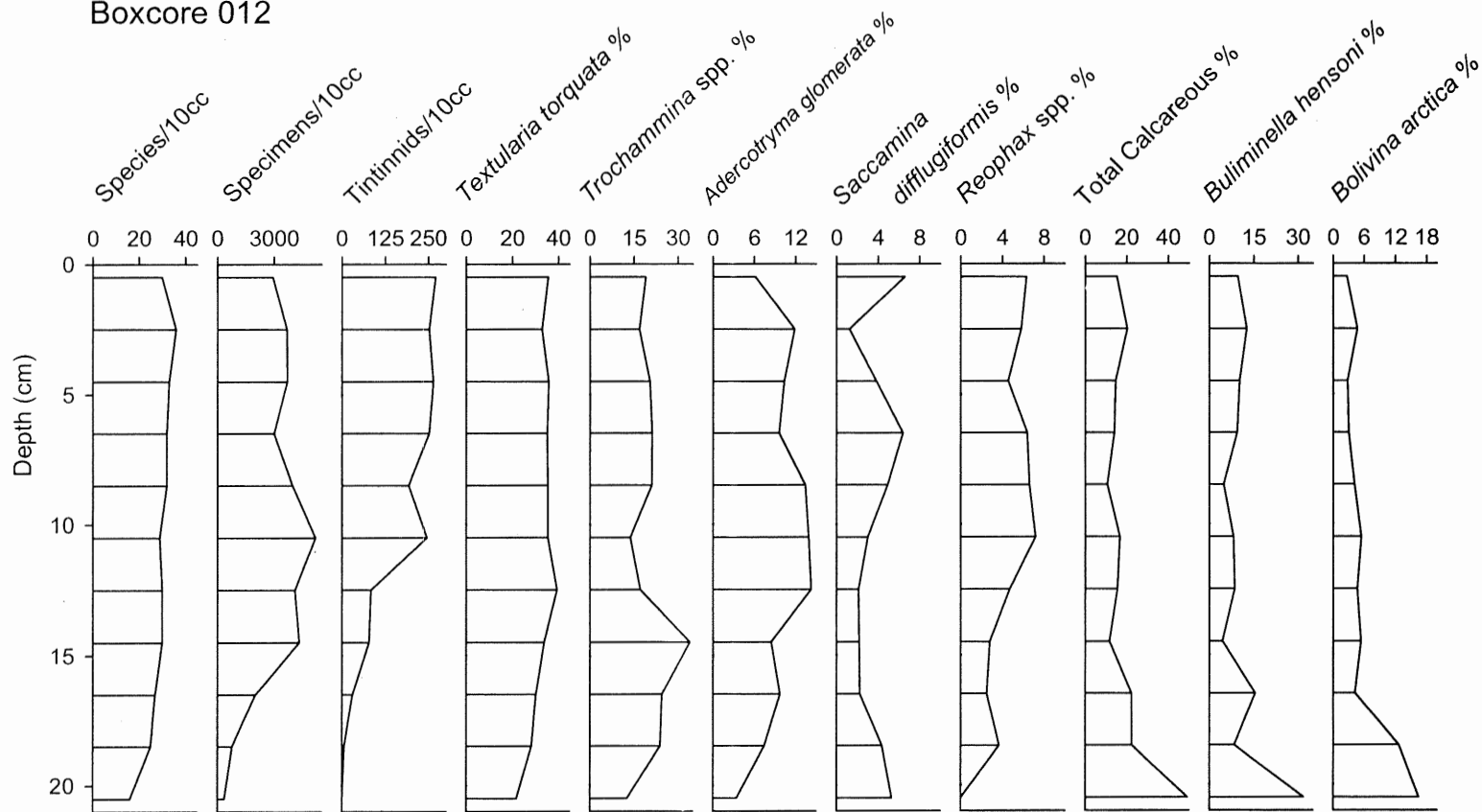


Fig. 4.7. The total number of species, specimens and tintinnids per 10 cm³, and relative fractional abundances (% of the total) for abundant or indicator species and total calcareous species as a function of depth for boxcore 012.

decreases to 239 in the bottom sample. The total number of tintinnids per 10 cm³ is nearly 300 at the top of the core, and from 10.5 cm to the end of the core the numbers decline to zero (Fig. 4.7). The average percent total number of calcareous specimens is 19.5 %, indicating that agglutinated fauna dominate the assemblage throughout the core. *Textularia torquata* and *Trochammina* spp. are the most abundant agglutinated species, the values of which are consistent through the core, with an average of 32 % and 20 % respectively. The minor agglutinated species, represented by *Adercotryma glomerata*, *Saccamina difflugiformis*, and *Reophax* spp., are somewhat variable through the core, each less than 20 % of the total (Fig. 4.7). The calcareous species range from 10 to 50 % of the total through the core, where the highest counts are at the bottom of the core (Fig. 4.7). The percent total calcareous species are primarily represented by *Buliminella hensoni* and *Bolivia arctica*, and also contain low abundances (< 1 %) of *Stetsonia arctica*, *Cyclogyra involvens*, and *Buccella frigida*. Although the proportion of total calcareous specimens reaches 20 %, these small species did not yield enough carbonate per sampling interval (> 1 mg) needed for a radiocarbon date.

4.4 Foraminiferal Assemblage Numerical Analyses – Amundsen Gulf

A total of 60 species (Appendix D) and 85 samples (Appendix B) were used in the Q-mode cluster analysis. Four species were removed due to high standard errors, and sample 109-6.5 (core 109, 6.5 cm) was removed due to small sample size. The cluster analysis has divided 96.5 % of the samples into four distinct groups based on their species assemblages, as demonstrated by the dendrogram (Fig. 4.8). The two main clusters are located at the top of the dendrogram, indicating they contain the samples with

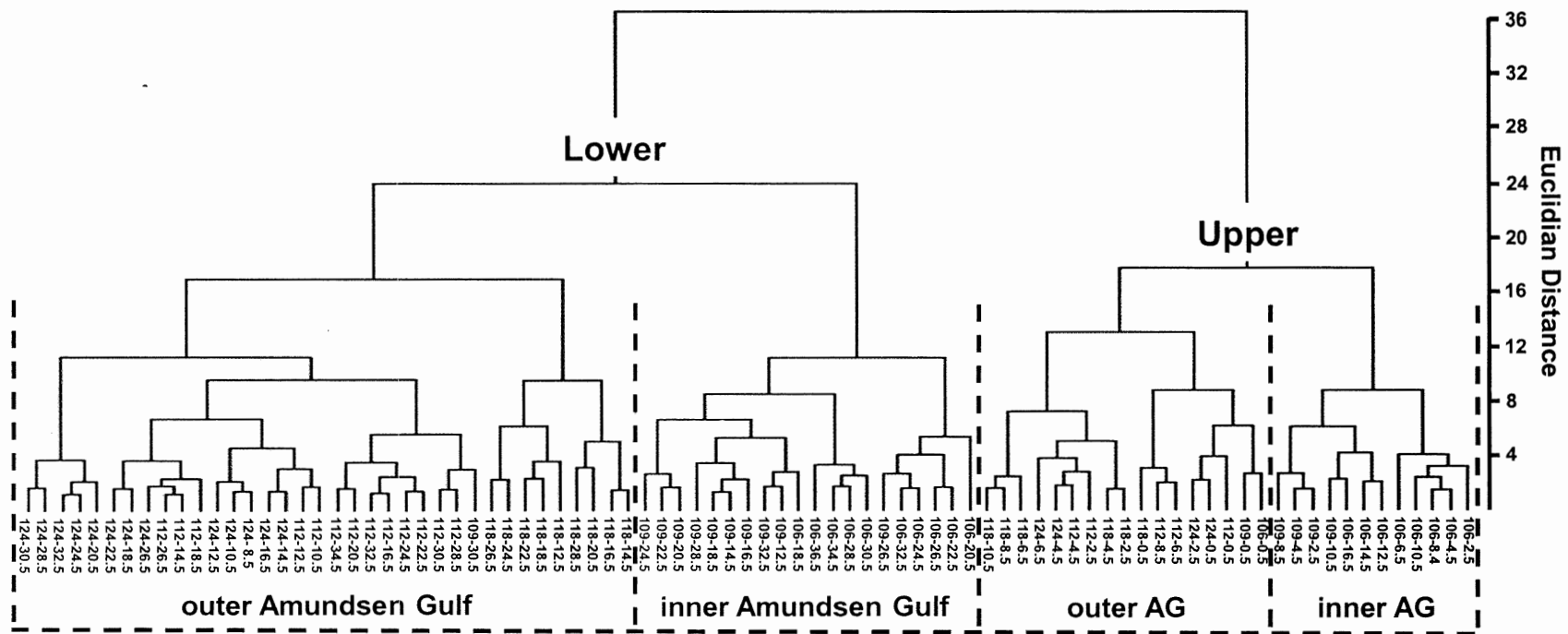


Fig. 4.8. Dendrogram produced by the Q-mode cluster analysis based on 60 species and 85 specimens. Four distinct clusters are identified as upper and lower sections of each core, and inner and outer Amundsen Gulf within the ice cover clusters.

the greatest dissimilarity. These two clusters, labelled Upper and Lower, divide all of the samples into an upper and lower section of each core, the upper section ranging from 6.5 to 16.5 cm (average 10.5 cm) of the total core length. The SIMPER analysis (Table 4.3a) provides the foraminiferal species assemblage responsible for the two main clusters (upper/lower) identified in the dendrogram. The species contributing to the similarity within the upper section assemblage consist of agglutinated fauna including *Trochammina* spp., *Bathysiphon rufus*, and *Textularia earlandi*, as well as other minor species. The species contributing to the lower section assemblage consist of the species listed above, as well as the calcareous species *Buliminella hensoni* and *Stetsonia arctica*. The species *Buliminella hensoni*, *Stetsonia arctica*, and *Neogloboquadrina pachyderma* are the most discriminating in their contribution to creating the two clusters, due to their large increases in abundance proceeding down each core from the upper to lower sections.

Also shown in the dendrogram (Fig. 4.8), are two clusters nested within both the Upper and Lower clusters. Except for the surface samples, all of the samples are subdivided into groups representing the inner Amundsen Gulf (toward NWT; cores 106, 109) and outer Amundsen Gulf (toward Beaufort Sea; core 112, 118, 124). A second SIMPER analysis (Table 4.3b) designates *Bathysiphon rufus*, *Buliminella hensoni*, *Stetsonia arctica*, and *Neogloboquadrina pachyderma* as the greatest contributors to the distinction between samples due to the large difference in mean fractional abundance of these species between the two groups. Three samples did not divide into their proper groups; 106-0.5 and 109-0.5 are grouped with the other surface samples, and 109-30.5 is grouped with the outer AG.

Table 4.3. Results of the SIMPER analysis listing the similarity within groups created by the Q-mode analysis. Dissimilarity is also shown between the (a) upper and lower sections, and (b) inner and outer Amundsen Gulf.

Species	Upper Section		Lower Section		Upper and Lower Section Difference % Dissimilarity
	Mean Fractional Abundance	% Similarity	Mean Fractional Abundance	% Similarity	
<i>Trochammina globogeriniformis</i>	16.88	12.83	13.81	10.46	2.50
<i>Bathysiphon rufus</i>	18.78	11.52	12.67	8.02	5.84
<i>Textularia earlandi</i>	12.20	9.78	8.82	8.05	3.23
<i>Trochammina nitida</i>	8.87	8.98	7.21	7.25	2.37
<i>Trochammina nana</i>	7.83	8.58	6.99	7.31	*
<i>Saccammina difflugiformis</i>	7.93	7.43	3.57	4.75	3.83
<i>Recurvoides turbinatus</i>	4.01	5.62	1.29	2.83	3.12
<i>Bolivina arctica</i>	3.60	5.61	3.09	4.76	*
<i>Buliminella hensoni</i>	5.10	3.73	17.23	10.62	8.29
<i>Rhizammina algaeformis</i>	3.37	3.78	0.11	*	5.23
<i>Reophax guttifer</i>	2.27	3.18	0.31	*	3.38
<i>Glomospira gordialis</i>	1.04	2.88	0.78	*	*
<i>Eggerella advena</i>	0.69	2.15	0.69	*	*
<i>Stetsonia arctica</i>	0.70	*	7.91	6.76	7.61
<i>Neogloboquadrina pachyderma</i>	0.05	*	4.66	4.48	6.46
<i>Cassidulina reniforme</i>	0.15	*	3.03	3.84	4.93
<i>Trochammina pseudoinflata</i>	0.50	*	0.83	2.06	*
<i>Islandiella teretis</i>	0.11	*	0.99	2.05	2.56
<i>Buccella frigid</i>	0.08	*	0.71	*	2.27

Species	Inner Amundsen Gulf		Outer Amundsen Gulf		Inner and Outer AG Difference % Dissimilarity
	Mean Fractional Abundance	% Similarity	Mean Fractional Abundance	% Similarity	
<i>Bathysiphon rufus</i>	24.19	14.54	8.15	7.38	8.46
<i>Trochammina globogeriniformis</i>	15.35	12.15	14.51	11.16	2.61
<i>Trochammina nana</i>	8.53	9.11	6.40	7.34	2.31
<i>Trochammina nitida</i>	8.09	8.31	7.55	7.84	2.53
<i>Textularia earlandi</i>	7.05	8.19	12.02	9.72	3.63
<i>Saccammina difflugiformis</i>	7.00	7.27	3.7	4.73	3.84
<i>Buliminella hensoni</i>	7.01	5.42	17.35	10.23	7.85
<i>Bolivina arctica</i>	2.98	5.07	3.46	5.33	*
<i>Recurvoides turbinatus</i>	2.78	4.14	1.82	3.19	2.55
<i>Stetsonia arctica</i>	3.17	2.64	7.05	4.95	6.13
<i>Glomospira gordialis</i>	0.96	2.40	0.81	2.11	*
<i>Eggerella advena</i>	1.01	2.47	0.47	*	*
<i>Textularia torquata</i>	0.30	*	1.36	3.13	2.76
<i>Cassidulina reniforme</i>	0.83	*	2.90	2.95	4.23
<i>Neogloboquadrina pachyderma</i>	2.32	*	3.63	2.54	5.03
<i>Cyclogyra involvens</i>	0.59	*	0.71	2.13	*
<i>Trochammina pseudoinflata</i>	0.59	*	0.80	2.02	*
<i>Rhizammina algaeformis</i>	1.51	*	1.02	*	3.56
<i>Reophax guttifer</i>	0.70	*	1.18	*	2.67
<i>Reophax ovicula</i>	0.66	*	0.12	*	2.02

4.5 $\delta^{18}\text{O}$ and $\delta^{13}\text{C}$ of Foraminifera – Amundsen Gulf

The $\delta^{13}\text{C}$ and $\delta^{18}\text{O}$ values for *I. teretis* and Npl are listed in Table 4.4, and plotted when available in Figs. 4.2-4.6. Samples available in cores 106, 109 and 118 are intermittent due to low numbers of specimens, and the $\delta^{13}\text{C}$ and $\delta^{18}\text{O}$ values within each core have a range of < 0.2 ‰. Since the analytical error is ~ 0.05 ‰, they are analytically significant values. Cores 112 and 124 contain the most complete records with some significant variation in their $\delta^{13}\text{C}$ and $\delta^{18}\text{O}$ values. The differences in $\delta^{13}\text{C}$ of both planktics and benthics and the $\delta^{18}\text{O}$ of the benthics in core 112 reach 0.2 ‰, while the difference in planktic $\delta^{18}\text{O}$ values is 0.64 ‰. The planktic $\delta^{13}\text{C}$ and $\delta^{18}\text{O}$ values from core 124 have a range of 0.4 ‰, while the benthic $\delta^{13}\text{C}$ and $\delta^{18}\text{O}$ range < 0.2 ‰. Due to the limited number of non-dissolving, clean foraminiferal tests and therefore number of samples, it is difficult to distinguish any patterns within and among cores, and to correlate them with the abundance data. The stable isotope records in core 112 and 124 vary similarly but not concurrently with the abundances of tintinnids and calcareous species shown in Figs. 4.2-4.6.

Table 4.4. Stable oxygen and carbon isotope values in cores 106, 109, 112, 118, 124 for (a) *Neogloboquadrina pachyderma* (b) *Islandiella teretis*.

<i>Neogloboquadrina pachyderma</i>										
Table 4.4a										
Midpoint (cm)	Oxygen Isotopes					Carbon Isotopes				
	106	109	112	118	124	106	109	112	118	124
0.5										
2.5										
4.5										
6.5										
8.5					1.66					0.65
10.5			1.51		1.33			0.84		0.87
12.5		1.72	0.92		1.76		0.86	0.75		0.88
14.5			1.51		1.28			0.82		0.63
16.5		1.44	1.49	1.96	1.28		0.84	0.88	0.48	0.45
18.5	1.01	1.31	1.59			0.88	0.78	0.84		
20.5				1.61	1.53				0.81	0.74
22.5			1.67					0.65		
24.5			1.66					0.76		
26.5			0.99		1.49			0.83		0.79
28.5	1.47		1.34	2.15	1.59	0.86		0.85	0.88	0.78
30.5	1.58	1.92	1.22		1.50	0.89	0.82	0.85		0.83
32.5	1.75	1.69	1.66		1.58	0.81	0.81	0.65		0.74
34.5	1.43					0.83				
36.5										
<i>Islandiella teretis</i>										
Table 4.4b										
Midpoint (cm)	Oxygen Isotopes					Carbon Isotopes				
	106	109	112	118	124	106	109	112	118	124
0.5										
2.5										
4.5										
6.5										
8.5					4.00					-0.05
10.5			3.56		3.96			-0.08		-0.04
12.5			3.28					-0.14		
14.5					3.91					-0.20
16.5			3.62	3.78				-0.12	-0.15	
18.5			3.90					-0.12		
20.5				3.66					-0.20	
22.5										
24.5										
26.5										
28.5			3.92	3.88	4.01			-0.17	-0.01	-0.07
30.5			3.90		3.89			-0.14		-0.07
32.5										
34.5					-0.12					0.16
36.5			-0.64					0.09		

Chapter 5 - Discussion

5.1 Amundsen Gulf

The objectives of this thesis were to: (1) determine the foraminiferal species assemblages associated with seasonal or perennial ice cover within this area of the Arctic; (2) associate differences among foraminiferal assemblages with their collection locations in Amundsen Gulf; (3) align cores temporally based on similarities in foraminiferal species assemblages and determine core chronology based on radiocarbon and ^{210}Pb dating, and; (4) interpret the local variability in foraminiferal assemblages and their stable isotopes in the context of known regional oceanographic changes and climate oscillations.

5.1.1 Objective 1: Foraminiferal Species Assemblages Associated with Sea Ice Cover

The cluster analysis identified two main groups which are associated with the upper and lower halves of each core, and are viewed schematically in Fig. 5.1. The SIMPER analysis (Table 4.3a) identified the abundance of calcareous species (*Buliminella hensoni*, *Stetsonia arctica*) in the lower halves of each core as the species responsible for the dissimilarity between the two groups (Figs. 4.2-4.6). The disappearance of calcareous foraminifera within each core may be caused either by dissolution or that they could not form within acidic conditions created by the increase in carbonic acid from reducing organic matter settling from plankton blooms in the open water (Hald and Steinsund, 1996). Evidence of etching and partially dissolved calcareous foraminifera also supported the hypothesis of acidic conditions during the relatively

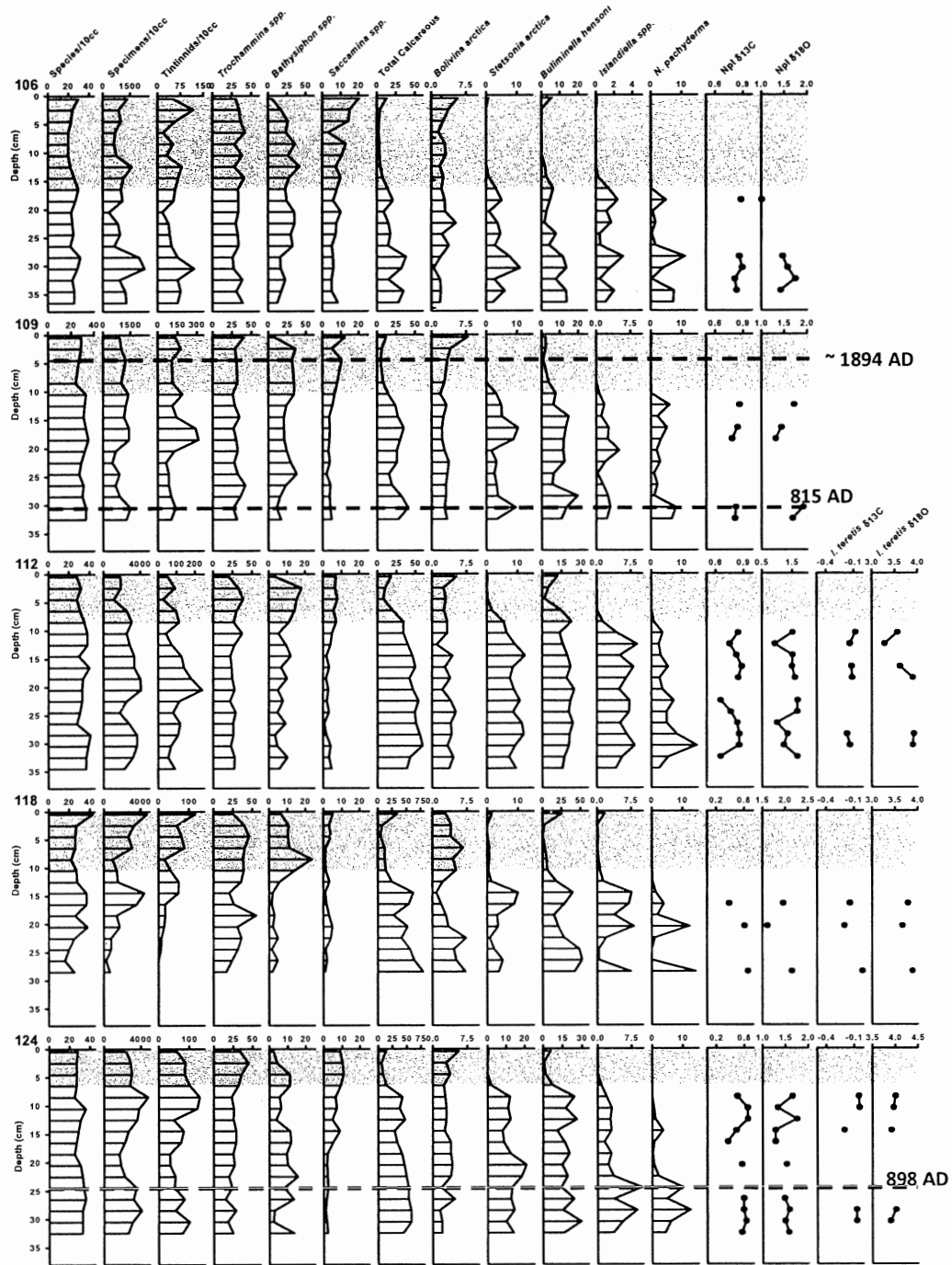


Fig. 5.1. The foraminiferal and isotopic profiles for all five cores as displayed in Figs. 3.2-3.6, with a visual representation of the two groups (upper and lower sections of each core) produced by the hierarchical clustering. Also plotted are the dates produced by the radiometric analyses in cores 109 and 124.

recent stanza. The top half of each of the five cores would then be represented by a seasonal ice cover proxy assemblage, which is nearly all composed of agglutinated species (*Trochammina* spp., *Bathysiphon rufus*, *Textularia earlandi*). The calcareous species would have been preserved due to reduced primary productivity in the water column during persistent ice cover (Wollenburg and Kuhnt, 2000; Carmack et al., 2004). This perennial ice-cover foraminiferal species assemblage is similar to that recovered by Scott et al., (2009) from piston core 124 at 12 ka, which may be associated with the beginning of deglaciation of the Amundsen Gulf. The cluster analysis has therefore identified a transition in ice cover from perennial to seasonal in each of the five cores along the transect through the Amundsen Gulf. This transition, which occurs in all five cores, is at different depths of each core, suggesting variable sedimentation rates at each core location.

The transition represents a disappearance of calcareous species due to dissolution, occurring in most calcareous species. Abundances of *Bolivina arctica* appear to be unaffected, however this species has been known to be particularly resistant to dissolution (Ishman et al., 1996). Not all of the *Buliminella hensoni* disappear in the cores, although reductions from 80-100% occur (Figs. 3.2-3.6). It is not known why these species may be resistant or somewhat resistant to dissolution. However, it is interesting that these species are mostly (over 85%) small (45-63 μm) in size. Other discrepancies in the statistical data include the placement of some of the samples within the hierarchical clustering.

Similar to the perennial-seasonal ice cover boundary identified by the foraminiferal clustering, there is a visually identifiable signal in the photographs of each

core as the transition from light to dark coloured mud (core photos-Appendix A). It is difficult however to correlate the two boundaries due to the gradient in colour, perhaps due to bioturbation. Therefore, it is possible that the dark mud in the seasonally ice-covered section of each core may be the organic matter from the increase in primary productivity during plankton blooms within summer's open sea (Arrigo and vanDijken, 2004). However, this hypothesis can only be confirmed with the organic content of the sediments. Piston core 124, which was investigated by Scott et al., (2009), had been analysed for %C_{org} at 10 cm intervals. There was a decreasing trend in the organic carbon content over the length of boxcore 124 (33.5 cm), although this could also be due to remineralization of organic matter with time (Meyers, 1997). Despite the uncertainties associated with the visual evidence for a potential perennial-seasonal shift in ice cover, the relative abundances and species compositions (Fig. 5.1) imply a change in sea ice cover that was consistent across the five areas sampled.

5.1.2 Objective 2: Foraminiferal Assemblages Associated with Core Location

The hierarchical clustering created two groups within each of the sea-ice groups: the inner (toward NWT; cores 106, 109) and outer (toward Beaufort Sea; cores 112, 118, 124) Amundsen Gulf (Fig. 4.8, Table 4.3b). The SIMPER analyses provided the foraminiferal species that account for the greatest dissimilarity, created by the large differences in the fractional abundances of these species, as well in the total number of specimens in each sample of each core. All of the surface samples are grouped within the outer Amundsen Gulf group, indicating their species assemblages are similar to one another.

In the Arctic, total numbers of foraminifera are dependent on the availability of food (Wollenburg and Kuhnt, 2000). The open water and continual production of sea ice in the flaw lead drives the upwelling of cold, saline, nutrient-rich waters up from the deep Arctic into the Amundsen Gulf (Arrigo and vanDijken, 2004; Conlan et al., 2008). These conditions produce a favourable environment for autotrophic fauna within the outer Amundsen Gulf, which is the trophic resource (food) for the heterotrophic foraminifera (Wollenburg et al., 2000). During perennial ice cover, the Beaufort undercurrent could have supplied the nutrient-rich Pacific water necessary for autotrophy, possibly diminishing in abundance as it reached the inner Gulf. There wouldn't be as much food during perennial ice cover and therefore produce fewer foraminifera, however the presence of calcareous foraminifera could offset that loss. The core sites of the inner Amundsen Gulf (106, 109) are the deepest, indicating a negative relationship between the total numbers of specimens and depth. Therefore both factors affect foraminiferal abundance due to the inverse relationship between available food and depth (Wollenburg et al., 2000). This relationship has also been observed between two cores from the Amundsen Gulf analysed by Schell et al. (2008), where the shallow site (CA-06, 253 m) contained up to 8000 specimens, and the deep site (CA-18, 600 m) only contained up to 600 specimens. The depth of core 112 however is not that different from the depth of core 106. The bathymetry of the Amundsen Gulf, as revealed by the 3-D image (Fig. 2.1) and by the bathymetry, backscatter and sub-bottom profiles for each cored location in Appendix A, is quite variable. Therefore, one potential, but untested hypothesis to explain these site-to-site variations in abundance is that this uneven surface may produce micro-scale variability in the bottom water environments for benthic communities across

the Amundsen Gulf that are unresolved using the average temperature, depth, and salinity measurements recorded (Table 3.1).

5.1.3 Objective 3: Chronology and Correlation among Cores

Radiocarbon and lead-210 measurements allowed the setting of chronological constraints in core 109. At the bottom of the core (31 cm), an age of 814 cal years AD was calculated from the ^{14}C measurement, and since unsupported lead-210 reaches 5 cm, it suggests that the top 5 cm span the last century (Fig. 5.1). Since the ^{210}Pb activities of the top two cm of core 109 are not significantly different, mixing occurred in the top two cm. The ^{210}Pb reaches a constant value below 5 cm, suggesting that the samples consist of the supported fraction of ^{210}Pb , which is confirmed by the fact that the ^{226}Rn is in secular equilibrium with the ^{210}Pb . The higher supported ^{210}Pb values of intervals 16-23 cm would require a change in the source of sedimentation influx, consisting of an increase in concentration of the mother elements to ^{210}Pb . For example, an increase in the input of ^{230}Th -rich clays would cause the supported ^{210}Pb to attain a higher value. Deciphering the intervals within this profile would require further radiometric and isotopic analyses. The sedimentation rates estimated from each of the ^{14}C and ^{210}Pb dates are not similar, suggesting variable sedimentation rates between 814 AD and the last century, which is confirmed by the changes in the supported ^{210}Pb values.

The timing of the foraminiferal (ice regime) transition in core 109 is constrained to occur between 815 AD and 1894 AD. This is also the timing of the transitions in all the cores in the transect, assuming that the change in ice regime represents the same event among all five cores. The radiocarbon date at 24.5 cm in core 124 of 897 AD represents

a similar time frame to core 109, indicating that the change in ice regime is most likely the same event in both cores.

5.1.4 Objective 4: Correlation of Foraminiferal and Isotopic Events with External Factors

According to the foraminiferal species assemblages, the Amundsen Gulf has been seasonally ice-covered since at least 1894 AD. Seasonal ice cover in this area during the last 30 years is confirmed with satellite data (Galley et al., 2008), and during the last 150 years confirmed by the Franklin expedition in 1850 AD (Pharand, 1984). Other climate proxies, such as pollen, tree ring widths, diatoms and chrysophytes (algae), chironomids (insects), cladocera (crustaceans), ice core melt, and varve thicknesses reconstructed from Arctic regions suggest that climate warming since 1850 AD is unprecedented (Overpeck et al., 1997; Smol et al., 2005). The presence of calcareous foraminifera in samples of the bottom half of each core analyzed here suggests that the Amundsen Gulf has been perennially ice-covered during 815 ± 140 AD, and for some time thereafter. The period of perennial ice cover corresponds to the cooling that occurred after the Holocene Climate Optimum called the neoglacial cooling. Perennial sea ice would have therefore persisted within the Amundsen Gulf during two climate anomalies of the neoglacial cooling: the Little Ice Age (LIA, ~1550-1750 AD, Bradley and Jones, 2003), and more interestingly, the Medieval Warm Period (MWP, ~900-1200 AD, Hughes and Diaz, 1994). The MWP is a warm climate anomaly observed in various proxy records throughout Europe and North America (Bradley et al., 2003).

The variability of the calcareous species abundances, specifically *Neogloboquadrina pachyderma* and *Islandiella tereris*, and their stable isotope values suggest variability in the oceanographic and sea ice conditions within the Amundsen Gulf during the prolonged period of perennial ice cover. The variability in abundances and isotope values, without dating in all cores, however, does not appear consistent among them. The planktic and benthic $\delta^{18}\text{O}$ and $\delta^{13}\text{C}$ records for cores 112 and 124 display fluctuations, where certain intervals appear to be negatively shifted (Table 4.4, Figs. 3.4, 3.6). Depleted values could be caused by periods of decreased ice cover, perhaps as a result of the opening of the flaw lead. Open water creates upwelling of nutrient-rich, depleted $\delta^{13}\text{C}_{\text{DIC}}$, which would decrease the $\delta^{13}\text{C}$ values, similarly to increases in primary productivity fluxes to the ocean floor with ice-free conditions (Ravelo and Hillaire-Marcel, 2008). Warmer, low salinity waters during sea ice melt in summers as well as the increase in depleted brines during sea ice production in winters would decrease $\delta^{18}\text{O}$ values. Increases in $\delta^{18}\text{O}$ -depleted land-derived freshwater, as shown by the increase in tintinnids in core 112 (Fig. 3.4) during warmer climates would also decrease planktic $\delta^{18}\text{O}$. Decreases in isotopic values and total calcareous foraminifera, and increases in tintinnids suggest short periods of seasonally open water, ice breakup, or the presence of the flaw lead. Although core 112 does not contain a radiocarbon date, these unstable ice conditions could reflect warmer climates of the MWP.

Recent satellite observations have revealed that a reduction in sea ice extent may not be coupled to atmospheric warming in all areas of the Arctic at any given time, but rather may reflect a divergence of sea ice (Howell et al., 2008). For example, a recent decline in sea ice extent has occurred across the Arctic, but is more pronounced in the

eastern Arctic than the western Arctic (Rigor et al., 2002). Rigor et al. (2002) attribute the decline to the diverging sea ice motion in the Eastern Arctic, which is predominantly cyclonic due to the westward movement of the Transpolar Drift (TPD). In the western Arctic, the anticyclonic motion of the ice pack within the Beaufort Gyre causes divergence along its edge, allowing seasonal ice breakup, thinning and thermodynamic melting, as well as further ice production (Galley et al., 2008). However, during summer reversals of the Beaufort Gyre (BG), multi-year ice is driven into the entrance of the Amundsen Gulf, increasing its amount of perennial ice, reducing the amount of open water, and providing cooler conditions (Galley et al., 2008). The variability in sea ice movement has been correlated with the multi-year to multi-decadal AO oscillations over the last few millennia (Mysak, 2001), specifically the MWP was driven by a persistently positive AO index similarly to recent decades (Trouet et al., 2009). Analyses of the Amundsen Gulf cores indicate seasonal ice cover during the recent century, the presence of perennial sea ice cover during the LIA, with perhaps periods of open water during the MWP. Although the MWP and recent climate are associated with similar atmospheric conditions, the current results indicate that the MWP did not produce seasonal ice cover similar to recent decades.

It has been suggested that the extreme losses in sea ice of the last two decades are no longer controlled by AO, but rather local thermodynamic processes (Lindsay and Zhang, 2005). Howell et al. (2008) suggest that the Arctic Ocean's response to warming may not be directly coupled to the atmosphere, and persistent increases in air temperature may not melt persistent sea ice cover. These findings could support the presence of sea ice in the Amundsen Gulf during a potentially warmer MWP. The differences in sea ice

conditions between the two periods of warmer climate within the Amundsen Gulf indicate that there may be more than oscillating climatic regimes controlling today's sea ice extent. Models have shown that solar and volcanic variance are not the only controls on sea ice in the Arctic today, and that the increase in warming is anthropogenically induced (Bertrand et al., 2002; Mann, 2007).

Records of past oceanographic currents also assist in determining the probability of the formation of sea ice. Utilizing both surface-dwelling dinoflagellates and subsurface-dwelling planktic foraminifera, de Vernal et al. (2005) demonstrated that during the early Holocene, surface conditions were decoupled from their respective subsurface conditions. Within the Chukchi Sea, an influx of warm, saline Atlantic water stratified with low salinity surface water produced a strong halocline and extensive sea ice cover by reducing the amount of the heat transfer to the surface. Increased influx of Atlantic and freshwater during the persistent positive AO of the MWP (Mysak, 2001; Trouet et al., 2009) could have stratified the Amundsen Gulf and increased sea ice production, indicating a decoupling of surface and subsurface water masses. De Vernal et al. (2005) also demonstrated persistent sea ice, decreasing salinity, and stable sea surface salinities during the last millennium within the Chukchi Sea cores, with slight interannual variability.

There are relatively few paleoceanographic sediment records extending into the last millennium from the Western Canadian Arctic Archipelago with which to compare the current results. Therefore, archaeological collections and interpretations are another useful source of information. Dyke et al. (1996) reported an absence of bowhead whale bones over the last 3000 years within the Archipelago, indicating an absence of summer

sea ice breakup. However, bowhead whale bones were found within the Eastern Canadian Arctic at 1.0 cal ka BP, corresponding to Thule migration during the MWP (Dyke et al., 1996). Thule sites containing whale bones are present on the northern mainland coast of the Northwest Territories, and Banks and Victoria Islands around 0.75-1.25 cal ka BP (Dyke et al., 1996; Dyke and Savelle, 2001). Their presence indicates ice-free waters between the coast and the Beaufort pack ice, which may represent ice-free summers within the Amundsen Gulf, the flaw lead system, or melting along the coast. Richerol et al. (2008) have assessed the sea surface temperature (SST) and sea ice history of the Beaufort Sea during the last several hundred years using dinoflagellate cyst assemblages. Their reconstructions indicate an increase in productivity, SST and ice cover, and decrease in salinity prior to the onset of the LIA. These trends abated upon the onset of the Anthropocene, and were heavily influenced by the Mackenzie River (Richerol et al., 2008). These few paleoceanographic records from the Western Canadian Arctic suggest periods of seasonal sea ice during the neoglacial cooling. However, they are variable in timing and length, and suggest that the trends may be a regional effect. Variability in sea ice cover is observed within the transect of Amundsen Gulf cores, as the seasonal and perennial ice covered periods, as well as the variability in the calcareous foraminiferal abundances and stable isotope values.

Paleoclimate proxy records created with diatom assemblages from areas surrounding the Amundsen Gulf, demonstrate the climate oscillations of the Anthropocene, LIA, and MWP (Joint and Wolfe, 2001; LeBlanc et al., 2004; Podrisky and Gajewski, 2007). Their reconstructions indicate a MWP that was nearly as warm or warmer than the Anthropocene. The Devon and Agassiz ice core oxygen isotopes and ice

melt records indicate that the last 1000 years have experienced the coldest and driest summers of the Holocene (Koerner and Fisher, 1990). The cooler climate was preceded however by temperatures as warm as during the last 100 summers. There is conflicting evidence, however, of the degree to which the MWP warmed, and for the geographic locations of such warming (Bradley et al., 2003). The transect of Amundsen Gulf cores examined here demonstrate variability in sea ice cover during the period of perennial ice cover as shown by the calcareous foraminiferal abundances and stable isotopes. Periods of seasonal ice cover during the MWP would have manifested as an absence of calcareous foraminifera. Therefore, the oceanographic conditions during the last millennium, based on proxies such as foraminifera, may not reflect the effect of changes in temperature and precipitation recreated by the land-based proxies, including diatoms:

The foraminiferal species assemblages within five cores through the Amundsen Gulf are clearly temporally distributed between two clusters spanning the last millennium, defined by a period of perennial ice cover followed by a period of seasonal ice cover for at least a century. Within those two ice regimes, the samples are clustered spatially between the inner and outer Amundsen Gulf. Higher numbers of foraminiferal specimens characterize the outer Amundsen Gulf cores, likely due to higher trophic resources caused by increased upwelled nutrients and shallower depths. Plankton blooms that occur during seasonally open waters in the Amundsen Gulf that would produce the food required for the agglutinated foraminifera, also created the corrosive conditions that dissolved the calcareous species or prevented them from forming. During the period of perennial ice cover, the calcareous foraminifera are preserved, but have been variable in abundance. Also variable are the planktic and benthic $\delta^{18}\text{O}$ and $\delta^{13}\text{C}$ values, specifically

in cores 112 and 124. Their depleted values could be caused by periods of decreased ice cover, warmer and fresher waters, as well as sea ice production, perhaps as a result of the opening of the flaw lead. Radiocarbon dating suggests that these periods of less sea ice could have occurred during the MWP. If there were periods of open water, the foraminiferal assemblages indicate that it was for a short period of time. Other paleoceanographic records from the Western Canadian Arctic suggest more sea ice during the Late Holocene, until recent warming (Dyke et al., 1996; Schell et al., 2008; Scott et al., 2009), and increased Atlantic influx and stratification, which contributes to sea ice production (de Vernal et al., 2005). Lastly, the MWP is suggested to be correlated with the Arctic Oscillation, which brings the perennial ice pack closer to the North American coast and prevents extreme ice loss within the Amundsen Gulf (Galley et al., 2008). The recent, unprecedented warming likely has a significant role in the extreme loss in Arctic sea ice, which may explain for the presence of sea ice in the bottom sections of these Amundsen Gulf cores during a similar climate regime.

5.2 Viscount Melville Sound

The recent oceanographic conditions and sea ice cover within the VMS are revealed through the foraminiferal species assemblage and abundances through the core. A clear shift in the assemblage occurs between 20 and 15 cm, where the total number of specimens and tintinnids, and the fractional abundance of calcareous foraminifera decreases. As shown in the photograph and X-rays (Appendix A), the core contains IRD, as well as a void below 19 cm which may previously have held a large rock. The lack of undisturbed stratigraphy due to ice scours (Appendix A), the presence of IRD, and the

fact that only 24 cm of core was collected together suggest that the sediments within the core accumulated post ice scouring. Although dependant on the age of the sediments, the scours could be due to glacial ice during the last glacial period, or ice-bergs passing by shortly thereafter. The increase in foraminifera after the presence of extremely low numbers at the bottom of the core may be associated with decreasing sea ice thickness. However, since the core could not be dated, it is difficult to know when the scouring occurred. The following discussion illustrates the oceanographic circulation and sea ice conditions suggested through analyses of the VMS with foraminifera, as well as the possible age of the sediment within the core.

The foraminiferal species assemblage in core 012 shows some similarities and differences with assemblages from adjacent areas in the CAA. The VMS core consists of a predominantly agglutinated foraminiferal assemblage (approximately 80 %) (Fig. 3.7), and a total calcareous fraction of approximately 20 %. Phleger first sampled the CAA in 1952, and the surface samples were dominated by the agglutinated species *Trochammina nana* and *Adercotryma glomerata* within Baffin Bay, Lancaster Sound, and VMS (Fig. 1.2). These two species are also present in the VMS core as major and minor species, respectively. *Textularia torquata*, the most abundant species found in the current VMS core, also dominated assemblages in samples from Lancaster Sound, and was present in Phleger's Eastern CAA surface samples. The calcareous species collected by Phleger (1952) in the Eastern CAA were dominated by *Cassidulina (Islandiella) norcrossi*, *Cassidulina islandica* var *minuta* (*Cassidulina reniforme*), *Elphidium* spp., and *Cibicides lobatulus*. These calcareous species are not found within core 012, while the small < 63 µm deep water Arctic species *Buliminella hensoni* and *Bolivina arctica* are found in the

VMS core. Importantly, Phleger's foraminiferal assemblage was sampled only based on individuals $> 75 \mu\text{m}$, which may account for the differences in the calcareous species assemblages. A core from Jones Sound also contains a similar foraminiferal species assemblage as the 2006 VMS core with *Textularia torquata* as the primary agglutinated species, and since the samples were sieved to $45 \mu\text{m}$ they produced up to 70 % *Buliminella hensoni* (Mudie et al., 2006). Vilks (1989) also sampled various regions of the NWP and described it as barren, where over half of the samples consisted of very low numbers. Samples with sufficient numbers contained over 90 % calcareous fauna, mainly the shelf genera *Islandiella* and *Elphidium*, an assemblage not observed by either Phleger (1952) or within this study. Vilks (1989) sampled other areas of the CAA, including within the Queen Elizabeth Islands, and reported similar assemblages as Phleger (1952). The foraminiferal distribution of M'Clure Strait, sampled by Iqbal (1973) while ice covered, is dominated by calcareous species at the entrance to the strait, gradually changing to agglutinated moving into the strait. M'Clure Strait, until recently, has been ice covered with multi-year ice. These assemblages are dominated by *Trochammina nana*, *Cassidulina laevigata*, *Recurvoides contortus*, which except for the *Trochammina* sp., does not resemble the VMS assemblage.

The agglutinated assemblage from the Amundsen Gulf located 900 km southwest of VMS, differs greatly from that of the VMS. In the Amundsen Gulf, surface samples collected within the last decade were analysed by Scott et al. (2008), whereas longer records of sediment cores were analysed in this thesis, Schell et al. (2008), and Scott et al. (2009). Both areas contain an abundance of *Trochammina* spp., but the Amundsen Gulf contains less than 5 % *Textularia torquata*, while VMS contains up to 40 %.

Adercotryma glomerata is a minor species present up to 14 % throughout the VMS core, but is limited within the cores of the Amundsen Gulf with an average of 0.4 % (Appendix B).

In contrast, the calcareous species are similar between the two sites, dominated by *Buliminella hensoni* and *Bolivina arctica*. The Amundsen Gulf cores also contain an abundance of *Stetsonia arctica*, as well as lower numbers of *Islandiella teretis* and *Neogloboquadrina pachyderma*. These species only occur in < 1 % of the total assemblage of the 2006 VMS core.

While the agglutinated foraminiferal species assemblage in the VMS resembles that of the Eastern CAA rather than the Amundsen Gulf or M'Clure Strait, the calcareous foraminiferal species assemblage appears to vary with time or space. For example, the VMS has been surface sampled several times during the last 60 years, initially collecting several species of large calcareous foraminifera (Phleger 1952), a second sampling revealed an absence of calcareous foraminifera (Vilks, 1989), and the VMS core contains the small-sized Arctic bottom water calcareous foraminifera. The presence and abundance of the deep Arctic calcareous species *Buliminella hensoni* indicates deep Arctic water is coming up and residing below the Atlantic water layer (Scott and Vilks, 1991; Mudie et al., 2006; Scott et al., 2008). The agglutinated foraminiferal assemblage of the VMS resembles those from the Eastern CAA rather than the Amundsen Gulf or M'Clure Strait in the west. The assemblages are associated with the water mass in which they reside, where the entrance of M'Clure Strait and the central Amundsen Gulf contain Beaufort Sea – Atlantic water, and the inner M'Clure Strait to Lancaster Sound and other areas of the CAA contain Baffin Bay – Atlantic water. The presence of calcareous

genera *Cassidulina*, *Islandiella*, and *Elphidium* indicates Atlantic shelf waters throughout the CAA. This assessment was similarly noted by Vilks (1989). He also demonstrated with plankton tows within Parry Channel that the number of planktics decreases with distance moving west through Lancaster Sound and Barrow Strait, and moving east through M'Clure Strait and Viscount Melville Sound. He attributed the decrease to sills within the NWP, specifically in Barrow Strait, that create a restriction in the movement of bottom water masses from entering the centre of the NWP. Mean ocean current velocities through the NWP are directed from the Arctic Ocean eastward to Baffin Bay due to differences in atmospheric and sea-level pressures (Prinsenber and Pettipas, 2008). However, Baffin Bay bottom water flows westward along the northern coast of Barrow Strait, with a strong current below 80 m during the winter months (Prinsenber and Pettipas, 2008). Vilks (1989) indicates that the sills in Barrow Strait prevent Baffin Bay water from further flowing into VMS, however the presence of Eastern Arctic fauna within the VMS core indicates some flow is reaching beyond the sill.

The change in the calcareous foraminiferal abundance within the bottom of the core, suggests changes in the benthic environment. The percent total calcareous foraminifera decreases from ~ 40 to 20 % from 20.5 to 14.5 cm, which is coupled with a large increase in total number of specimens from 300 to more than 5000. There is also an increase in the total number of tintinnids (freshwater indicator) at this level, from 0 to 246. The decrease in the abundance of calcareous fauna and increases in both total numbers of specimens and tintinnids indicate an increase in productivity and/or freshwater (Hald and Steinsund, 1996; Scott et al., 1995). These are indications of a continuous decrease in sea ice, perhaps from perennial to periods of open water.

Despite the evident changes in foraminifera and tintinnid abundances, it is difficult to know when this change in sea ice cover occurred since the core is not chronologically controlled. One could, however, compare this record to others of the NWP. The recent sedimentation rate in Barrow Strait is extrapolated from a radiocarbon date to be 7 yrs/cm (Vare et al., 2009) assuming constant sedimentation rates. Applying this rate to the VMS core would suggest a 145 year old core, extending through the Industrial Age. However, a radiocarbon dated core from Jones Sound contains a similar foraminiferal assemblage to the VMS core, suggesting VMS may as old as 4.5 cal ka B.P., (Mudie et al., 2006).

There are few paleoceanographic and paleo-sea ice records from the VMS and CAA. Since bowhead whales only occur within waters that are partially ice-covered, the presence of their bones is an indicator of seasonal sea ice (Dyke et al., 1996; Savelle et al., 2000). Radiocarbon-dated whale bones found within the CAA indicate several periods of seasonal ice cover prior to 8.0 ka B.P., and 2.5 - 5.5 ka B.P., suggesting perennial ice from 2.5 ka B.P. to present (Dyke et al., 1996; Savelle et al., 2000). Paleo-sea ice and sea-surface conditions have been however documented within the Eastern CAA. Sediments from northernmost Baffin Bay, Jones Sound, Lancaster Sound and Barrow Strait have been analysed for species assemblages of dinoflagellate cysts, foraminifera and diatoms (Levac et al., 2001; Mudie et al., 2005, 2006; Ledu et al., 2008; Vare et al., 2009). These records document a warm, seasonally ice-free climate from approximately 6 – 4 ka B.P., followed by continuous cooling until present, with evidence of large fluctuations.

An additional, historical source of comparative data comes from records of voyages into and through the NWP. Navigation through NWP has been attempted within the last 150 years. Various areas of the CAA were ice free during 1-2 months in summers ~ 1850 AD as reported by Sir John Franklin, but it wasn't until the early 20th century that the trip was completed by Roald Amundsen (Pharand, 1984). Although Amundsen's voyage in 1903-1906 AD brought him south just before the VMS core site to the east of Prince of Wales Island, historical accounts therefore suggest that if the VMS core is in fact 150 years old, it is possible that the foraminiferal assemblages indicate a change from perennial to seasonal sea ice cover. However, without chronological reference or a physically longer record in order to correlate with foraminifera from Jones Sound, it is difficult to pinpoint the timescale and correlate the cause of changes in foraminifera with any accuracy.

The sediment core collected in Viscount Melville Sound contains primarily an agglutinated foraminiferal assemblage (*Textularia torquata*, *Trochammina* spp.) with a small fraction (< 20 %) of small sized (45-63 μ m) calcareous species (*Buliminella hensoni*, *Bolivina arctica*). The agglutinated assemblage resembles other samples collected from the Eastern CAA, while the calcareous assemblage contains mainly Arctic deep water species, with few Atlantic shelf species as documented by others (Phleger, 1952; Vilks, 1989; Mudie et al., 2006). This indicates that Baffin Bay – Atlantic water is reaching the VMS, beyond the sill in Barrow Strait. A change in total foraminifera and species assemblage occurs at 14.5 cm, suggesting changes in sea ice cover. Without chronological control or a longer foraminiferal record, it is difficult to interpret any changes that have occurred throughout the core. Comparing the core to others within the

CAA then suggests that the change in the foraminiferal assemblage represents the transition from the end of the neoglacial cooling into the Industrial Age, ~ 150 years, as documented by early Arctic explorers, or a 4500 year old record similar to that of Jones Sound.

Chapter 6 - Conclusion

The oceanographic and sea-ice histories of the Amundsen Gulf (AG) and Viscount Melville Sound (VMS), both located within the Western Canadian Arctic Archipelago (CAA) were assessed in this thesis. Paleoceanographic records were produced using foraminiferal species assemblages from a transect spanning the AG (five boxcores), and a single boxcore from the VMS. It is difficult to know how the records from these two locations, separated by ~900 km, are chronologically correlated since the VMS core could not be radiometrically dated due to low numbers of small calcareous foraminifera. Additionally, the samples from these two locations cannot be correlated using foraminiferal assemblages since they contain different foraminiferal species assemblages. The VMS species assemblage more closely resembled those found in other areas of the Eastern CAA than those from the Amundsen Gulf and Western CAA.

All five cores within the Amundsen Gulf demonstrated a sharp transition from a calcareous (historic) to agglutinated (recent) foraminiferal assemblage, which I have interpreted as the transition from perennial to seasonal ice cover. ^{210}Pb dating of one of the transect cores suggests that this boundary occurred prior to 1894 AD, while radiocarbon dating indicates that the Gulf had been perennially ice-covered at least since ~ 800 AD. My confidence in these age estimations would have been increased with the dating of more cores. Ideally, both methods of radiometric dating would have been performed on all cores to chronologically correlate all five cores, and to identify the age of the shift in foraminiferal assemblages. Although the stable isotope data contribute to the dataset of values throughout the Arctic, more complete records would provide a better

account of the changes in oceanographic conditions in the Amundsen Gulf. Increased sediment volume and/or unlimited access to isotopic analyses could have led to more complete isotopic records among and within cores.

In retrospect, additional geochemical parameters may have been useful in determining the cause of changes in the foraminiferal assemblages. For example, total organic carbon down core could indicate the amount of primary productivity in the overlying water column, and carbonate content through each core could reflect the amount of dissolution among sites. Also, in my future foraminiferal research, I will certainly examine live-dead ratio analyses. Such an analysis is used in identifying which foraminifera are living at the surface (epifaunally) as well as further down core (infaunally). Methodologically, when sediment samples are stained with Rose Bengal immediately after collection, the living foraminifera incorporate the stain and can be differentiated from dead specimens of the same species. Important differences in habitat selection are species-specific and may be overlooked without such analyses. Unfortunately this staining procedure was not performed on the ship that collected the cores in 2004 due to logistical difficulties. Transfer functions, performed with other proxies such as diatoms, pollen and dinoflagellates, are another powerful tool in environmental reconstructions by relating known assemblages to their corresponding environmental parameters. If surface samples could have been collected below perennial ice cover—obviously limited by sampling inaccessibility—a transfer function could have been developed for the Amundsen Gulf corresponding to perennial ice conditions. Lastly, coupling several proxies, such as foraminiferal and dinoflagellate cyst

assemblages will certainly increase the validity of any reconstruction based on a single proxy.

Finally, in future research, in order to collect data on the time scales originally envisioned for these research questions, I will also examine sediment samples from piston cores. The boxcores examined here are all less than 40 cm long. Therefore, piston cores collected from those same locations could yield much longer records, perhaps up to 600 cm and representing perhaps >10000 years rather than 1000 years. For example, within the Amundsen Gulf, boxcore 124 was collected near the site of piston core 124, presented by Scott et al. (2009). The foraminiferal assemblages from that longer record indicate some variability in sea ice cover since the deglacial (12 ka). Sampling piston core 124 at finer resolution comparable to my intervals within boxcore 124 could create a similar high resolution (decadal to centennial scale) sea-ice history. Additionally, a piston core collected from the western end of the Northwest Passage (VMS area) may both increase the probability of successful radiocarbon dating by providing sufficient carbonate, and correlate temporally with the few records from the eastern Northwest Passage (e.g., Mudie et al., 2006; Ledu et al., 2008; Vare et al., 2009). Such comparisons would provide a more complete account of the spatio-temporal oceanographic and sea-ice history across the Northwest Passage. Finally, the VMS core has highlighted the necessity of chronological dating. Without strong foraminiferal species correlations among different sites, it is difficult or impossible to establish the rate of change of the species assemblages, or to correlate them with known changes in oceanography or sea ice based on other cores.

References

- Amiel, D., 2007. Terrestrial and marine POC fluxes derived from ^{234}Th distributions and $\delta^{13}\text{C}$ measurements on the Mackenzie River Shelf. PhD dissertation, Stony Brook University, 120 pp.
- Andersen, H.V., 1952. *Buccella*, a new genus of the rotalid foraminifera. *Journal of Washington Academy of Sciences* 42, 143-151.
- Anderson, G.J., 1963. Distribution patterns of recent foraminifera of the Bering Sea. *Micropaleontology*, 9 (3), 305-317, figs 1-12. pl 1.
- Arrigo, K.R., van Dijken, G.L., 2004. Annual cycles of sea ice and phytoplankton in Cape Bathurst polynya, southeastern Beaufort Sea, Canadian Arctic. *Geophysical Research Letters* 31, L08304, doi:10.1029/2003GL018978.
- Barber, D.G., Massom, R.A., 2007. The Role of Sea Ice in Arctic and Antarctic Polynyas processes. In W. O. Smith, & D. G. Barber (Eds), *Polynyas: Windows to The World*, 74, Elsevier Series in Oceanography, pp. 1–54.
- Barker, R.W., 1960. Taxonomic notes on the species figured by H.B. Brady in his report on the foraminifera dredged by *H.M.S. Challenger* during the years 1873-76. *Society of Economic Paleontology and Mineralogy, Special Publication* 9, 238 p., 114 pls.
- Bé, A.W.H., 1960. Some observations on the Arctic planktonic foraminifera. *Cushman Foundation for Foraminiferal Research, Contributions* 11, 64-68.
- Bergsten, H., 1994. Recent benthic foraminifera of a transect from the North Pole to Yermak Plateau, eastern central Arctic Ocean. *Marine Geology* 119, 252–267.
- Bertrand, C., Loutre, M.F., Crucifix, M., Berger, A., 2002. Climate of the last millennium: a sensitivity study. *Tellus* 54A, 221–244.
- Besonen, M.R., Patridge, W., Bradley, R.S., Francus, P., Stoner, J.S., Abbott, M.B., 2008. A record of climate over the last millennium based on varved lake sediments from the Canadian High Arctic. *The Holocene* 18 (1), 169–180.
- Bourgeois, J.C., Koerner, R.M., Alt, B.T., Fisher, D.A., 2000. Present and past environments inferred from Agassiz Ice Cap ice-core records. *Bulletin of the Geological Survey of Canada* 529, 271-282.
- Bradley, R.S. and Jones, P.D., 2003. “Little Ice Age” summer temperature variations: their nature and relevance to recent global warming trends. *The Holocene* 3 (4), 367-376.
- Bradley, R.S., Hughes, M.K., Diaz, H.F., 2003. Climate in Medieval Time. *Science* 302, 404–405.

Brady, H.B., 1871. On *Saccamina cateri*, a new foraminifera from the Carboniferous Limestone of Northumberland. *Annales and Magazines of Natural History* 7 ser. 4 (39), 177-184, pl 12.

Brady, H.B., 1878. On the reticularian and radiolarian Rhizopoda (Foraminifera and Polycystina) of North Polar Expedition of 1875-76. *Annales and Magazine of Natural History* 1 (5), 425-440, pl. 20-21.

Brady, H.B., 1879. Notes on some of the Reticularian Rhizopoda of the *Challenger* Expedition. *Quarterly Journal of Microscopical Science* 19, 20-62.

Brady, H.B., 1881a. On some Arctic foraminifera from soundings obtained on the Austro-Hungarian North Polar Expedition of 1872-76. *Annales and Magazine of Natural History* 8, 393-418.

Brady, H.B., 1881b. Über einige arktische tiefsee-Foraminiferen gesammelt während der österreichisch-ungarischen Nordpol-Expedition den Jahren 1872-74. *Denkschriften der Kaiserlichen Akademie der Wissenschaften Wien Mathematisch-naturwissenschaften Classe* 43, 9-110.

Brady, H.B., 1884. Report on the foraminifera dredged by *H. M. S. Challenger* during the years 1873-76. In "Reports of the Scientific Results of the Voyage of the *H.M.S.Challenger*, Zoology", London, 9, 1-814.

Carmack, E.C., Macdonald, R.W., 2002. Oceanography of the Canadian Shelf of the Beaufort Sea: a setting for marine life. *Arctic* 55, 29-45.

Carmack, E.C., Macdonald, R.W., Jasper, S., 2004. Phytoplankton productivity on the Canadian Shelf of the Beaufort Sea. *Marine Ecology Progress Series* 277, 37-50.

Chaster, G.W., 1892. Foraminifera. First Report of the Southport Society of Natural Science 1890-91, 54-72.

Clarke, K.R., 1993. Non-parametric multivariate analyses of changes in community structure. *Australian Journal of Ecology* 18, 117-143.

Comiso, J.C., Parkinson, C.L., 2004. Satellite-observed changes in the Arctic. *Physics Today* 57, 38-44.

Conlan, K., Aitken, A., Hendrycks, E., McClelland, C., Melling, H., 2008. Distribution patterns of Canadian Beaufort Shelf macrobenthos. *Journal of Marine Systems* 74, 864-886.

Cushman, J.A., 1910 A monograph of the foraminifera of the North Pacific Ocean. Pt. 1. Astrorhizidae and Lituolidae. *Bulletin of the U.S. National Museum* 71 (6), 1-134.

Cushman, J.A., 1917. A monograph of the foraminifera of the North Pacific Ocean; Part VI-Miliolidae. U.S. Natural Museum, Bulletin 71 (6), 1-108.

Cushman, J.A., 1920. The foraminifera of the Atlantic Ocean, Pt. 2, Lituolidae. U.S. National Museum Bulletin 104, 1-111, pls 1-18.

Cushman, J.A., 1922. Results of the Hudson Bay expedition, 1920, I - the foraminifera. Canada, Biological Board, Contributions to Canadian Biology (1921) 9, 135-147.

Cushman, J.A., 1925. Recent foraminifera from British Columbia. Cushman Laboratory for Foraminiferal Research Contributions 1 (2), 38-47.

Cushman, J.A., 1927a. Some characteristic Mexican fossil foraminifera. Journal of Paleontology 1, 147-172.

Cushman, J.A., 1927b. An outline of a re-classification of the foraminifera. Contributions from the Cushman Laboratory for Foraminiferal Research 3, 1-105.

Cushman, J.A., 1933. New Arctic foraminifera collected by Capt. R.A. Bartlett from Fox Basin and off the northeast coast of Greenland. Smithsonian Miscellaneous Collections 89(9), 1-8.

Cushman, J.A., 1937. A monograph of the foraminiferal family Valvulinidae. Cushman Laboratory for Foraminiferal Research, Special Publication 8, 210 p.

Cushman, J.A., 1941. Some fossil foraminifera from Alaska. Contributions to the Cushman Laboratory for Foraminiferal Research 17, 33-38.

Cushman, J.A., 1944. Foraminifera from the shallow water of the New England Coast. Cushman Laboratory for Foraminiferal Research, Contributions 23, 60-72.

Cushman, J.A., 1948. Arctic Foraminifera. Cushman Laboratory for Foraminiferal Research, Special Publication 23, 79 pp.

Cushman, J.A., Cole, W.S., 1930. Pleistocene foraminiferid from Maryland. Contributions to the Cushman Laboratory for Foraminiferal Research 6, 49-62.

Cushman, J.A., Todd, R., 1947. A foraminiferal fauna from Amchitka Island, Alaska. Contributions from the Cushman Laboratory for Foraminiferal Research 23, 60-72.

Darby, D.A., Bischof, J.F., 2004. A Holocene record of changing Arctic Ocean ice drift analogous to the effects of the Arctic Oscillation. Paleoceanography 19, PA1027, doi:10.1029/2003PA000961.

Dawson, J.W., 1860. Notice of Tertiary fossils from Labrador, Maine, etc., and remarks on the climate of Canada in the newer Pliocene or Pleistocene period. *Canadian Naturalist* 5, 188-200.

de Folin, L., 1886. Les Bathysiphons; premières pages d'une monographie du genre. *Actes de la Société Linnéenne de Bordeaux* 40, 271-289, pls. 5-8.

Delage, Y., Hérouard, E., 1896. *Traité de zoologie concrète. Tome I: La cellule et les Protozoaires.* Schleicher Frères, Paris, 584 pp.

de Vernal, A., Hillaire-Marcel, C., Darby, D., 2005. High variability of sea ice cover in the Chukchi Sea (western Arctic Ocean) during the Holocene. *Paleoceanography* 20, PA4018, doi:10.1029/2005PA001157.

Dickson, R., Rudels, B., Dye, S., Karcher, M., Meincke, J., Yashayaev, I., 2007. Current estimates of freshwater flux through Arctic and subarctic seas. *Progress in Oceanography* 73, 210–230.

d'Orbigny, A.D., 1826. Tableau méthodique de la classe des Cephalopodes. *Annales des Sciences Naturelles* 7, 245-314.

d'Orbigny, A.D., 1839a. Foraminifères. In de la Sagra, R., (ed) *Histoire physique, politique et naturelle de l'île de Cuba.* A. Bertrand, Paris, 224 pp.

Dyke, A.S., Hooper, J., Savelle, J.M., 1996. A history of sea ice in the Canadian Arctic Archipelago based on postglacial remains of the bowhead whale (*Balaena mysticetus*). *Arctic* 49, 235–255.

Dyke, A.S., Savelle, J.M., 2001. Holocene history of the Bering Sea bowhead whale (*Balaena mysticetus*) in its Beaufort Sea summer grounds off Southwestern Victoria Island, Western Canadian Arctic. *Quaternary Research* 55, 371–379.

Ehrenberg, G. C., 1861. Elemente des tiefen Meeresgrundes in Mexikansichen Golfstromen bei Florida; uber die Tiefgrund-Verhältnisse des Oceans am Eingange der Davisstrasse und bei Island. *Monatsbericht der Königlichen Preussischen Akademie der Wissenschaften zu Berlin* (1861), p. 275-315.

Feyling-Hanssen, R.W., Buzas, M.A., 1976. Emendation of *Cassidulina* and *Islandiella helenae* new species. *Journal of Foraminiferal Research* 6, 154-158.

Finkelstein, S.A., Gajewski, K., 2007. A palaeolimnological record of diatom-community dynamics and late-Holocene climatic changes from Prescott Island, Nunavut, central Canadian Arctic. *The Holocene* 17 (6), 803–812.

Flint, J.M., 1899. Recent Foraminifera. A descriptive catalogue of specimens dredged by the U.S. Fish-Commission Steamer Albatross. Report of the United States National Museum for 1897, 149-349.

Fortier, L., Barber, D.G., 2008. An introduction to the Canadian Arctic Shelf Exchange Study. In: Fortier, L., Barber, D.G., Michaud, J. (Eds), *On Thin Ice: a synthesis of the Canadian Arctic Shelf Exchange Study (CASES)*. Aboriginal Issues Press, University of Manitoba, pp. 1–11.

Gajewski, K., Mott, R.J., Ritchie, J.C., Hadden, K., 2000. Holocene vegetation history of Banks Island, Northwest Territories, Canada. *Canadian Journal of Botany* 78, 430–436.

Galley, R.J., Key, E., Barber, D.G., Hwang, B.J., Ehn, J.K., 2008. Spatial and temporal variability of sea ice in the southern Beaufort Sea and Amundsen Gulf: 1980–2004. *Journal of Geophysical Research* 113, C05S95, doi:10.1029/2007JC004553.

Ghaleb, B., 2009. Overview of the methods for the measurement and interpretation of short-lived radioisotopes and their limits. *Deep-sea to Coastal Zones: Methods and Techniques for Studying Paleoenvironments IOP Publishing IOP Conf. Series: Earth and Environmental Science* 5, 13 pp.

Green, K.E., 1960. Ecology of some Arctic foraminifera. *Micropaleontology* 6, 57–78.

Gregory, M.R., 1970. Distribution of benthic foraminifera in Halifax Harbour, Nova Scotia, Canada. PhD Thesis, Department of Geology, Dalhousie University, Halifax, Nova Scotia.

Hald, M., Steinsund, P.I., 1996. Benthic foraminifera and carbonate dissolution in surface sediments of the Barents and Kara Sea. In: Stein, R., Ivanov, G.I., Levitan, M.A., Fahl, K. (Eds.), *Surface-sediment composition and sedimentary processes in the central Arctic Ocean and along the Eurasian Continental Margin*. *Berichte Zur Polarforschung*, 212, 285–307.

Herb, R., 1971. Distribution of Recent benthonic foraminifera in the Drake Passage. *Antarctic Research Series* 17, *Biology of the Antarctic Seas IV*, 251-300.

Herman, Y., 1974. Arctic Ocean sediments, microfauna, and the climatic record in Late Cenozoic time. In Herman, Y.(ed.), *Marine Geology and Oceanography of the Arctic Seas*, Springer-Verlag, New York, 283-348.

Hessland, I., 1943. Marine Schalenablager-ungen Nord-Borduslans. *Geological Institute of Uppsala, Bulletin*, 31pp.

Hillaire-Marcel, C., de Vernal, A., Polyak, L., Darby, D., 2004. Size-dependent isotopic composition of planktic foraminifers from Chukchi Sea vs. NW Atlantic sediments — implications for the Holocene paleoceanography of the western Arctic. *Quaternary Science Reviews* 23, 245–260.

Hillaire-Marcel, C., de Vernal, A., 2008. Stable isotope clue to episodic sea ice formation in the glacial North Atlantic. *Earth and Planetary Science Letters* 268, 143–150.

Howell, S.E.L., Tivy, A., Yackel, J.J., McCourt, S., 2008. Multi-year sea ice conditions in the western Canadian Arctic Archipelago region of the Northwest Passage: 1968 – 2006. *Atmospheric-Ocean* 46(2), 229 – 242.

Howell, S.E.L., Duguay, C.R., Markus, T., 2009. Sea ice conditions and melt season duration variability within the Canadian Arctic Archipelago: 1979–2008. *Geophysical Research Letters* 36, L10502, doi:10.1029/2009GL037681.

Hughes, M.K. and Diaz, H.F., 1994. Was there a “Medieval Warm Period”, and if so, where and when? *Climate Change* 26, 109-142.

Iqbal, J., 1973. Sedimentology and benthonic foraminifera in M’Clure Strait (Canadian Arctic Archipelago). MSc. Thesis, unpublished, Dalhousie University, 265 pp.

Ingram R.G., Williams, W.J., van Hardenberg, B., Dawe, J.T., Carmack, E.C., 2008. Seasonal circulation over the Canadian Beaufort Shelf. In: Fortier, L., Barber, D.G., Michaud, J., (Eds), *On Thin Ice: a synthesis of the Canadian Arctic Shelf Exchange Study (CASES)*. Aboriginal Issues Press, University of Manitoba, 13-35.

Ishman, S.E., Polyak, L.V., Poore, R.Z., 1996. Expanded record of Quaternary oceanographic change: Amerasian Arctic Ocean. *Geology* 24, 139–142.

Iwasa, S., 1955. Biostratigraphy of the Iswasagawa Group in Honjo and its environment, Akita prefecture. *Journal of the Geological Society Tokyo* 61, 1-18.

Jennings, A.E., Knudsen, K.L., Hald, M., Hansen, C.V., Andrews, J.T., 2002. A mid-Holocene shift in Arctic sea-ice variability on the East Greenland Shelf. *The Holocene* 12 (1), 49–58.

Joynt, E.H., Wolfe, A.P., 2001. Paleoenvironmental inference models from sediment diatom assemblages in Baffin Island lakes (Nunavut, Canada) and reconstruction of summer water temperature. *Canadian Journal of Fisheries and Aquatic Science* 58, 1222–1243.

Jones, P.D., Osborn, T.J., Briffa, K.R., 2001. The evolution of climate over the last millennium. *Science* 292, 662–667.

Jones, E.P., Swift, J.H., Anderson, L.G., Lipizer, M., Civitarese, G., Falkner, K.K., Kattner, G., McLaughlin, F., 2003. Tracing Pacific water in the North Atlantic Ocean. *Journal of Geophysical Research* 108, 3116.

Keatley, B.E., Douglas, M.S.V., Smol, J.P., 2006. Early-20th century environmental changes inferred using subfossil diatoms from a small pond on Melville Island, N.W.T., Canadian high Arctic. *Hydrobiologia* 553, 15–26.

Koerner, R.M., Fisher, D.A., 1990. A record of Holocene summer climate from a Canadian high-Arctic ice core. *Nature* 343, 630–631.

Lagoë, M.B., 1977. Recent benthic foraminifera from the Central Arctic Ocean. *Journal of Foraminiferal Research* 7(46), 106–129.

Lagoë, M.B., 1980. Recent arctic foraminifera - overview. *AAPG Bulletin-American Association of Petroleum Geologists* 64 (3), 445–445.

LeBlanc, M., Gajewski, K., Hamilton, P.B., 2004. A diatom-based Holocene palaeoenvironmental record from a mid-Arctic lake on Boothia Peninsula, Nunavut, Canada. *Holocene* 14, 417–425.

Ledu, L., Rochon, A., de Vernal, A., St-Onge, G., 2008. Palynological evidence of Holocene climate change in the eastern Arctic: a possible shift in the Arctic oscillation at the millennial time scale. *Canadian Journal of Earth Sciences* 45, 1363–1375.

Levac, E., De Vernal, A., Blake, W., 2001. Sea-surface conditions in northernmost Baffin Bay during the Holocene: palynological evidence. *Journal of Quaternary Science* 16, 353–363.

Lim, D.S.S., Smol, J.P., Douglas, M.S.V., 2008. Recent environmental changes on Banks Island (N.W.T., Canadian Arctic) quantified using fossil diatom assemblages. *Journal of Paleolimnology* 40, 385–398.

Lindsay, R.W., Zhang, J., 2005. The Thinning of Arctic Sea Ice, 1988–2003: Have We Passed a Tipping Point? *Journal of Climate* 18, 4879–4894.

Linné, C., 1758. *Systema naturae per regna tria naturae, secundum classes, ordines, genera, species, cum characteribus, differentiis, synonymis, locis*. G. Engelmann (Lipsiae), ed 10 (1), 1–824.

Loeblich, A.R.Jr., Tappan, H., 1953. Studies of Arctic Foraminifera: Smithsonian Miscellaneous Collections 121, 150 pp.

Loeblich, A.R. jr., Tappan, H., Beckman, J.P., Bolli, H.M., Gallitelli, E.M., Troelsen, J.C., 1957. Studies in Foraminifera. United States National Museum, Bulletin 215, 321 pp.

Lukovich, J.V., Barber, D.G., 2006. Atmospheric controls on sea ice motion in the southern Beaufort Sea. *Journal of Geophysical Research* 111, D18103, doi:10.1029/2005JD006408.

- Mann, M.E., 2007. Climate over the past two millennia. *Annual Review of Earth and Planetary Sciences* 35, 111–136.
- Mann, M.E., Zhang, Z., Rutherford, R., Bradley, R.S., Hughes, M.K., Shindell, D., Ammann, C., Faluvegi, G., Ni, F., 2009. Global signatures and dynamical origins of the Little Ice Age and Medieval Climate Anomaly. *Science* 326, 1256–1260.
- Markussen, B., Zahn, R., Thiede, J., 1985. Late Quaternary sedimentation in the eastern Arctic Basin: stratigraphy and depositional environment. *Palaeogeography, Palaeoclimatology, Palaeoecology* 50, 271–284.
- Marlowe, J.I., Vilks, G., 1963. Marine geology, eastern part of the Prince Gustaf Adolph Sea, District of Franklin. Polar Continental Shelf Project: Geological Survey of Canada, Paper 63-22, 1-23.
- Meyers, P.A., 1997. Organic geochemical proxies of paleoceanographic, paleolimnologic and paleoclimatic processes. *Organic Geochemistry* 27 (5/6), 213–250.
- McNeely, R., Dyke, A.S., Southon, J.R., 2006. Canadian marine reservoir ages, preliminary data assessment. Geological Survey of Canada, Open File Report 5049, 3 pp.
- Medioli, F.S., Scott, D.B., 1983. Holocene Arcellacea (Thecamoebians) from Eastern Canada. Cushman Foundation for Foraminiferal Research, Special Publication 21, 63 pp.
- Milam, R.W., Anderson, J.B., 1981. Distribution and ecology of recent benthonic foraminifera of the Adelie-George V Continental shelf and slope, Antarctica. *Marine Micropaleontology* 6, 297–325.
- Miller, A.A.L., Scott, D.B., Medioli, F.S., 1982. *Elphidium excavatum* (Terquem): ecophenotypic versus subspecific variation. *Journal of Foraminiferal Research* 12, 116–144.
- Montfort de, P.D., 1808. *Conchyliologie systématique et classification méthodique des coquilles 1*. F. de Schoell, Paris, 409 pp.
- Mudie, P.J., Rochon, A., Levac, E., 2005. Decadal-scale sea-ice changes in the Canadian Arctic and their impacts on humans during the past 4,000 years. *Environmental Archaeology* 10, 113–126.
- Mudie, P.J., Rochon, A., Prins, M.A., Soenarjo, D., Troelstra, S.R., Levac, E., Scott, D.B., Roncaglia, L., Kuijpers, A., 2006. Late Pleistocene–Holocene marine geology of Nares Strait region: palaeoceanography from foraminifera and dinoflagellate cysts, sedimentology and stable isotopes. *Polarforschung* 74, 169–183.

Mudroch, A. and MacKnight, S., 1994. Handbook of techniques for aquatic sediment sampling. CRC Press, 236 pp.

Mysak, L.A., 2001. Patterns of Arctic Circulation. *Science* 293, 1269–1270.

Norman, A.M., 1892. *Museum Normanianum, or, A catalogue of the Invertebrata of Europe and the Arctic and the North Atlantic Oceans, which are contained in the collection of A.M. Norman. 2nd Edition, pt. 8, Rhizopoda (together with Pt. 7, Spongozoa)*, Durham, 1901-1905, 21 pp.

Nørvang, A., 1945. The zoology of Iceland. *Foraminifera* 2, (2). Ejnar Munksgaard, Copenhagen and Reykjavik, p. 1-79.

Osborn, T.J. and Briffa, K.R., 2006. The spatial extent of 20th-century warmth in the context of the past 1200 years. *Science* 311, 841-844.

Osterman, L.E., Poore, R.Z., Foley, K.M., 1999. Distribution of benthic foraminifers (>125 μ m) in the surface sediments of the Arctic Ocean. *U.S. Geological Survey Bulletin* 2164, 28 pp.

Overpeck, J., Hughen, K., Hardy, D., Bradley, R., Case, R., Douglas, M., Finney, B., Gajewski, K., Jacoby, G., Jennings, A., Lamoureux, S., Lasca, A., MacDonald, G., Moore, J., Retelle, M., Smith, S., Wolfe, A., Zielinski, G., 1997. Arctic environmental change of the last four centuries. *Science* 278, 1251–1256.

Parker, F.L., 1952. Foraminiferal distribution in the Long Island Sound-Buzzards Bay area. *Bulletin of the Harvard Museum of Comparative Zoology* 106, 391-423.

Parker, W.K., Jones, T.R., 1865. On some foraminifera from the North Atlantic and Arctic Oceans, including Davis Strait and Baffin's Bay. *Philosophical Transactions of the Royal Society* 155, 325-441.

Parkinson, C.L., Cavalieri, D.J., 2008. Arctic sea ice variability and trends, 1979–2006. *Journal of Geophysical Research* 113, C07003, doi:10.1029/2007JC004558.

Patterson, T.R., Fishbein, E., 1989. Re-examination of the statistical methods used to determine the number of point counts needed for micropaleontological quantitative research. *Journal of Paleontology* 63 (2), 245–248.

Pharand, D., 1984. *The Northwest Passage: Arctic straits*. Martinus Nijhoff Publishers, Dordrecht, 176 pp.

Phleger, F.B., 1952. Foraminifera distribution in some sediment samples from the Canadian and Greenland Arctic. *Cushman Foundation for Foraminiferal Research, Contributions* 3, 80–89, pls. 13,14.

- Podrifske, B., Gajewski, K., 2007. Diatom community response to multiple scales of Holocene climate variability in a small lake on Victoria Island, NWT, Canada. *Quaternary Science Reviews* 26, 3179–3196.
- Polyak, L., Korsun, S., Febo, L., Stanovoy, V., Khusind, T., Hald, M., Paulsen, B.E., Lubinski, D.J., 2002. Benthic foraminiferal assemblages from the southern Kara Sea, a river-influenced Arctic marine environment. *Journal of Foraminiferal Research* 32, 252–273.
- Poore, R.Z., Ishman, S.E., Phillips, R.L., McNeil, D.H., 1994. Quaternary stratigraphy and paleoceanography of the Canada Basin, Western Arctic Ocean. *United States Geological Survey Bulletin* 2080, 32 pp.
- Prinsenbergh, S.J., Bennett, E.B., 1987. Mixing and transports in Barrow Strait, the central part of the Northwest Passage. *Continental Shelf Research* 7(8), 913–935.
- Prinsenbergh, S., Pettipas, R., 2008. Ice and Ocean Mooring Data Statistics from Barrow Strait, Central Section of NW Passage in Canadian Arctic Archipelago International *Journal of Offshore and Polar Engineering* 18 (4), 277–281.
- Proshutinsky, A., Bourke, R.H., McLaughlin, F.A., 2002. The role of the Beaufort Gyre in Arctic climate variability: Seasonal to decadal climate scales. *Geophysical Research Letters* 29 (23), 2100, doi:10.1029/2002GL015847.
- Ravelo, A.C., Hillaire-Marcel, C., 2008. The use of oxygen and carbon isotopes of foraminifera in paleoceanography. In: Hillaire-Marcel, C., de Vernal, A., (Eds), *Proxies in Late Cenozoic Paleoceanography*. Elsevier, The Netherlands, 735–764.
- Reuss, A.E., 1850. Neue Foraminiferen aus den Schichten des österreichischen Tertiärbeckens. *Königliche Akademie der Wissenschaften Wien, mathematisch-naturwissenschaftliche Klasse, Denkschriften* 1, 365–390.
- Reuss, A.E., 1851. Über die fossilen Foraminiferen und Entomostraceen der septarienthonen Umgegend von Berlin: *Zeitschrift der Deutschen Geologischen Gesellschaft*, Berlin, 3, 49–91.
- Rhumbler, L., 1911. Die foraminiferen (thalamophoren) der Plankton-Expedition; Teil 1. Die allgemeinen Organisationsverhältnisse der foraminiferen. *Plankton-Expedition der Humboldt-Stiftung, Ergebnisse*, 3 (L.C.), 331 pp.
- Richerol, T., Rochon, A., Blasco, S., Scott, D.B., Schell, T.M., Bennett, R.J., 2008. Evolution of paleo sea-surface conditions over the last 600 years in the Mackenzie Trough, Beaufort Sea (Canada). *Marine Micropaleontology* 68, 6–20.

Rigor, I.G., Wallace, J.M., Colony R.L., 2002. Response of sea ice to the Arctic oscillation. *Journal of Climate* 15, 2648–2663.

Rögl, F., Bolli, H.M., 1973. Holocene to Pleistocene planktonic foraminifera of DSDP Leg 15, Site 147 (Cariaco Basin [French], Caribbean Sea) and their climatic interpretation. In Edgar, N.T., Saunders, J.B. et al., (eds), *Initial Reports of the Deep Sea Drilling Project 15*, 553-615.

Rühland, K., Priesnitz, A., Smol, J.P., 2003. Paleolimnological evidence from diatoms for recent environmental changes in 50 lakes across Canadian Arctic treeline. *Arctic, Antarctic, and Alpine Research* 35 (1), 110–123.

Sars G.O., 1872. On some remarkable forms of animal life from the great deeps off the Norwegian coast. Part 1, partly from posthumous manuscripts of the late prof. Mich. Sars. University Program for the 1rs half-year 1869. Brøgger & Christie, Christiania, 74 pp.

Savelle, J.M., Dyke, A.S., McCartney, A.P., 2000. Holocene bowhead whale (*Balaena mysticetus*) mortality patterns in the Canadian Arctic Archipelago. *Arctic* 53, 414–421.

Schell, T.M., Moss, T.J., Scott, D.B., Rochon, A., 2008. Paleo-sea ice conditions of the Amundsen Gulf, Canadian Arctic Archipelago: implications from the foraminiferal record of the last 200 years. *Journal of Geophysical Research* 113, C03S02, doi:10.1029/2007JC004202.

Schafer, C.T., Cole, F.E., 1978. Distribution of Foraminifera in Chaleur Bay, Gulf of St. Lawrence. *Geological Survey of Canada Paper 77-30*, 55 pp.

Schröder, C.J., Medioli, F.S., Scott, D.B., 1989. Fragile abyssal foraminifera (including new Komokiacea) from Nares Abyssal Plain. *Micropaleontology* 35 (1), 10-48, pls. 1-9.

Schröder-Adams, C.J., Cole, F.E., Medioli, F.S., Mudie, P.J., Scott, D.B., Dobbin, L., 1990. Recent Arctic shelf foraminifera: Seasonally ice covered vs. perennial ice covered areas. *Journal of Foraminiferal Research* 20, 8–36.

Schulze, F.E., 1875. Rhizopoden. In "Zoologische Ergebnisse der Nord-Seefahrt vom 21 Luli bius 9 September 1872" (series of articles). *Jahresbericht der Kommission zur wissenschaftlichen Untersuchung der deutschen Meere in Kiel*, 1(2-3), 97-114, pl. 2.

Scott, D.B., 1987. Quaternary benthic foraminifers from Deep Sea Drilling Project Sites 612 and 613, Leg 95, New Jersey transect. In Poag, C.W., Watts, A.B. et al.: (eds.) "Initial Reports of the Deep Sea Drilling Project", XCV, Washington (U.S. Government Printing Office), 313-337.

Scott, D.B., Martini, I.P., 1982. Marsh foraminiferal zonations in western James-Hudson Bay. *Naturaliste Canadien* 109, 399-414.

Scott, D.B., Vilks, G., 1991. Benthonic foraminifera in the surface sediments of the deep-sea Arctic Ocean. *Journal of Foraminiferal Research* 21, 20–38.

Scott, D.B., Hermelin, J.O.R., 1993. A device for precision splitting of micropaleontological samples in liquid suspension. *Journal of Paleontology* 67, 151–154.

Scott, D.B., Schafer, C.T., Medioli, F.S., 1980. Eastern Canadian estuarine foraminifera: a framework for comparison. *Journal of Foraminiferal Research* 10, 205–234.

Scott, D.B., Mudie, P.J., Baki, V., MacKinnon, K.D., Cole, F.E., 1989. Biostratigraphy and late Cenozoic paleoceanography of the Arctic Ocean: foraminiferal, lithostratigraphic, and isotopic evidence. *Geological Society of America Bulletin* 101, 260–277.

Scott, D.B., Brown, K., Collins, E.S., Medioli, F.S., 1995. A new sea-level curve from Nova Scotia: evidence for a rapid acceleration of sea-level rise in the late mid-Holocene. *Canadian Journal of Earth Sciences* 32, 2071–2080.

Scott, D.B., Schell, T., Rochon, A., Blasco S., 2008. Modern benthic foraminifera in the surface sediments of the Beaufort Shelf, Slope and Mackenzie Trough, Beaufort Sea, Canada: Taxonomy and summary of surficial distributions. *Journal of Foraminiferal Research* 38, 228–250.

Scott, D.B., Schell, T., St-Onge, G., Rochon, A., Blasco, S., 2009. Foraminiferal assemblage changes over the last 15,000 years on the Mackenzie-Beaufort Sea Slope and Amundsen Gulf, Canada: Implications for past sea ice conditions. *Paleoceanography* 24, PA2219, doi:10.1029/2007PA001575.

Seidenkrantz, M.-S., Aagaard-Sørensen, S., Sulsbrück, H., Kuijpers, A., Jensen, K.G., Kunzendorf, H., 2007. Hydrography and climate of the last 4400 years in a SW Greenland fjord: implications for Labrador Sea palaeoceanography. *Holocene* 17 (3), 387–401.

Seidenkrantz, M.-S., Roncaglia, L., Fischel, A., Heilmann-Clausen, C., Kuijpers, A., Moros, M., 2008. Variable North Atlantic climate seesaw patterns documented by a late Holocene marine record from Disko Bugt, West Greenland. *Marine Micropaleontology* 68, 66–83.

Serreze, M.C. and Barry, R.G., 2005. *The Arctic Climate System*. Cambridge University Press, Cambridge UK, 385 pp.

Serreze, M.C., Maslanik, J.A., Scambos, T.A., Fetterer, F., Stroeve, J., Knowles, K., Fowler, C., Drobot, S., Barry, R.G., Haran, T.M., 2003. A record minimum Arctic sea ice extent and area in 2002. *Geophysical Research Letters* 30 (3), 1110, doi:10.1029/2002GL016406.

Smol, J.P., Wolfe, A.P., Birks, H.J.B., Douglas, M.S.V., Jones, V.J., Korhola, A., Pienitz, R., Rühland, K., Sorvari, S., Antoniades, D., Brooks, S.J., Fallu, M.-A., Hughes, M., Keatley, B.E., Laing, T.E., Michelutti, N., Nazarova, L., Nyman, M., Paterson, A.M., Perren, B., Quinlan, R., Rautio, M., Saulnier-Talbot, E., Siitonen, S., Solovieva, N., Weckström, J., 2005. Climate-driven regime shifts in the biological communities of arctic lakes. *Proceedings of the National Academy of Sciences* 102 (12), 4397–4402.

Souto, S., 1973. Contribucion al conocimiento de los tintinnidos de agua dulce de la Republica Argentina. I Rio de la Plata y delta del Parana. *Physis, Seccion B*, 32 (85), 249-254.

Stroeve, J., Frei, A., McCreight, J., Ghatak, D., 2008. Arctic sea-ice variability revisited. *Annals of Glaciology* 48, 71–81.

Stuiver, M., Reimer, P.J., 1993. Extended 14C data-base and revised CALIB 3.0 14C age calibration program. *Radiocarbon* 35, 215–230.

Swift, J.H., Aagaard, K., Timokhov, L., Nikiforov, E.G., 2005. Long-term variability of Arctic Ocean waters: Evidence from a reanalysis of the EWG data set. *Journal of Geophysical Research* 110, C03012, doi:10.1029/2004JC002312.

Tappan, H., 1951. Northern Alaska index foraminifera. Cushman Foundation for Foraminiferal Research, Contributions 2, 1-8.

Terquem, O., 1876. Essai sur le classement des animaux qui vivent sur la plage et dans les environs de Denkerque, Pt. 1. *Mémoires de la Société Dunkerquoise pour l'Encouragement des Sciences des Lettres et des Arts* (1874-1875) 19, 405-457.

Thomas, E.K., Briner, J.P., 2009. Climate of the past millennium inferred from varved proglacial lake sediments on northeast Baffin Island, Arctic Canada. *Journal of Paleolimnology* 41, 209–224.

Thomas, F.C., Medioli, F.S., Scott, D.B., 1990. Holocene and latest Wisconsinan benthic foraminiferal assemblages and paleocirculation history, Lower Scotian Slope and Rise. *Journal of Foraminiferal Research* 20, 212-245.

Todd, R., 1965. The foraminifera of the tropical Pacific collections of the *Albatross*, 1899-1900. Part 4-Rotaliform families and planktonic families. *U.S. National Museum Bulletin* 161, 1-139.

Todd, R., Low, D., 1961. Near-shore foraminifera of Martha's Vineyard Island, Massachusetts. Cushman Foundation for Foraminiferal Research, Contributions 12, 5-21.

Trouet, V., Esper, J., Graham, N.E., Baker, A., Scourse, J.D., Frank, D.C., 2009. Persistent positive North Atlantic Oscillation mode dominated the Medieval Climate Anomaly. *Science* 324, 78–80.

Vare, L.L., Massé, G., Gregory, T.R., Smart, C.W., Belt, S.T., 2009. Sea ice variations in the central Canadian Arctic Archipelago during the Holocene. *Quaternary Science Reviews* 28, 1354–1366.

Vilks, G., 1969. Recent foraminifera in the Canadian Arctic. *Micropaleontology* 15, 35–60, pls. 1–3.

Vilks, G., 1973. A study of *Globorotalia pachyderma* (Ehrenberg) = *Globergina pachyderma* (Ehrenberg) in the Canadian Arctic: unpublished Ph.D. thesis, Dalhousie University, 256 pp.

Vilks, G., 1989. Ecology of recent foraminifera on the Canadian Continental Shelf of the Arctic Ocean. In: Herman, Y. (Ed.), *The Arctic Seas: Climatology, Oceanography, Geology, and Biology*. Van Nostrand Reinhold, New York, 497–569 pp.

Walker, G., Boys, W., 1784. *Testacea Minuta Rariora*; a collection of the minute and rare shells lately discovered in the sand of the sea-shore near Sandwich by William Boys. London: J. March, 25 pp.

Walker, G., Jacob, E., 1798. In Kanmacher F., *Adam's Essays on the Microscope*. 2nd Edition, London. Printed by Dillon and Keating, 712 pp.

Williams, W.J., Carmack, E.C., 2008. Combined effect of wind-forcing and isobath divergence on upwelling at Cape Bathurst, Beaufort Sea. *Journal of Marine Research* 66, 645–663.

Williamson, M.A., Keen, C.E., Mudie, P.J., 1984. Foraminiferal distribution on the continental margin off Nova Scotia. *Marine Micropaleontology* 9, 219–239.

Williamson, W.C., 1858. *On recent foraminifera of Great Britain*. Ray Society, London, 107 pp.

Wollenburg, J.E., Knies, J., Mackensen, A., 2004. High-resolution paleoproductivity fluctuations during the past 24 kyr as indicated by benthic foraminifera in the marginal Arctic Ocean. *Palaeogeography, Palaeoclimatology, Palaeoecology* 204, 209–238.

Wollenburg, J.E., Kuhnt, W., 2000. The response of benthic foraminifers to carbon flux and primary production in the Arctic Ocean. *Marine Micropaleontology* 40, 189–231.

Wollenburg, J.E., Kuhnt, W., Mackensen, A., 2001. Changes in Arctic Ocean paleoproductivity and hydrography during the last 145 kyr: The benthic foraminiferal record. *Paleoceanography* 16, 65–77.

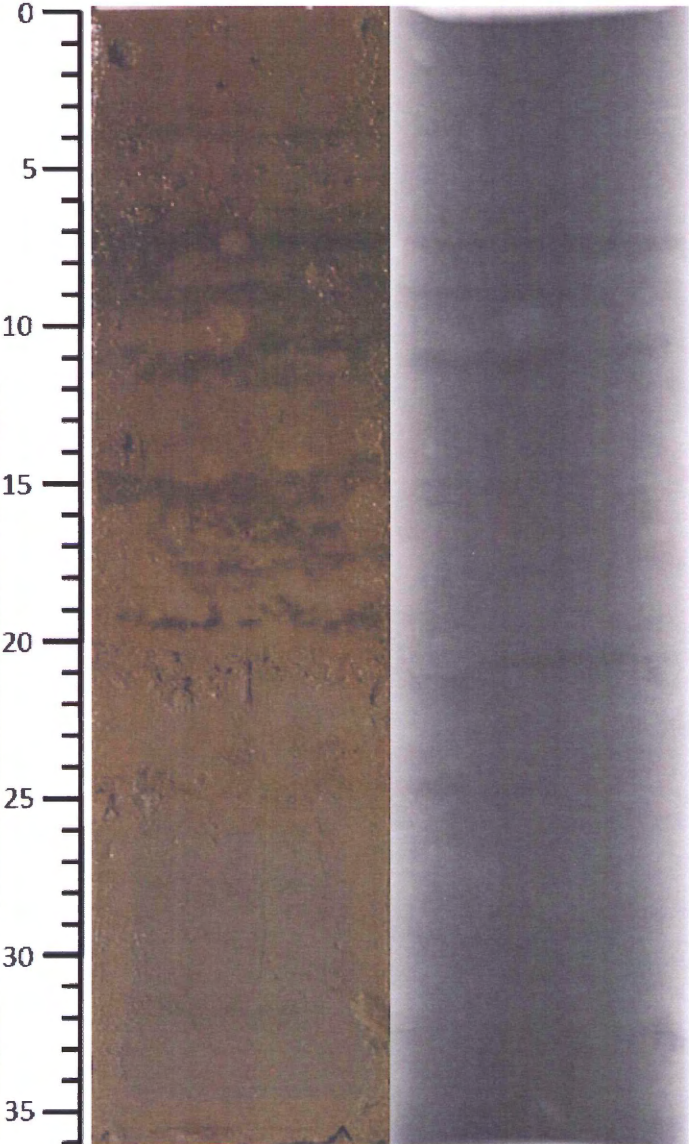
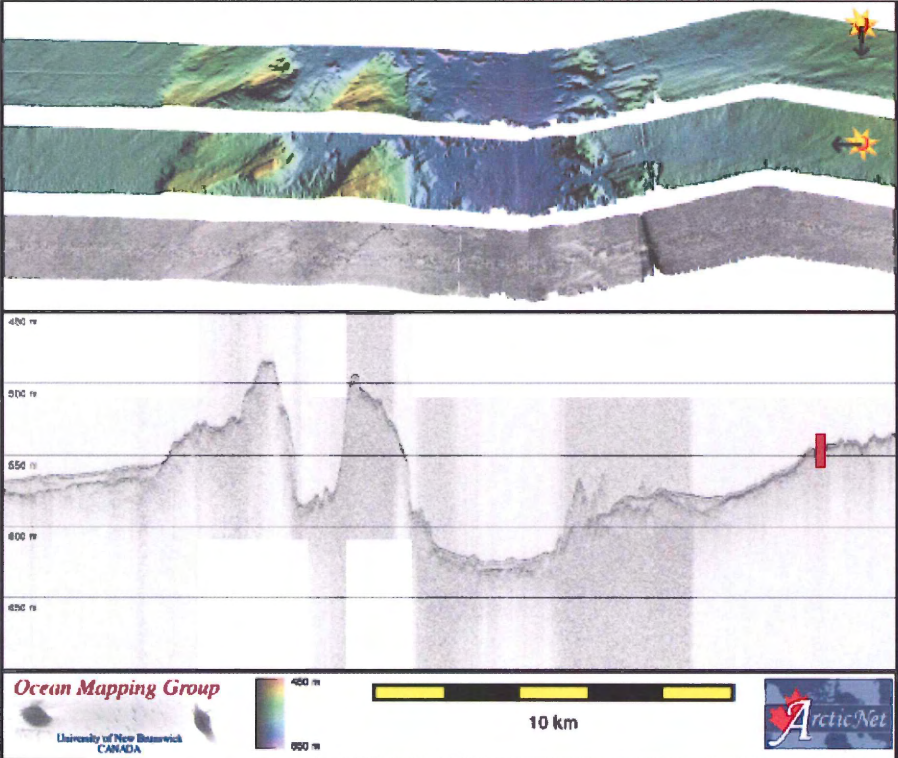
Wollenburg, J.E., Mackensen, A., 1998. Living benthic foraminifers from the central Arctic Ocean: faunal composition, standing stock and diversity. *Marine Micropaleontology* 34, 153–185.

Appendices

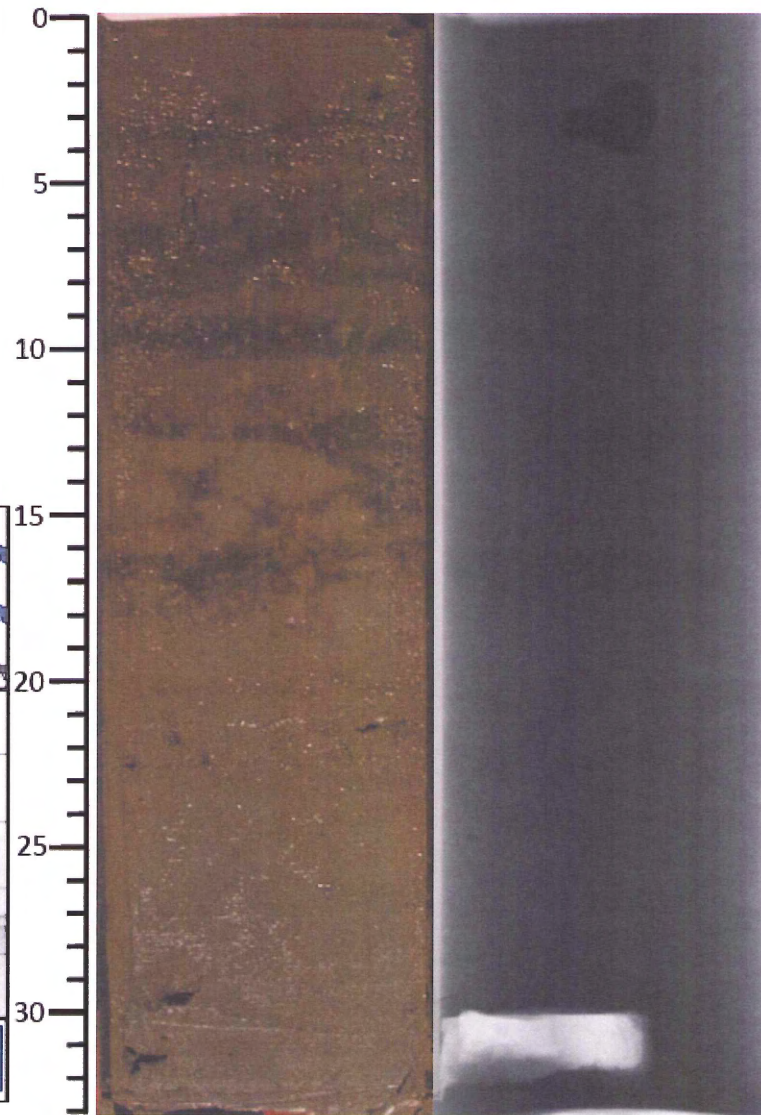
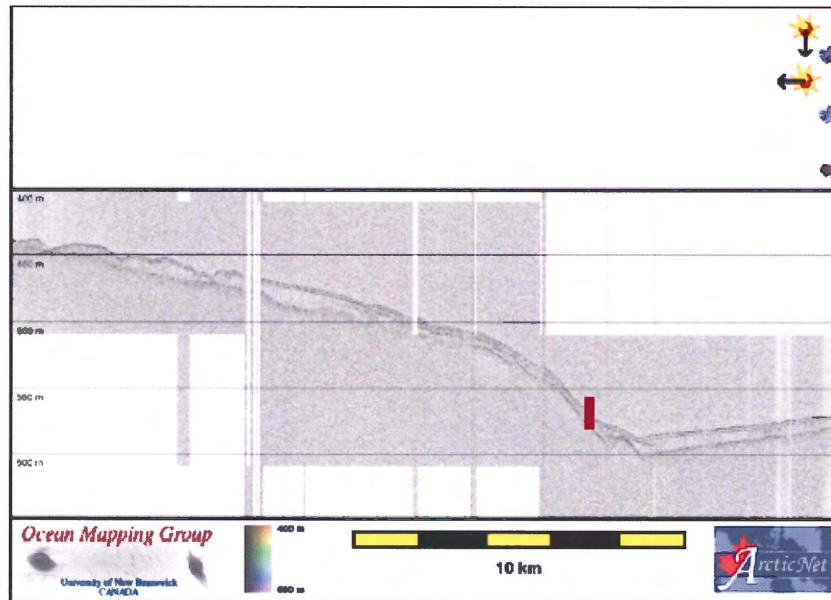
Appendix A - Boxcore and Sub-bottom Imaging

Visualizations of sampling locations and longitudinally split cores from five Amundsen Gulf boxcore samples (106, 109, 112, 118, 124), and from the boxcore from Viscount Melville Sound (012). For most cores, the Figure shows bathymetry, backscatter and sub-bottom data gathered by the EM300 & 3.5kHz transducer array onboard the CCGS Amundsen (images provided by the University of New Brunswick Ocean Mapping Group). Latitudes and longitudes for each sample are presented in Table 3.1. Photographs and X-rays of each split core are shown at the right of each Figure. Depth scales beside each core indicate cm increments.

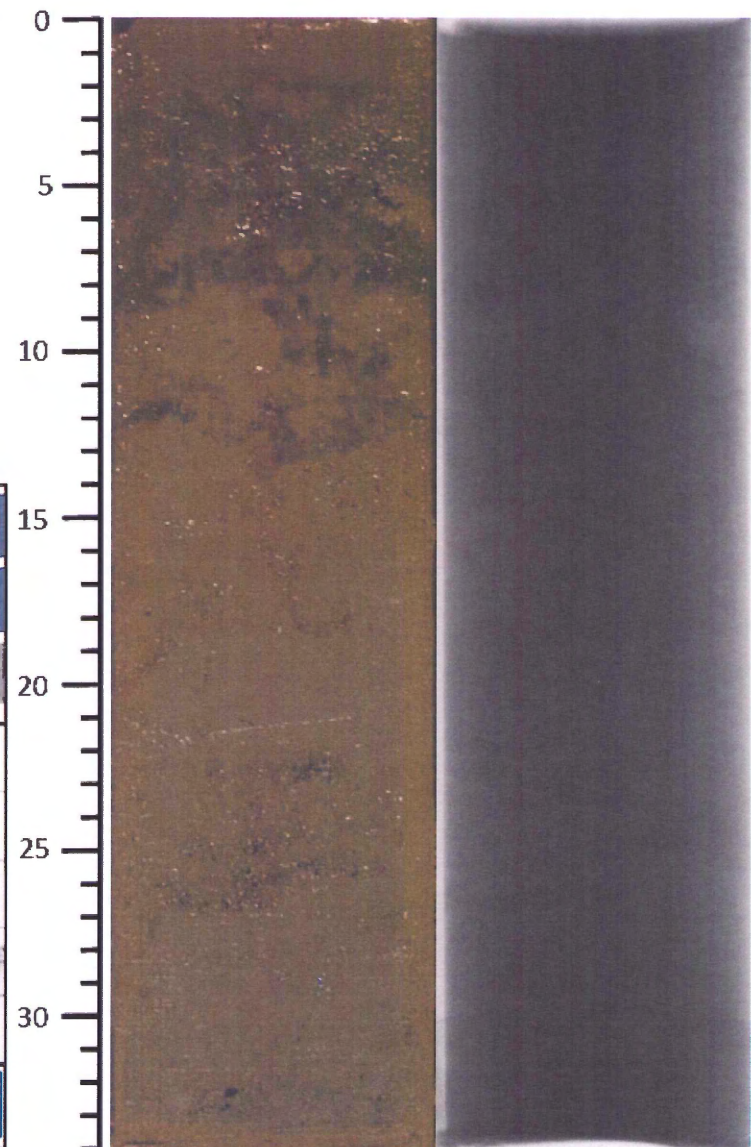
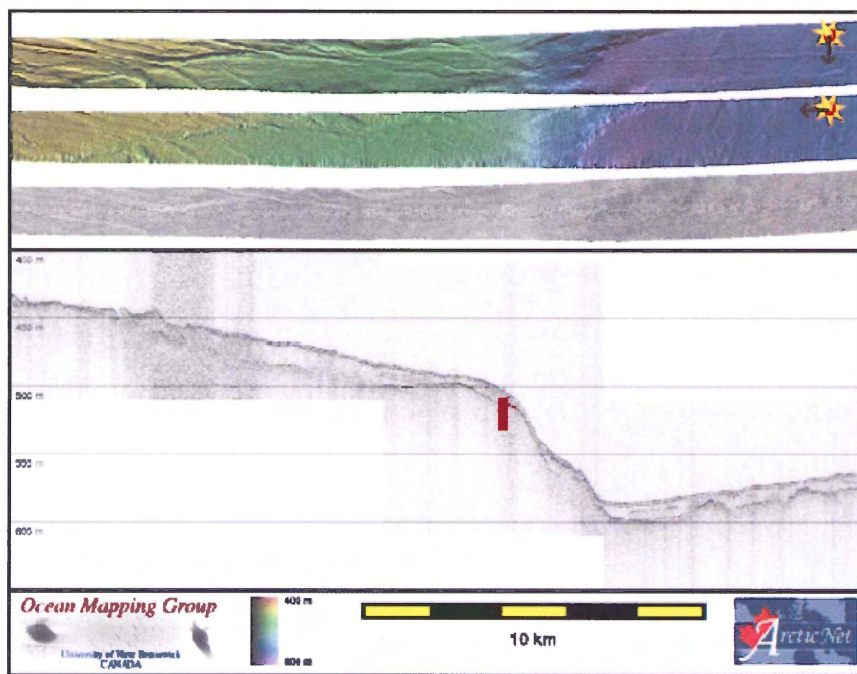
2004-804-106A



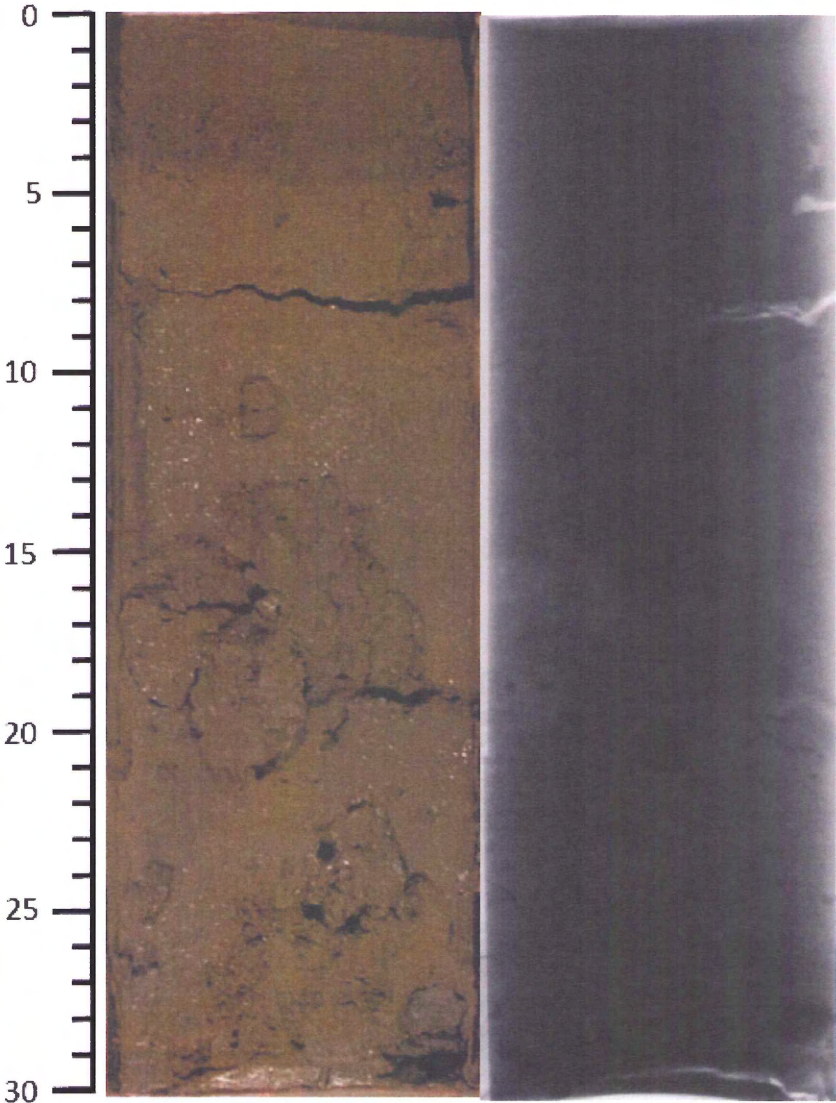
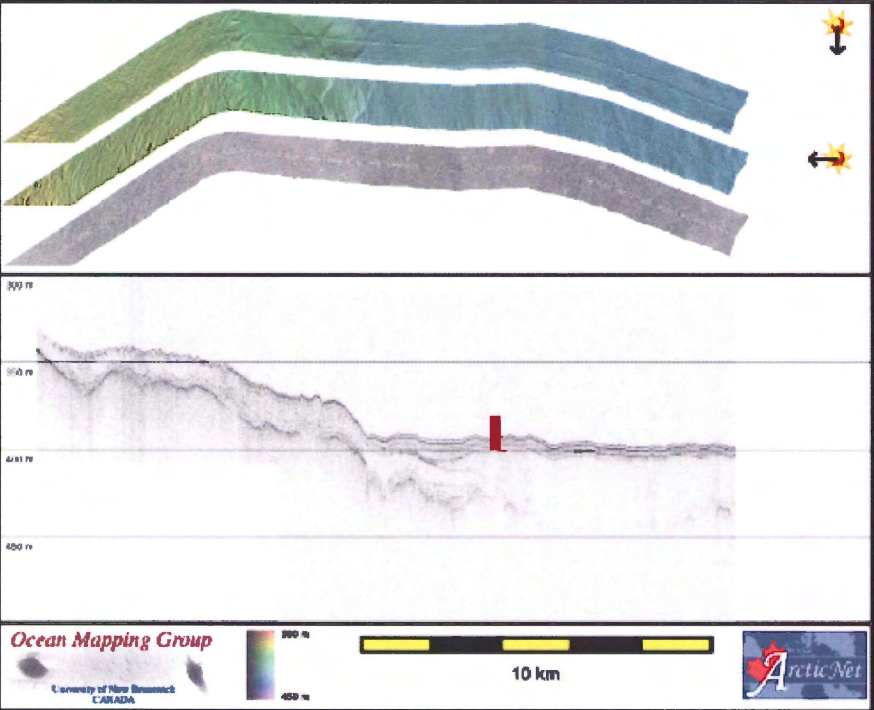
2004-804-109A



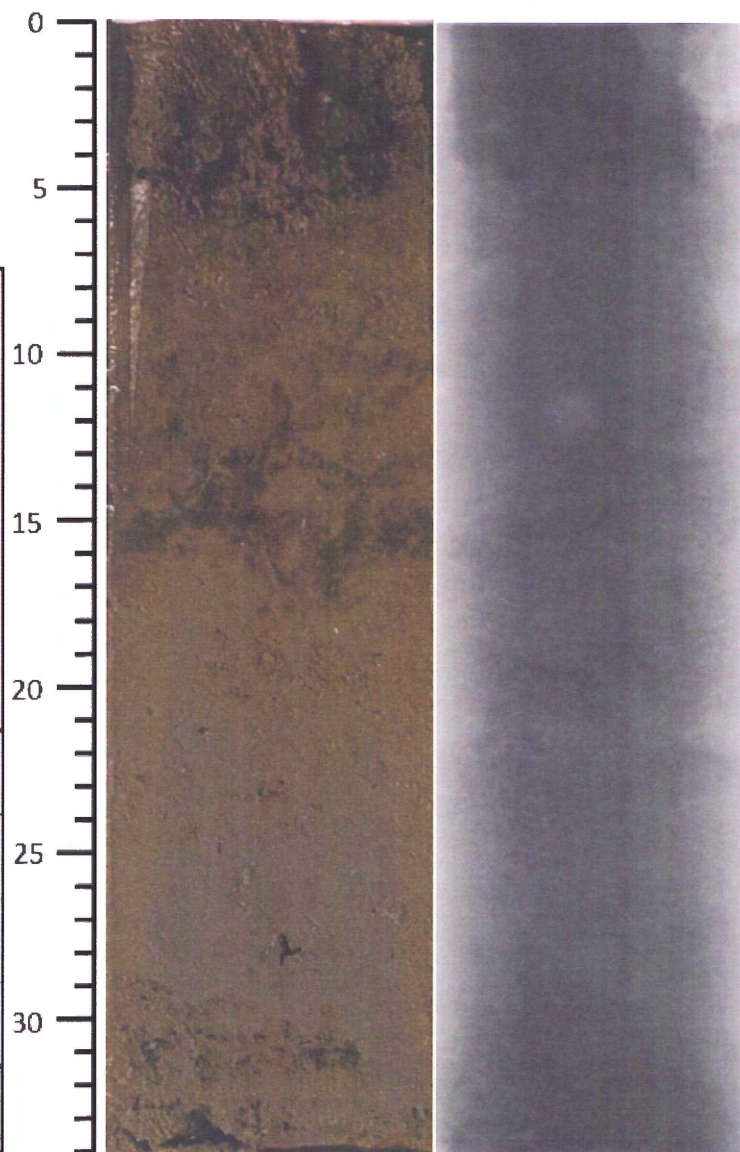
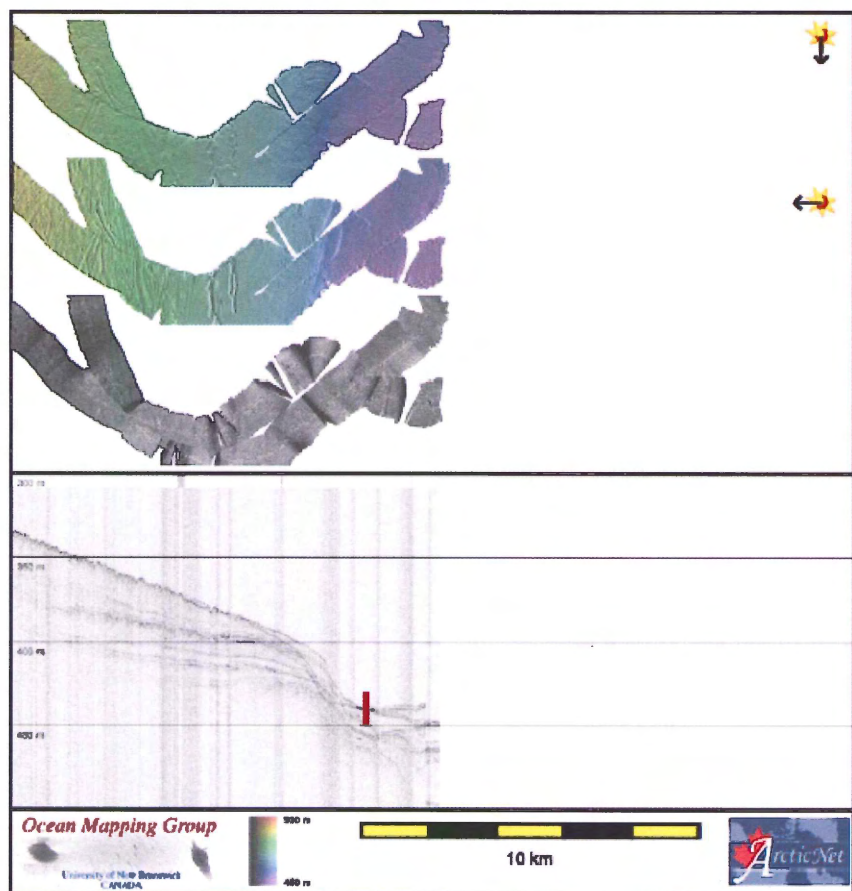
2004-804-112A



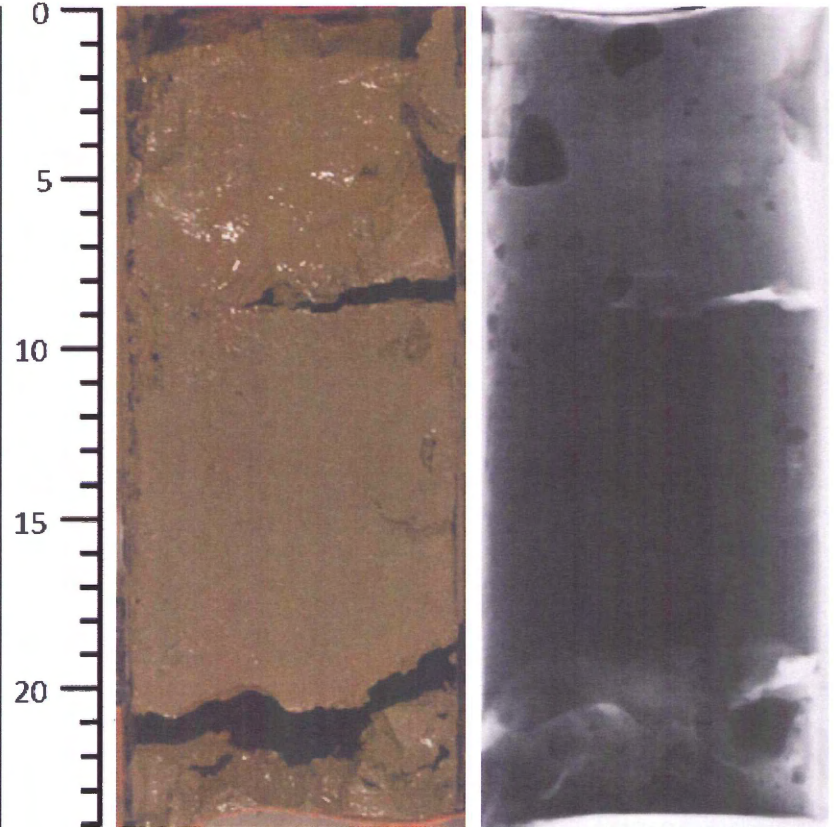
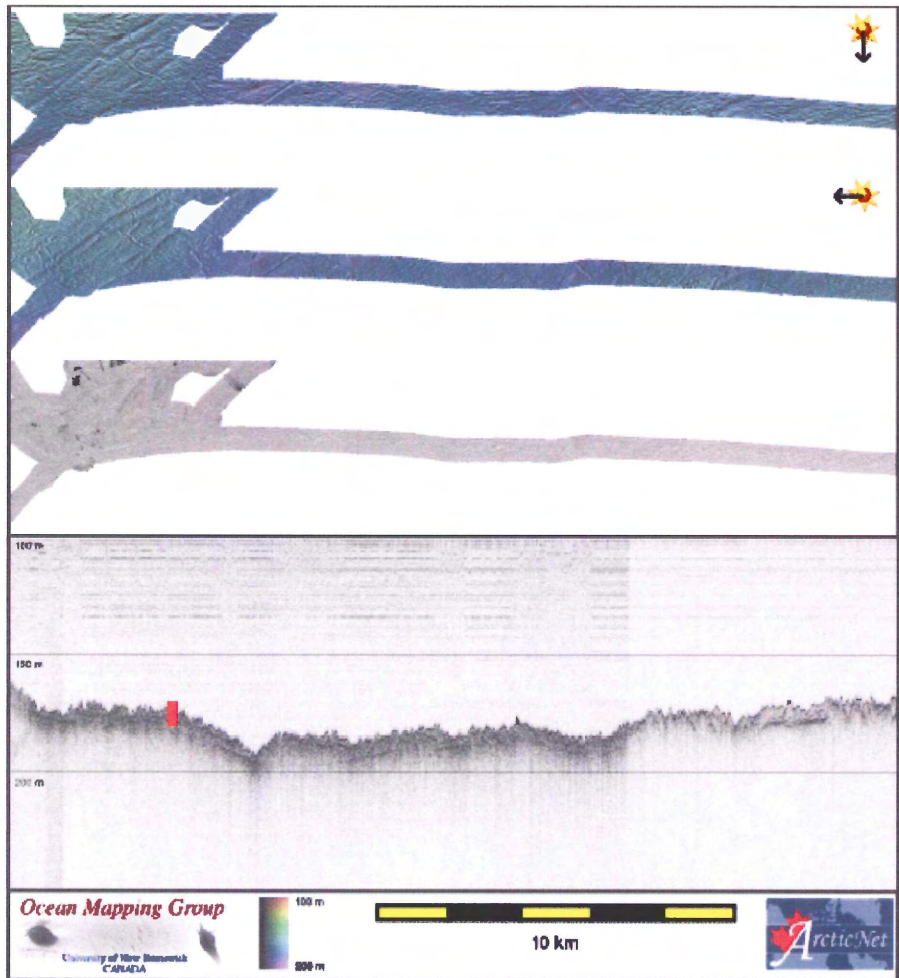
2004-804-118A



2004-804-124B



2006-804-012



Appendix B - Abundance Data – Amundsen Gulf

Depth-specific data summaries from the five Amundsen Gulf boxcore samples. The following Tables (B1-B5) contain the data for each boxcore, consisting of the percentage contribution of $n = 32$ foraminiferal species and their standard errors in the row immediately beneath. Species per 10 cc, specimens per 10 cc and tintinnid counts are presented above the species-specific percentages.

Table B1. Data summary from Amundsen Gulf Core 106. Rows below tintinnid counts are 32 species-specific percentages (\pm SE).

Sample	106-0.5	106-2.5	106-4.5	106-6.5	106-8.5	106-10.5	106-12.5	106-14.5	106-16.5	106-18.5	106-20.5	106-22.5	106-24.5	106-26.5	106-28.5	106-30.5	106-32.5	106-34.5	106-36.5
Interval (cm)	0-1	2-3	4-5	6-7	8-9	10-11	12-13	14-15	16-17	18-19	20-21	22-23	24-25	26-27	28-29	30-31	32-33	34-35	36-37
Midpoint (cm)	0.50	2.50	4.50	6.50	8.50	10.50	12.50	14.50	16.50	18.50	20.50	22.50	24.50	26.50	28.50	30.50	32.50	34.50	36.50
Species/10cc	30	24	23	20	20	20	22	26	30	27	23	24	25	22	32	29	24	26	26
Specimens/10cc	1334	890	1001	672	614	765	1582	1135	1015	1102	337	838	971	633	1976	2282	933	1243	1291
Tintinnids (counts/10cc)	50	117	58	18	50	30	80	68	58	52	15	36	40	46	66	120	66	76	66
<i>Adercotryma glomerata</i>				0.15		0.39													
standard error (\pm)				0.29		0.44													
<i>Bathysiphon rufus</i>	5.10	16.52	25.67	23.21	35.18	26.01	41.34	27.31	22.27	24.23	34.12	34.96	29.56	32.23	15.84	16.61	22.51	17.62	12.24
standard error (\pm)	1.18	2.44	2.71	3.19	3.78	3.11	2.43	2.59	2.56	2.53	5.06	3.23	2.87	3.64	1.61	1.53	2.68	2.12	1.79
<i>Bolivina arctica</i>	5.70	3.71	2.60	1.49	2.93	3.14	1.77	2.64	2.17	2.90	2.97	5.25	2.27	3.79	2.02	0.53	1.93	2.09	1.86
standard error (\pm)	1.24	1.24	0.99	0.92	1.33	1.24	0.65	0.93	0.90	0.99	1.81	1.51	0.94	1.49	0.62	0.30	0.88	0.80	0.74
<i>Buccella frigida</i>								0.44	0.39		0.30		1.24	0.16	1.11	0.66	0.86	1.21	0.62
standard error (\pm)								0.39	0.39		0.58		0.69	0.31	0.46	0.33	0.59	0.61	0.43
<i>Bulinimella hensoni</i>	5.70	0.22			0.33		2.02	2.82	6.50	4.90	2.97	1.91	8.03	4.42	11.74	13.67	7.93	13.35	13.94
standard error (\pm)	1.24	0.31			0.45		0.69	0.96	1.52	1.27	1.81	0.93	1.71	1.60	1.42	1.41	1.73	1.89	1.89
<i>Cassidulina reniforme</i>									0.79	1.81	0.89	0.84	0.21	0.47	2.13	1.14	0.43	1.61	0.77
standard error (\pm)									0.54	0.79	1.00	0.62	0.29	0.54	0.64	0.44	0.42	0.70	0.48
<i>Cibicides lobatus</i>																			
standard error (\pm)																			
<i>Cribr stomoides crassimargo</i>	0.07	0.11						0.09	0.39	0.09	1.78	0.12			0.15	0.26	0.75	0.24	0.23
standard error (\pm)	0.15	0.22						0.17	0.39	0.18	1.41	0.23			0.17	0.21	0.55	0.27	0.26
<i>Cribr stomoides jeffreysi</i>									0.20			0.24	0.10	0.63	0.15	0.04	0.64		
standard error (\pm)									0.27			0.33	0.20	0.62	0.17	0.09	0.51		
<i>Cribr stomoides subglobosum</i>	0.15		0.10				0.44	0.26	1.18	0.73	0.59	0.36	0.31	0.63	0.35	0.22	0.54		0.08
standard error (\pm)	0.21		0.20				0.33	0.30	0.66	0.50	0.82	0.40	0.35	0.62	0.26	0.19	0.47		0.15
<i>Cylogyra involvens</i>			0.40	0.89		0.78	0.76	0.35	0.59	0.91		0.48	0.62	1.58	0.40	0.26	1.07	1.61	1.39
standard error (\pm)			0.39	0.71		0.63	0.43	0.34	0.47	0.56		0.47	0.49	0.97	0.28	0.21	0.66	0.70	0.64
<i>Dentalina sp.</i>																			
standard error (\pm)																			
<i>Eggerella advena</i>	0.30	0.67	0.80	1.49	0.65	0.26	0.63	0.70	0.99	0.36	0.59	1.91	0.62	1.26	1.11	3.86	1.50	2.90	2.32
standard error (\pm)	0.29	0.54	0.55	0.92	0.64	0.36	0.39	0.49	0.61	0.36	0.82	0.93	0.49	0.87	0.46	0.79	0.78	0.93	0.82

Sample	106-0.5	106-2.5	106-4.5	106-6.5	106-8.5	106-10.5	106-12.5	106-14.5	106-16.5	106-18.5	106-20.5	106-22.5	106-24.5	106-26.5	106-28.5	106-30.5	106-32.5	106-34.5	106-36.5
Interval (cm)	0-1	2-3	4-5	6-7	8-9	11	13	15	17	19	21	23	25	27	29	31	33	35	37
Midpoint (cm)	0.50	2.50	4.50	6.50	8.50	10.50	12.50	14.50	16.50	18.50	20.50	22.50	24.50	26.50	28.50	30.50	32.50	34.50	36.50
Species/10cc	30	24	23	20	20	20	22	26	30	27	23	24	25	22	32	29	24	26	26
Specimens/10cc	1334	890	1001	672	614	765	1582	1135	1015	1102	337	838	971	633	1976	2282	933	1243	1291
Tintinnids (counts/10cc)	50	117	58	18	50	30	80	68	58	52	15	36	40	46	66	120	66	76	66
<i>Elphidiella groenlandica</i>																			
standard error (±)																			
<i>Elphidium exc. F. clavata</i>																			
standard error (±)																			
<i>Elphidium subarcticum</i>																			
standard error (±)																			
<i>Epistominella takayanagii</i>								0.18											
standard error (±)								0.24											
<i>Fissurina sp.</i>																			
standard error (±)																			
<i>Fursenkoina fusiformis</i>	0.15								0.20					0.40	0.18		0.16	0.08	
standard error (±)	0.21								0.27					0.28	0.17		0.22	0.15	
<i>Glomospira gordialis</i>	1.27	1.69	0.80	1.19	1.30	0.26	0.95	0.97	0.79	1.72		0.60	0.41	0.95	0.30	0.13	0.86	1.61	0.77
standard error (±)	0.60	0.85	0.55	0.82	0.90	0.36	0.48	0.57	0.54	0.77		0.52	0.40	0.75	0.24	0.15	0.59	0.70	0.48
<i>Haynesina orbiculare</i>																			
standard error (±)																			
<i>Hemisphaerammina bradyi</i>																			
standard error (±)																			
<i>Hyperammina spp.</i>																			
standard error (±)																			
<i>Islandiella narcrossi</i>																			
standard error (±)																			
<i>Islandiella teretis</i>	0.15							0.18	0.59	0.54	0.30	0.84	0.21		0.86	0.48		0.40	0.31
standard error (±)	0.21							0.24	0.47	0.43	0.58	0.62	0.29		0.41	0.28		0.35	0.30
<i>Lagena sp.</i>												0.12			0.15	0.18			
standard error (±)												0.23			0.17	0.17			
<i>Miliolids</i>															0.10			0.16	
standard error (±)															0.14			0.22	

Sample	106-0.5	106-2.5	106-4.5	106-6.5	106-8.5	106-10.5	106-12.5	106-14.5	106-16.5	106-18.5	106-20.5	106-22.5	106-24.5	106-26.5	106-28.5	106-30.5	106-32.5	106-34.5	106-36.5
Interval (cm)	0-1	2-3	4-5	6-7	8-9	11	13	15	17	19	21	23	25	27	29	31	33	35	37
Midpoint (cm)	0.50	2.50	4.50	6.50	8.50	10.50	12.50	14.50	16.50	18.50	20.50	22.50	24.50	26.50	28.50	30.50	32.50	34.50	36.50
Species/10cc	30	24	23	20	20	20	22	26	30	27	23	24	25	22	32	29	24	26	26
Specimens/10cc	1334	890	1001	672	614	765	1582	1135	1015	1102	337	838	971	633	1976	2282	933	1243	1291
Tintinnids (counts/10cc)	50	117	58	18	50	30	80	68	58	52	15	36	40	46	66	120	66	76	66
<i>Neogloboquadrina pachyderma</i>									0.10	4.99	0.59	1.55	0.31	1.58	11.18	4.08	0.32	7.64	7.36
standard error (±)									0.19	1.29	0.82	0.84	0.35	0.97	1.39	0.81	0.36	1.48	1.42
<i>Nonion barleeaanum</i>	0.30	0.11													0.10			0.24	
standard error (±)	0.29	0.22													0.14			0.27	
<i>Nonionellina labradorica</i>																			
standard error (±)																			
<i>Ordisalis umbonatus</i>																			
standard error (±)																			
<i>Psammosphaera fusca</i>	0.07			0.15															
standard error (±)	0.15			0.29															
<i>Quinqueloculina agglutinans</i>																			
standard error (±)																			
<i>Quinqueloculina lamarckiana</i>																			
standard error (±)																			
<i>Quinqueloculina seminulum</i>	0.45	0.45													0.05			0.16	
standard error (±)	0.36	0.44													0.10			0.22	
<i>Recurvoides turbinatus</i>	11.02	6.63	3.40	4.91	3.91	4.18	3.60	1.85	1.08	1.63	0.59	0.84	1.85	0.16	1.21	1.31	1.29	0.80	0.77
standard error (±)	1.68	1.63	1.12	1.63	1.53	1.42	0.92	0.78	0.64	0.75	0.82	0.62	0.85	0.31	0.48	0.47	0.72	0.50	0.48
<i>Reophax arctica</i>	0.45	1.35	0.20		0.65		0.13		0.20										
standard error (±)	0.36	0.76	0.28		0.64		0.18		0.27										
<i>Reophax bilocularis</i>	1.42	0.45	0.20	0.60	0.49		0.32	0.79	0.59	0.73	1.78	0.36	0.21	0.16	1.06	0.44	0.75	0.24	0.46
standard error (±)	0.64	0.44	0.28	0.58	0.55		0.28	0.52	0.47	0.50	1.41	0.40	0.29	0.31	0.45	0.27	0.55	0.27	0.37
<i>Reophax dentaliniformis</i>									1.87	1.45									
standard error (±)									0.83	0.71									
<i>Reophax fusiformis</i>																			
standard error (±)																			

Sample	106-0.5	106-2.5	106-4.5	106-6.5	106-8.5	106-10.5	106-12.5	106-14.5	106-16.5	106-18.5	106-20.5	106-22.5	106-24.5	106-26.5	106-28.5	106-30.5	106-32.5	106-34.5	106-36.5
Interval (cm)	0-1	2-3	4-5	6-7	8-9	11	12-13	14-15	16-17	18-19	20-21	22-23	24-25	26-27	28-29	30-31	32-33	34-35	36-37
Midpoint (cm)	0.50	2.50	4.50	6.50	8.50	10.50	12.50	14.50	16.50	18.50	20.50	22.50	24.50	26.50	28.50	30.50	32.50	34.50	36.50
Species/10cc	30	24	23	20	20	20	22	26	30	27	23	24	25	22	32	29	24	26	26
Specimens/10cc	1334	890	1001	672	614	765	1582	1135	1015	1102	337	838	971	633	1976	2282	933	1243	1291
Tintinnids (counts/10cc)	50	117	58	18	50	30	80	68	58	52	15	36	40	46	66	120	66	76	66
<i>Reophax guttifer</i>	1.65	1.01	2.60	1.79	0.81	2.35	0.25	0.62	0.99	1.27	0.89		1.03		0.51	0.26	0.21		0.08
standard error (±)	0.68	0.66	0.99	1.00	0.71	1.07	0.25	0.46	0.61	0.66	1.00		0.64		0.31	0.21	0.30		0.15
<i>Reophax nodulosa</i>	0.67	1.35	0.90	1.34	0.81	1.05	0.32		0.59	0.54	1.19								
standard error (±)	0.44	0.76	0.58	0.87	0.71	0.72	0.28		0.47	0.43	1.16								
<i>Reophax ovicula</i>	0.30	0.22								0.18									
standard error (±)	0.29	0.31								0.25									
<i>Reophax pilulifer</i>	0.15						0.63												
standard error (±)	0.21						0.39												
<i>Reophax scorpiurus</i>	0.60	0.45	0.80		0.49	0.13	0.32	0.79	0.79	0.18	0.89		0.93	0.16	0.46	0.35	0.11		0.08
standard error (±)	0.41	0.44	0.55		0.55	0.26	0.28	0.52	0.54	0.25	1.00		0.60	0.31	0.30	0.24	0.21		0.15
<i>Reophax scottii</i>	0.15					0.26									0.10				
standard error (±)	0.21					0.36									0.14				
<i>Rhizammina algaeformis</i>	6.52	7.53	5.29	9.52	4.40	1.83	3.54	0.79	2.76										
standard error (±)	1.32	1.73	1.39	2.22	1.62	0.95	0.91	0.52	1.01										
<i>Robertinoides charlottensis</i>																			
standard error (±)																			
<i>Saccammina difflugiformis</i>	20.16	15.17	13.79	3.27	12.70	10.72	7.21	9.87	7.39	5.81	10.09	7.64	7.21	5.21	5.87	5.87	4.93	5.15	8.13
standard error (±)	2.15	2.36	2.14	1.35	2.63	2.19	1.27	1.74	1.61	1.38	3.22	1.80	1.63	1.73	1.04	0.96	1.39	1.23	1.49
<i>Saccammina sphaerica</i>			0.40						0.49							0.18	0.21		0.31
standard error (±)			0.39						0.43							0.17	0.30		0.30
<i>Sorosphaera confusa</i>	0.75		0.50	0.15			0.19	0.09											
standard error (±)	0.46		0.44	0.29			0.21	0.17											
<i>Spiroplectammina biformis</i>		0.67	0.60		0.33	0.52		0.44	0.79	0.18				0.95					0.93
standard error (±)		0.54	0.48		0.45	0.51		0.39	0.54	0.25				0.75					0.52
<i>Stetsonia arctica</i>	0.60							0.79	3.15	5.08	0.89	3.70	4.74	2.84	7.69	10.96	2.57	5.95	2.17
standard error (±)	0.41							0.52	1.08	1.30	1.00	1.28	1.34	1.29	1.17	1.28	1.02	1.32	0.79

Sample	106-0.5	106-2.5	106-4.5	106-6.5	106-8.5	106-10.5	106-12.5	106-14.5	106-16.5	106-18.5	106-20.5	106-22.5	106-24.5	106-26.5	106-28.5	106-30.5	106-32.5	106-34.5	106-36.5
Interval (cm)	0-1	2-3	4-5	6-7	8-9	10-11	12-13	14-15	16-17	18-19	20-21	22-23	24-25	26-27	28-29	30-31	32-33	34-35	36-37
Midpoint (cm)	0.50	2.50	4.50	6.50	8.50	10.50	12.50	14.50	16.50	18.50	20.50	22.50	24.50	26.50	28.50	30.50	32.50	34.50	36.50
Species/10cc	30	24	23	20	20	20	22	26	30	27	23	24	25	22	32	29	24	26	26
Specimens/10cc	1334	890	1001	672	614	765	1582	1135	1015	1102	337	838	971	633	1976	2282	933	1243	1291
Tintinnids (counts/10cc)	50	117	58	18	50	30	80	68	58	52	15	36	40	46	66	120	66	76	66
<i>Textularia earlandi</i>	6.00	6.18	4.60	7.44	6.84	9.41	7.33	6.34	9.26	5.99	3.86	7.76	7.21	9.16	8.40	10.25	11.79	5.79	6.04
standard error (±)	1.27	1.58	1.30	1.98	2.00	2.07	1.28	1.42	1.78	1.40	2.06	1.81	1.63	2.25	1.22	1.24	2.07	1.30	1.30
<i>Textularia torquata</i>	0.75	0.90	0.30	0.45	0.33	0.52	0.38	0.44		0.36	1.19	0.24	0.21			0.61		0.16	
standard error (±)	0.46	0.62	0.34	0.50	0.45	0.51	0.30	0.39		0.36	1.16	0.33	0.29			0.32		0.22	
<i>Thurammina papillata</i>																			
standard error (±)																			
<i>Trifarina fluens</i>													0.10						
standard error (±)													0.20						
<i>Triloculina carinata</i>																0.04			
standard error (±)																0.09			
<i>Trochammina globigeriniformis</i>	8.77	19.10	18.78	21.28	11.73	13.59	15.42	17.44	17.54	18.51	6.82	14.32	15.65	14.38	14.47	12.05	18.44	17.30	23.16
standard error (±)	1.52	2.58	2.42	3.09	2.54	2.43	1.78	2.21	2.34	2.29	2.69	2.37	2.29	2.73	1.55	1.34	2.49	2.10	2.30
<i>Trochammina nana</i>	10.12	6.85	8.59	9.08	9.28	11.24	5.75	9.69	7.68	8.44	8.01	8.47	11.23	13.59	8.25	9.33	13.93	7.00	12.16
standard error (±)	1.62	1.66	1.74	2.17	2.30	2.24	1.15	1.72	1.64	1.64	2.90	1.89	1.99	2.67	1.21	1.19	2.22	1.42	1.78
<i>Trochammina nitida</i>	10.49	8.43	7.69	10.71	6.51	13.07	6.70	13.92	7.68	5.72	17.21	6.56	5.36	5.21	3.44	5.17	4.93	4.67	3.25
standard error (±)	1.64	1.83	1.65	2.34	1.95	2.39	1.23	2.01	1.64	1.37	4.03	1.68	1.42	1.73	0.80	0.91	1.39	1.17	0.97
<i>Trochammina pseudoinflata</i>		0.22	1.00	0.89	0.33	0.26		0.18		0.73	1.48	0.48	0.41	0.47	0.10	0.88	1.50	1.77	0.46
standard error (±)		0.31	0.62	0.71	0.45	0.36		0.24		0.50	1.29	0.47	0.40	0.54	0.14	0.38	0.78	0.73	0.37
<i>Uvigerina canariensis</i>															0.05			0.16	
standard error (±)															0.10			0.22	
<i>Valvulinaria artica</i>												0.48			0.20				
standard error (±)												0.47			0.20				

Table B2. Data summary from Amundsen Gulf Core 109. Rows below tintinnid counts are 32 species-specific percentages (\pm SE).

Sample	109-0.5	109-2.5	109-4.5	109-6.5	109-8.5	109-10.5	109-12.5	109-14.5	109-16.5	109-18.5	109-20.5	109-22.5	109-24.5	109-26.5	109-28.5	109-30.5	109-32.5
Interval (cm)	0-1	2-3	4-5	6-7	8-9	10-11	12-13	14-15	16-17	18-19	20-21	22-23	24-25	26-27	28-29	30-31	32-33
Midpoint (cm)	0.50	2.50	4.50	8.50	10.50	12.50	14.50	16.50	18.50	20.50	22.50	24.50	26.50	28.50	30.50	32.50	0.50
Species/10cc	29	29	27	8	24	33	32	31	33	35	32	29	27	31	30	33	33
Specimens/10cc	928	1018	1250	140	1018	1395	1258	1152	1421	1421	687	512	915	672	941	1497	1272
Tintinnids (counts/10cc)	136	174	106	0	113	187	111	142	290	311	126	62	84	84	101	136	102
<i>Adercotryma glomerata</i>		0.39	0.12						0.14		0.15	0.20	0.11				
standard error (\pm)		0.38	0.19						0.19		0.29	0.38	0.21				
<i>Bathysiphon rufus</i>	8.84	35.66	31.04	91.43	33.69	33.69	23.53	20.40	20.55	20.90	24.02	29.30	37.05	22.77	15.52	10.42	16.82
standard error (\pm)	1.83	2.94	2.56	4.64	2.90	2.48	2.34	2.33	2.10	2.11	3.19	3.94	3.13	3.17	2.31	1.55	2.06
<i>Bolivina arctica</i>	7.76	4.13	3.36	0.71	2.75	1.94	3.22	2.60	2.25	2.32	2.77	3.71	3.39	3.13	3.08	2.81	3.30
standard error (\pm)	1.72	1.22	1.00	1.39	1.00	0.72	0.98	0.92	0.77	0.78	1.23	1.64	1.17	1.32	1.10	0.84	0.98
<i>Buccella frigida</i>						0.07	0.44	0.09	0.49	0.14	0.87	0.39	0.33	0.60	0.64	0.73	0.47
standard error (\pm)						0.14	0.36	0.17	0.36	0.19	0.70	0.54	0.37	0.58	0.51	0.43	0.38
<i>Bulinimella hensoni</i>	2.16	2.36	0.80		3.93	7.74	6.44	14.84	13.30	12.24	11.94	12.50	6.56	5.95	19.77	13.49	10.85
standard error (\pm)	0.93	0.93	0.49		1.19	1.40	1.36	2.05	1.77	1.70	2.42	2.86	1.60	1.79	2.54	1.73	1.71
<i>Cassidulina reniforme</i>						0.50	1.15	0.78	1.90	1.83	3.78	1.17	0.22	1.04	2.13	2.00	1.57
standard error (\pm)						0.37	0.59	0.51	0.71	0.70	1.43	0.93	0.30	0.77	0.92	0.71	0.68
<i>Cibicides lobatus</i>																	
standard error (\pm)																	
<i>Cribrostomoides crassimargo</i>	0.54	0.49		0.29		0.32	1.04	0.63	1.13	0.73	0.39	0.98	0.74	2.66	1.80	1.34	
standard error (\pm)	0.47	0.43		0.33		0.31	0.59	0.41	0.55	0.64	0.54	0.64	0.65	1.03	0.67	0.63	
<i>Cribrostomoides jeffreysi</i>		0.10	0.24			0.07			0.07				0.15	0.21	0.40	0.16	
standard error (\pm)		0.19	0.27			0.14			0.14				0.29	0.29	0.32	0.22	
<i>Cribrostomoides subglobosum</i>	0.22				0.07	0.16		0.14	0.07	0.29	0.20		0.45	1.81	0.80	0.16	
standard error (\pm)	0.30				0.14	0.22		0.19	0.14	0.40	0.38		0.50	0.85	0.45	0.22	
<i>Cyclogyra involvens</i>	0.65		0.16	0.20	0.22	0.48	0.78		0.35	0.87	0.39	1.20	1.79	0.64	0.53	0.16	
standard error (\pm)	0.52		0.22	0.27	0.24	0.38	0.51		0.31	0.70	0.54	0.71	1.00	0.51	0.37	0.22	
<i>Dentalina sp.</i>													0.15				
standard error (\pm)													0.29				
<i>Eggerella advena</i>	0.86	0.20	1.12	1.57	0.93		0.26	0.28	1.27	1.16	0.39	0.87	0.60	0.85	1.07	0.94	
standard error (\pm)	0.59	0.27	0.58	0.76	0.50		0.29	0.28	0.58	0.80	0.54	0.60	0.58	0.59	0.52	0.53	

Sample	109- 0.5	109- 2.5	109- 4.5	109- 6.5	109- 8.5	109- 10.5	109- 12.5	109- 14.5	109- 16.5	109- 18.5	109- 20.5	109- 22.5	109- 24.5	109- 26.5	109- 28.5	109- 30.5	109- 32.5
Interval (cm)	0-1	2-3	4-5	6-7	8-9	11	13	15	17	19	21	23	25	27	29	31	33
Midpoint (cm)	0.50	2.50	4.50	8.50	10.50	12.50	14.50	16.50	18.50	20.50	22.50	24.50	26.50	28.50	30.50	32.50	0.50
Species/10cc	29	29	27	8	24	33	32	31	33	35	32	29	27	31	30	33	33
Specimens/10cc	928	1018	1250	140	1018	1395	1258	1152	1421	1421	687	512	915	672	941	1497	1272
Tintinnids (counts/10cc)	136	174	106	0	113	187	111	142	290	311	126	62	84	84	101	136	102
<i>Elphidiella groenlandica</i> standard error (±)																	
<i>Elphidium exc. F. clavata</i> standard error (±)									0.09		0.29						
<i>Elphidium subarcticum</i> standard error (±)									0.17		0.40						
<i>Epistominella takayanagii</i> standard error (±)							0.12			0.07							0.16
<i>Fissurina sp.</i> standard error (±)							0.19			0.14							0.22
<i>Fursenkoina fusiformis</i> standard error (±)					0.79	0.22	0.36	0.17		0.21	0.29			0.30	0.21	0.13	
<i>Glomospira gordialis</i> standard error (±)	0.54	0.98	1.68		0.10	2.08	1.19	0.61	1.34	0.07	1.75	1.37	1.97	0.45	0.21	1.60	1.10
<i>Haynesina orbiculare</i> standard error (±)	0.47	0.61	0.71		0.19	0.75	0.60	0.45	0.60	0.14	0.98	1.01	0.90	0.50	0.29	0.64	0.57
<i>Hemisphaerammina bradyi</i> standard error (±)		0.10												0.30	0.11		
<i>Hyperammina spp.</i> standard error (±)	0.32		0.36											0.41	0.21		
<i>Islandiella narcrossi</i> standard error (±)						0.07	0.08		0.35	0.14	0.87			0.30	0.11	0.40	0.63
<i>Islandiella teretis</i> standard error (±)						0.14	0.16		0.31	0.19	0.70			0.41	0.21	0.32	0.43
<i>Lagena sp.</i> standard error (±)						0.14	0.56	0.35	0.56	0.63	0.44	0.78	0.11	0.15	0.32	0.73	0.24
<i>Miliolids</i> standard error (±)						0.20	0.41	0.34	0.39	0.41	0.49	0.76	0.21	0.29	0.36	0.43	0.27
<i>Miliolids</i> standard error (±)												0.39					
<i>Miliolids</i> standard error (±)												0.54					
<i>Miliolids</i> standard error (±)								0.09		0.07		0.20					
<i>Miliolids</i> standard error (±)								0.17		0.14		0.38					

Sample	109- 0.5	109- 2.5	109- 4.5	109- 6.5	109- 8.5	109- 10.5	109- 12.5	109- 14.5	109- 16.5	109- 18.5	109- 20.5	109- 22.5	109- 24.5	109- 26.5	109- 28.5	109- 30.5	109- 32.5
Interval (cm)	0-1	2-3	4-5	6-7	8-9	10-11	12-13	14-15	16-17	18-19	20-21	22-23	24-25	26-27	28-29	30-31	32-33
Midpoint (cm)	0.50	2.50	4.50	8.50	10.50	12.50	14.50	16.50	18.50	20.50	22.50	24.50	26.50	28.50	30.50	32.50	0.50
Species/10cc	29	29	27	8	24	33	32	31	33	35	32	29	27	31	30	33	33
Specimens/10cc	928	1018	1250	140	1018	1395	1258	1152	1421	1421	687	512	915	672	941	1497	1272
Tintinnids (counts/10cc)	136	174	106	0	113	187	111	142	290	311	126	62	84	84	101	136	102
<i>Neogloboquadrina pachyderma</i>	0.22					0.07	6.08	2.26	5.35	3.38	1.89	3.13	0.98	2.23	1.06	8.08	6.84
standard error (±)	0.30					0.14	1.32	0.86	1.17	0.94	1.02	1.51	0.64	1.12	0.66	1.38	1.39
<i>Nonion barleeaanum</i>	0.86												0.11				
standard error (±)	0.59												0.21				
<i>Nonionellina labradorica</i>							0.12		0.07							0.67	
standard error (±)							0.19		0.14							0.41	
<i>Ordisalis umbonatus</i>																	
standard error (±)																	
<i>Psammosphaera fusca</i>		0.10															0.08
standard error (±)		0.19															0.15
<i>Quinqueloculina agglutinans</i>		0.49	0.24			0.07											
standard error (±)		0.43	0.27			0.14											
<i>Quinqueloculina lamarckiana</i>																	
standard error (±)																	
<i>Quinqueloculina seminulum</i>									0.07			0.20					
standard error (±)									0.14			0.38					
<i>Recurvoides turbinatus</i>	5.60	4.62	4.88	1.43	5.50	3.37	2.62	2.69	2.18	1.48	1.60	1.95	1.31	3.27	1.59	1.74	1.89
standard error (±)	1.48	1.29	1.19	1.97	1.40	0.95	0.88	0.93	0.76	0.63	0.94	1.20	0.74	1.35	0.80	0.66	0.75
<i>Reophax arctica</i>				0.71		0.43			0.21	0.21				0.89			
standard error (±)				1.39		0.34			0.24	0.24				0.71			
<i>Reophax bilocularis</i>	0.97				0.39		0.52	0.61	0.28	0.49	0.44	0.59	0.11	0.15	0.64	0.53	0.24
standard error (±)	0.63				0.38		0.40	0.45	0.28	0.36	0.49	0.66	0.21	0.29	0.51	0.37	0.27
<i>Reophax dentaliniformis</i>	0.32																
standard error (±)	0.37																
<i>Reophax fusiformis</i>	0.75	0.10	0.32		0.10	0.07				0.28							
standard error (±)	0.56	0.19	0.31		0.19	0.14				0.28							

Sample	109-0.5	109-2.5	109-4.5	109-6.5	109-8.5	109-10.5	109-12.5	109-14.5	109-16.5	109-18.5	109-20.5	109-22.5	109-24.5	109-26.5	109-28.5	109-30.5	109-32.5
Interval (cm)	0-1	2-3	4-5	6-7	8-9	10-11	12-13	14-15	16-17	18-19	20-21	22-23	24-25	26-27	28-29	30-31	32-33
Midpoint (cm)	0.50	2.50	4.50	8.50	10.50	12.50	14.50	16.50	18.50	20.50	22.50	24.50	26.50	28.50	30.50	32.50	0.50
Species/10cc	29	29	27	8	24	33	32	31	33	35	32	29	27	31	30	33	33
Specimens/10cc	928	1018	1250	140	1018	1395	1258	1152	1421	1421	687	512	915	672	941	1497	1272
Tintinnids (counts/10cc)	136	174	106	0	113	187	111	142	290	311	126	62	84	84	101	136	102
<i>Reophax guttifer</i>	0.97	0.79	0.76		0.69	0.22	0.76	0.26	0.14	0.21	0.44	0.39		0.15	0.53	0.40	1.34
standard error (±)	0.63	0.54	0.48		0.51	0.24	0.48	0.29	0.19	0.24	0.49	0.54		0.29	0.46	0.32	0.63
<i>Reophax nodulosa</i>	0.11	0.20	0.32		0.69	0.29	0.16	0.26		0.14							
standard error (±)	0.21	0.27	0.31		0.51	0.28	0.22	0.29		0.19							
<i>Reophax ovicula</i>	3.23	3.83	3.28	0.71	2.46	1.94	1.07	1.39	1.76	0.99	0.87	0.39	0.22			0.67	0.31
standard error (±)	1.14	1.18	0.99	1.39	0.95	0.72	0.57	0.68	0.68	0.51	0.70	0.54	0.30			0.41	0.31
<i>Reophax pilulifer</i>		0.29														1.94	0.94
standard error (±)		0.33														0.70	0.53
<i>Reophax scorpiurus</i>	0.22	0.20	0.84			0.65	0.48	0.69	0.28	1.41	0.44		0.11	0.30	0.43		0.16
standard error (±)	0.30	0.27	0.51			0.42	0.38	0.48	0.28	0.61	0.49		0.21	0.41	0.42		0.22
<i>Reophax scottii</i>																	
standard error (±)																	
<i>Rhizamina algaeformis</i>	3.56	3.54	1.40		0.69	0.36	0.48	0.17		0.49							
standard error (±)	1.19	1.13	0.65		0.51	0.31	0.38	0.24		0.36							
<i>Robertinoides charlottensis</i>																	
standard error (±)																	
<i>Saccammina difflugiformis</i>	11.64	4.42	9.92		7.66	6.09	5.09	3.04	3.59	3.52	2.91	3.71	1.53	4.32	3.40	3.54	4.32
standard error (±)	2.06	1.26	1.66		1.63	1.26	1.21	0.99	0.97	0.96	1.26	1.64	0.80	1.54	1.16	0.94	1.12
<i>Saccammina sphaerica</i>	0.43	0.69	0.48		0.20	0.36	0.24	0.52	0.28	0.28	0.15	0.20	0.55		0.43	0.47	0.47
standard error (±)	0.42	0.51	0.38		0.27	0.31	0.27	0.42	0.28	0.28	0.29	0.38	0.48		0.42	0.35	0.38
<i>Sorosphaera confusa</i>	1.51	0.20	0.24					0.17		0.07			0.11				
standard error (±)	0.78	0.27	0.27					0.24		0.14			0.21				
<i>Spiroplectammina biformis</i>	0.22	0.20	0.28		0.59	0.65		0.26		0.21	0.29				0.21	0.13	
standard error (±)	0.30	0.27	0.29		0.47	0.42		0.29		0.24	0.40				0.29	0.19	
<i>Stetsonia arctica</i>					3.23	4.89	5.12	10.27	8.94	1.60	3.32	2.51	3.27	3.72	9.49	3.46	
standard error (±)					0.93	1.19	1.27	1.58	1.48	0.94	1.55	1.01	1.35	1.21	1.48	1.00	

Sample	109-0.5	109-2.5	109-4.5	109-6.5	109-8.5	109-10.5	109-12.5	109-14.5	109-16.5	109-18.5	109-20.5	109-22.5	109-24.5	109-26.5	109-28.5	109-30.5	109-32.5
Interval (cm)	0-1	2-3	4-5	6-7	8-9	10-11	12-13	14-15	16-17	18-19	20-21	22-23	24-25	26-27	28-29	30-31	32-33
Midpoint (cm)	0.50	2.50	4.50	8.50	10.50	12.50	14.50	16.50	18.50	20.50	22.50	24.50	26.50	28.50	30.50	32.50	0.50
Species/10cc	29	29	27	8	24	33	32	31	33	35	32	29	27	31	30	33	33
Specimens/10cc	928	1018	1250	140	1018	1395	1258	1152	1421	1421	687	512	915	672	941	1497	1272
Tintinnids (counts/10cc)	136	174	106	0	113	187	111	142	290	311	126	62	84	84	101	136	102
<i>Textularia earlandi</i>	7.11	6.88	7.48	1.43	5.01	8.39	10.37	5.99	5.77	5.70	4.80	5.86	7.43	4.32	4.14	7.62	10.38
standard error (±)	1.65	1.55	1.46	1.97	1.34	1.45	1.68	1.37	1.21	1.21	1.60	2.03	1.70	1.54	1.27	1.34	1.68
<i>Textularia torquata</i>					0.98	0.14	0.24		0.42	0.42	0.29	0.78	0.11			0.13	0.31
standard error (±)					0.61	0.20	0.27		0.34	0.34	0.40	0.76	0.21			0.19	0.31
<i>Thurammina papillata</i>		0.39	0.12				0.12										
standard error (±)		0.38	0.19				0.19										
<i>Trifarina fluens</i>																	
standard error (±)																	
<i>Triloculina carinata</i>										0.15			0.15				
standard error (±)										0.29			0.29				
<i>Trochammina globigeriniformis</i>	12.61	15.03	17.08	1.43	18.57	11.61	13.71	14.67	9.71	13.37	11.64	9.96	13.11	22.17	20.72	16.10	18.55
standard error (±)	2.14	2.20	2.09	1.97	2.39	1.68	1.90	2.04	1.54	1.77	2.40	2.59	2.19	3.14	2.59	1.86	2.14
<i>Trochammina nana</i>	10.13	7.47	6.80		6.19	6.81	6.68	9.98	8.66	8.16	8.15	7.03	6.67	9.97	5.84	6.21	5.11
standard error (±)	1.94	1.61	1.40		1.48	1.32	1.38	1.73	1.46	1.42	2.05	2.21	1.62	2.27	1.50	1.22	1.21
<i>Trochammina nitida</i>	17.03	5.30	6.44	2.14	6.68	7.46	7.87	9.38	8.30	8.23	11.06	9.57	11.26	9.52	7.97	3.21	7.23
standard error (±)	2.42	1.38	1.36	2.40	1.53	1.38	1.49	1.68	1.43	1.43	2.35	2.55	2.05	2.22	1.73	0.89	1.42
<i>Trochammina pseudoinflata</i>	0.65	0.88	0.24		0.29	0.07	0.12	0.43	0.35	0.49	1.31	1.17	1.09	0.30	0.96	0.94	0.16
standard error (±)	0.52	0.58	0.27		0.33	0.14	0.19	0.38	0.31	0.36	0.85	0.93	0.67	0.41	0.62	0.49	0.22
<i>Uvigerina canariensis</i>																	
standard error (±)																	
<i>Valvulinaria artica</i>																0.80	0.16
standard error (±)																0.45	0.22

Table B3. Data summary from Amundsen Gulf Core 112. Rows below tintinnid counts are 32 species-specific percentages (\pm SE).

Sample	112-0.5	112-2.5	112-4.5	112-6.5	112-8.5	112-10.5	112-12.5	112-14.5	112-16.5	112-18.5	112-20.5	112-22.5	112-24.5	112-26.5	112-28.5	112-30.5	112-32.5	112-34.5
Interval (cm)	0-1	2-3	4-5	6-7	8-9	10-11	12-13	14-15	16-17	18-19	20-21	22-23	24-25	26-27	28-29	30-31	32-33	34-35
Midpoint (cm)	2.50	4.50	6.50	8.50	10.50	12.50	14.50	16.50	18.50	20.50	22.50	24.50	26.50	28.50	30.50	32.50	34.50	0.50
Species/10cc	28	32	28	32	35	38	38	30	40	34	33	33	31	28	41	39	37	37
Specimens/10cc	1899	1918	1126	2523	3090	2535	2879	3387	3390	4019	4072	2527	1811	2818	3677	3680	3228	2331
Tintinnids (counts/10cc)	52	92	25.5	96	114	42	75	126	141	180	240	114	81	120	108	69	54	90
<i>Adercotryma glomerata</i>	0.84	0.31	0.80		0.10	0.24	0.31		0.09	0.15	0.22							0.64
standard error (\pm)	0.41	0.25	0.52		0.11	0.19	0.20		0.10	0.12	0.14							0.32
<i>Bathysiphon rufus</i>	3.16	17.88	15.36	14.19	11.07	5.17	9.27	12.05	6.73	10.03	4.86	7.84	4.75	9.16	3.26	4.48	10.16	5.92
standard error (\pm)	0.79	1.72	2.11	1.36	1.11	0.86	1.06	1.10	0.84	0.93	0.66	1.05	0.98	1.06	0.57	0.67	1.04	0.96
<i>Bolivina arctica</i>	5.27	2.50	3.02	2.62	3.30	3.31	1.04	4.43	2.83	3.88	2.21	4.04	5.14	4.05	4.16	3.34	4.55	3.73
standard error (\pm)	1.00	0.70	1.00	0.62	0.63	0.70	0.37	0.69	0.56	0.60	0.45	0.77	1.02	0.73	0.65	0.58	0.72	0.77
<i>Buccella frigida</i>				0.12	0.10	0.51	0.45	0.47	0.47	0.45	0.79	0.47	1.49	0.60	1.12	0.68	0.74	0.77
standard error (\pm)				0.13	0.11	0.28	0.24	0.23	0.23	0.21	0.27	0.27	0.56	0.29	0.34	0.27	0.30	0.36
<i>Bulinimella hensoni</i>	11.80	5.01	1.95	14.74	22.52	13.49	15.84	19.31	21.95	18.51	24.75	21.61	20.21	23.63	20.89	20.54	17.10	15.70
standard error (\pm)	1.45	0.98	0.81	1.38	1.47	1.33	1.33	1.33	1.39	1.20	1.33	1.60	1.85	1.57	1.31	1.31	1.30	1.48
<i>Cassidulina reniforme</i>					0.78	1.93	5.73	2.92	4.42	3.88	3.36	5.62	3.92	4.05	4.46	6.44	3.75	3.52
standard error (\pm)					0.31	0.54	0.85	0.57	0.69	0.60	0.55	0.90	0.89	0.73	0.67	0.79	0.66	0.75
<i>Cibicides lobatus</i>												0.16	0.06		0.05			
standard error (\pm)												0.16	0.11		0.08			
<i>Cribratomoides crassimargo</i>		0.05	0.09			0.04	0.03		0.12	0.07	0.10	0.75	0.39	0.04	0.46	0.49	0.56	0.90
standard error (\pm)		0.10	0.17			0.08	0.07		0.12	0.08	0.10	0.34	0.29	0.07	0.22	0.23	0.26	0.38
<i>Cribratomoides jeffreysi</i>					0.29										0.33	0.33		
standard error (\pm)					0.19										0.18	0.18		
<i>Cribratomoides subglobosum</i>	0.05	0.10	0.62	0.04			0.03						0.17		0.05			0.09
standard error (\pm)	0.10	0.14	0.46	0.08			0.07						0.19		0.08			0.12
<i>Cyclogyra involvens</i>	0.42	1.20	2.22	0.71	0.19	0.59	0.94	0.71	0.62	1.42	1.03	0.95	0.17	0.43	0.52	0.57	0.65	0.90
standard error (\pm)	0.29	0.49	0.86	0.33	0.16	0.30	0.35	0.28	0.26	0.37	0.31	0.38	0.19	0.24	0.23	0.24	0.28	0.38
<i>Dentalina sp.</i>																		
standard error (\pm)																		
<i>Eggerella advena</i>	0.21	1.36	0.36	0.48		1.30	0.52	0.35	0.21	0.45	0.52	0.24	0.11	0.71	0.33	0.08	0.19	0.26
standard error (\pm)	0.21	0.52	0.35	0.27		0.44	0.26	0.20	0.15	0.21	0.22	0.19	0.15	0.31	0.18	0.09	0.15	0.21

Sample	112- 0.5	112- 2.5	112- 4.5	112- 6.5	112- 8.5	112- 10.5	112- 12.5	112- 14.5	112- 16.5	112- 18.5	112- 20.5	112- 22.5	112- 24.5	112- 26.5	112- 28.5	112- 30.5	112- 32.5	112- 34.5
Interval (cm)	0-1	2-3	4-5	6-7	8-9	10-11	12-13	14-15	16-17	18-19	20-21	22-23	24-25	26-27	28-29	30-31	32-33	34-35
Midpoint (cm)	2.50	4.50	6.50	8.50	10.50	12.50	14.50	16.50	18.50	20.50	22.50	24.50	26.50	28.50	30.50	32.50	34.50	0.50
Species/10cc	28	32	28	32	35	38	38	30	40	34	33	33	31	28	41	39	37	37
Specimens/10cc	1899	1918	1126	2523	3090	2535	2879	3387	3390	4019	4072	2527	1811	2818	3677	3680	3228	2331
Tintinnids (counts/10cc)	52	92	25.5	96	114	42	75	126	141	180	240	114	81	120	108	69	54	90
<i>Elphidiella groenlandica</i> standard error (±)															0.33	0.03		
<i>Elphidium exc. F. clavata</i> standard error (±)						0.12	0.07					0.08		0.11	0.11	0.19	0.09	0.39
<i>Elphidium subarcticum</i> standard error (±)						0.13	0.10								0.11	0.11	0.14	0.25
<i>Epistominella takayanagii</i> standard error (±)									0.18	0.02		0.04						
<i>Fissurina sp.</i> standard error (±)		1.25							0.14	0.05		0.08						
<i>Fursenkoina fusiformis</i> standard error (±)		0.50							0.09	0.47		0.24	0.22	0.07	0.05	0.16	0.19	0.13
<i>Glomospira gordialis</i> standard error (±)				0.12	0.29	0.36	0.31	0.09	0.27	0.07	0.15	0.24	0.22	0.14	0.24	0.16	0.37	0.39
<i>Haynesina orbiculare</i> standard error (±)				0.13	0.19	0.23	0.20	0.10	0.17	0.08	0.12	0.19	0.22	0.14	0.16	0.13	0.21	0.25
<i>Hemisphaerammina bradyi</i> standard error (±)	1.00	0.89	0.62	1.11	0.91	0.83	1.22	0.89	0.80	1.22	0.81	0.95	0.99	0.43	0.49	0.76	0.68	1.93
<i>Hyperammina spp.</i> standard error (±)	0.45	0.42	0.46	0.41	0.33	0.35	0.40	0.32	0.30	0.34	0.28	0.38	0.46	0.24	0.23	0.28	0.28	0.56
<i>Islandiella narcrossi</i> standard error (±)					0.06	1.07	0.56	0.65	1.50	0.45	0.47	0.47	0.66	0.32	0.11	0.73	1.02	0.60
<i>Islandiella teretis</i> standard error (±)				0.09	0.40	0.27	0.27	0.41	0.21	0.21	0.27	0.37	0.21	0.11	0.28	0.35	0.31	
<i>Lagena sp.</i> standard error (±)			0.13	0.12	0.42	1.46	2.64	1.54	2.18	2.14	1.20	1.15	2.54	0.85	2.04	1.14	0.84	0.17
<i>Miliolids</i> standard error (±)			0.21	0.13	0.23	0.47	0.59	0.41	0.49	0.45	0.33	0.42	0.72	0.34	0.46	0.34	0.31	0.17
					0.04	0.10			0.12	0.10					0.16	0.19	0.09	0.17
					0.08	0.12			0.12	0.10					0.13	0.14	0.11	0.17
									0.15	0.05	0.08				0.03	0.03	0.03	0.09
									0.12	0.07	0.11				0.05	0.05	0.06	0.12

Sample	112-0.5	112-2.5	112-4.5	112-6.5	112-8.5	112-10.5	112-12.5	112-14.5	112-16.5	112-18.5	112-20.5	112-22.5	112-24.5	112-26.5	112-28.5	112-30.5	112-32.5	112-34.5
Interval (cm)	0-1	2-3	4-5	6-7	8-9	11	13	15	17	19	21	23	25	27	29	31	33	35
Midpoint (cm)	2.50	4.50	6.50	8.50	10.50	12.50	14.50	16.50	18.50	20.50	22.50	24.50	26.50	28.50	30.50	32.50	34.50	0.50
Species/10cc	28	32	28	32	35	38	38	30	40	34	33	33	31	28	41	39	37	37
Specimens/10cc	1899	1918	1126	2523	3090	2535	2879	3387	3390	4019	4072	2527	1811	2818	3677	3680	3228	2331
Tintinnids (counts/10cc)	52	92	25.5	96	114	42	75	126	141	180	240	114	81	120	108	69	54	90
<i>Neogloboquadrina pachyderma</i>					0.68	3.75	2.43	3.13	5.46	2.71	3.63	7.32	5.02	4.97	8.32	14.81	5.61	2.57
standard error (±)					0.29	0.74	0.56	0.59	0.76	0.50	0.57	1.02	1.01	0.80	0.89	1.15	0.79	0.64
<i>Nonion barleeianum</i>				0.12	0.03	0.04		0.03	0.03	0.02	0.05				0.08	0.03		
standard error (±)				0.13	0.06	0.08		0.06	0.06	0.05	0.07				0.09	0.05		
<i>Nonionellina labradorica</i>									0.09						0.41	0.82		
standard error (±)									0.10						0.21	0.29		
<i>Ordisalis umbonatus</i>																		
standard error (±)																		
<i>Psammosphaera fusca</i>																		
standard error (±)																		
<i>Quinqueloculina agglutinans</i>	0.26	0.36																
standard error (±)	0.23	0.27																
<i>Quinqueloculina lamarckiana</i>									0.09						0.08	0.03		
standard error (±)									0.10						0.09	0.05		
<i>Quinqueloculina seminulum</i>					0.03				0.09	0.02					0.03		0.12	0.04
standard error (±)					0.06				0.10	0.05					0.05		0.12	0.08
<i>Recurvoides turbinatus</i>	5.11	5.11	5.46	4.16	2.23	1.42	2.50	1.42	1.77	1.19	1.40	1.07	1.16	0.64	1.14	0.98	1.21	1.80
standard error (±)	0.99	0.99	1.33	0.78	0.52	0.46	0.57	0.40	0.44	0.34	0.36	0.40	0.49	0.29	0.34	0.32	0.38	0.54
<i>Reophax arctica</i>		0.31		0.24		0.24				0.45						0.08	0.19	
standard error (±)		0.25		0.19		0.19				0.21						0.09	0.15	
<i>Reophax bilocularis</i>	0.32	0.31	0.44	1.19	0.55	0.71	0.10	0.30	0.44		0.22	0.51	0.61		0.46	0.08	0.43	0.47
standard error (±)	0.25	0.25	0.39	0.42	0.26	0.33	0.12	0.18	0.22		0.14	0.28	0.36		0.22	0.09	0.23	0.28
<i>Reophax dentaliniformis</i>		0.10																
standard error (±)		0.14																
<i>Reophax fusiformis</i>	0.11	0.10	0.09	0.20	0.23	0.08	0.07	0.06	0.21		0.02						0.06	
standard error (±)	0.15	0.14	0.17	0.17	0.17	0.11	0.10	0.08	0.15		0.05						0.09	

Sample	112-0.5	112-2.5	112-4.5	112-6.5	112-8.5	112-10.5	112-12.5	112-14.5	112-16.5	112-18.5	112-20.5	112-22.5	112-24.5	112-26.5	112-28.5	112-30.5	112-32.5	112-34.5
Interval (cm)	0-1	2-3	4-5	6-7	8-9	10-11	12-13	14-15	16-17	18-19	20-21	22-23	24-25	26-27	28-29	30-31	32-33	34-35
Midpoint (cm)	2.50	4.50	6.50	8.50	10.50	12.50	14.50	16.50	18.50	20.50	22.50	24.50	26.50	28.50	30.50	32.50	34.50	0.50
Species/10cc	28	32	28	32	35	38	38	30	40	34	33	33	31	28	41	39	37	37
Specimens/10cc	1899	1918	1126	2523	3090	2535	2879	3587	3390	4019	4072	2527	1811	2818	3677	3680	3228	2331
Tintinnids (counts/10cc)	52	92	25.5	96	114	42	75	126	141	180	240	114	81	120	108	69	54	90
<i>Reophax guttifer</i>	5.85	1.72	4.88	2.38	1.72	0.87	0.24	0.18	0.03	0.10	0.29	0.12	0.17	0.07	0.35	1.14	0.25	0.17
standard error (±)	1.06	0.58	1.26	0.59	0.46	0.36	0.18	0.14	0.06	0.10	0.17	0.13	0.19	0.10	0.19	0.34	0.17	0.17
<i>Reophax nodulosa</i>	0.11	0.16	0.58	0.32	0.13	0.08		0.03										
standard error (±)	0.15	0.18	0.44	0.22	0.13	0.11		0.06										
<i>Reophax ovicula</i>	0.53	0.73	0.67	0.36			0.10					0.24					0.19	
standard error (±)	0.33	0.38	0.48	0.23			0.12					0.19					0.15	
<i>Reophax pilulifer</i>											0.15				0.30	0.16		
standard error (±)											0.12				0.18	0.13		
<i>Reophax scorpiurus</i>	0.11	0.21	0.27	0.28	0.36	0.43	0.10		0.03	0.05	0.02	0.08	0.28	0.04	0.27	0.05	0.50	0.21
standard error (±)	0.15	0.20	0.30	0.21	0.21	0.26	0.12		0.06	0.07	0.05	0.11	0.24	0.07	0.17	0.08	0.24	0.19
<i>Reophax scottii</i>		0.16					0.21								0.33	0.08		
standard error (±)		0.18					0.17								0.18	0.09		
<i>Rhizammina algaeformis</i>	17.69	2.61	2.80	0.99	1.26	0.51	0.80											
standard error (±)	1.72	0.71	0.96	0.39	0.39	0.28	0.33											
<i>Robertinoides charlottensis</i>									0.03									
standard error (±)									0.06									
<i>Saccammina difflugiformis</i>	6.42	5.74	7.06	5.43	6.54	4.02	3.92	1.56	3.04	1.62	2.53	1.82	3.15	0.60	1.79	3.70	2.73	4.08
standard error (±)	1.10	1.04	1.50	0.88	0.87	0.76	0.71	0.42	0.58	0.39	0.48	0.52	0.80	0.29	0.43	0.61	0.56	0.80
<i>Saccammina sphaerica</i>	0.53	0.78	0.67	0.36	0.55	0.79	0.21	0.18	0.27		0.22	0.24		0.07	0.03	0.43	0.37	0.39
standard error (±)	0.33	0.39	0.48	0.23	0.26	0.34	0.17	0.14	0.17		0.14	0.19		0.10	0.05	0.21	0.21	0.25
<i>Sorosphaera confusa</i>	0.95	0.05	0.18	0.08	0.16	0.08	0.35											0.04
standard error (±)	0.44	0.10	0.25	0.11	0.14	0.11	0.21											0.08
<i>Spiroplectammina biformis</i>		0.47		0.12	0.29	0.95	0.42	0.62	0.35	0.15	0.15		0.22	0.21			0.37	0.51
standard error (±)		0.31		0.13	0.19	0.38	0.24	0.26	0.20	0.12	0.12		0.22	0.17			0.21	0.29
<i>Stetsonia arctica</i>	0.21		0.18	1.66	5.53	6.39	9.17	12.40	8.50	7.54	8.84	10.68	8.50	11.43	11.91	9.21	7.25	9.40
standard error (±)	0.21		0.25	0.50	0.81	0.95	1.05	1.11	0.94	0.82	0.87	1.20	1.28	1.17	1.05	0.93	0.89	1.18

Sample	112-0.5	112-2.5	112-4.5	112-6.5	112-8.5	112-10.5	112-12.5	112-14.5	112-16.5	112-18.5	112-20.5	112-22.5	112-24.5	112-26.5	112-28.5	112-30.5	112-32.5	112-34.5
Interval (cm)	0-1	2-3	4-5	6-7	8-9	11	13	15	17	19	21	23	25	27	29	31	33	35
Midpoint (cm)	2.50	4.50	6.50	8.50	10.50	12.50	14.50	16.50	18.50	20.50	22.50	24.50	26.50	28.50	30.50	32.50	34.50	0.50
Species/10cc	28	32	28	32	35	38	38	30	40	34	33	33	31	28	41	39	37	37
Specimens/10cc	1899	1918	1126	2523	3090	2535	2879	3387	3390	4019	4072	2527	1811	2818	3677	3680	3228	2331
Tintinnids (counts/10cc)	52	92	25.5	96	114	42	75	126	141	180	240	114	81	120	108	69	54	90
<i>Textularia earlandi</i>	17.38	16.63	11.28	16.41	10.19	8.88	9.48	13.20	11.06	16.12	13.41	9.14	9.61	10.50	7.26	4.48	10.13	15.06
standard error (±)	1.70	1.67	1.85	1.45	1.07	1.11	1.07	1.14	1.06	1.14	1.05	1.12	1.36	1.13	0.84	0.67	1.04	1.45
<i>Textularia torquata</i>	1.16	1.15	1.38	1.07	1.55	1.66	1.67	1.06	1.24	1.34	0.74	1.31	0.61	1.06	1.55	0.57	1.77	1.42
standard error (±)	0.48	0.48	0.68	0.40	0.44	0.50	0.47	0.35	0.37	0.36	0.26	0.44	0.36	0.38	0.40	0.24	0.45	0.48
<i>Thurammina papillata</i>	0.05																	
standard error (±)	0.10																	
<i>Trifarina fluens</i>										0.03								
standard error (±)										0.06								
<i>Triloculina carinata</i>					0.10	0.24	0.10	0.12	0.21						0.22		0.09	
standard error (±)					0.11	0.19	0.12	0.12	0.15						0.15		0.11	
<i>Trochammina globigeriniformis</i>	9.53	17.73	22.07	21.48	15.95	22.45	16.95	11.78	14.87	13.54	15.94	11.00	16.23	13.20	18.68	16.25	18.06	18.32
standard error (±)	1.32	1.71	2.42	1.60	1.29	1.62	1.37	1.09	1.20	1.06	1.12	1.22	1.70	1.25	1.26	1.19	1.33	1.57
<i>Trochammina nana</i>	3.05	4.33	5.77	3.92	5.73	7.93	4.38	4.07	4.45	4.58	3.61	4.08	5.47	5.46	3.75	3.75	5.02	2.83
standard error (±)	0.77	0.91	1.36	0.76	0.82	1.05	0.75	0.67	0.69	0.65	0.57	0.77	1.05	0.84	0.61	0.61	0.75	0.67
<i>Trochammina nitida</i>	7.79	9.65	10.92	4.56	4.85	6.39	5.42	5.85	4.07	5.90	7.81	5.82	6.68	6.32	3.35	2.20	3.62	5.15
standard error (±)	1.21	1.32	1.82	0.81	0.76	0.95	0.83	0.79	0.67	0.73	0.82	0.91	1.15	0.90	0.58	0.47	0.64	0.90
<i>Trochammina pseudoinflata</i>	0.11	1.04	0.13	0.40	0.13	0.95	0.83	0.18	0.56	0.75	0.15	0.83	0.72	0.85	0.49	0.71	0.93	1.07
standard error (±)	0.15	0.45	0.21	0.25	0.13	0.38	0.33	0.14	0.25	0.27	0.12	0.35	0.39	0.34	0.23	0.27	0.33	0.42
<i>Uvigerina canariensis</i>																		
standard error (±)																		
<i>Valvulinaria artica</i>					0.19	0.36	0.42	0.18	0.53	0.22	0.15	0.83	0.44			0.08	0.09	0.13
standard error (±)					0.16	0.23	0.24	0.14	0.24	0.15	0.12	0.35	0.31			0.09	0.11	0.15

Table B4. Data summary from Amundsen Gulf Core 118. Rows below tintinnid counts are 32 species-specific percentages (\pm SE).

Sample	118-0.5	118-2.5	118-4.5	118-6.5	118-8.5	118-10.5	118-12.5	118-14.5	118-16.5	118-18.5	118-20.5	118-22.5	118-24.5	118-26.5	118-28.5
Interval (cm)	0-1	2-3	4-5	6-7	8-9	10-11	12-13	14-15	16-17	18-19	20-21	22-23	24-25	26-27	28-29
Midpoint (cm)	0.50	2.50	4.50	6.50	8.50	10.50	12.50	14.50	16.50	18.50	20.50	22.50	24.50	26.50	28.50
Species/10cc	43	27	26	26	22	27	28	37	37	26	37	25	20	16	25
Specimens/10cc	4700	3324	2676	3091	961	1413	1552	4424	3618	1400	1783	798	824	256	678
Tintinnids (counts/10cc)	120	60	75	84	19.5	39	66	66	21	22	18	10	9	0	0
<i>Adercotryma glomerata</i>			0.22						0.07						
standard error (\pm)			0.18						0.08						
<i>Bathysiphon rufus</i>	6.70	10.59	10.09	10.97	23.58	14.05	5.64	2.12	1.41	3.14	2.02	4.76	1.46	4.69	1.77
standard error (\pm)	0.71	1.05	1.14	1.10	2.68	1.81	1.15	0.42	0.38	0.91	0.65	1.48	0.82	2.59	0.99
<i>Bolivina arctica</i>	2.94	3.97	3.92	6.60	4.37	5.10	2.32	0.81	1.91	2.86	3.42	7.27	4.61	5.08	7.08
standard error (\pm)	0.48	0.66	0.74	0.88	1.29	1.15	0.75	0.26	0.45	0.87	0.84	1.80	1.43	2.69	1.93
<i>Buccella frigida</i>	0.13	0.18				0.32	0.42	1.51	1.24	0.43	1.01	0.50		0.78	1.77
standard error (\pm)	0.10	0.14				0.29	0.32	0.36	0.36	0.34	0.46	0.49		1.08	0.99
<i>Bulinimella hensoni</i>	25.28	2.53		3.11	5.62	6.16	17.98	39.60	28.69	15.00	20.19	28.32	48.06	51.56	42.48
standard error (\pm)	1.24	0.53		0.61	1.46	1.25	1.91	1.44	1.47	1.87	1.86	3.13	3.41	6.12	3.72
<i>Cassidulina reniforme</i>	0.13		0.22		0.31	0.53	1.06	5.92	4.51	2.79	3.48	1.00	0.36		5.75
standard error (\pm)	0.10		0.18		0.35	0.38	0.51	0.70	0.68	0.86	0.85	0.69	0.41		1.75
<i>Cibicides lobatus</i>	0.15								0.03	0.07	0.17				
standard error (\pm)	0.11								0.05	0.14	0.19				
<i>Cribrostomoides crassimargo</i>	0.02	0.24	0.11	0.06	0.62	2.09	3.93	0.97	0.97	1.50	0.90	1.00	2.18	0.78	0.15
standard error (\pm)	0.04	0.17	0.13	0.09	0.50	0.75	0.97	0.29	0.32	0.64	0.44	0.69	1.00	1.08	0.29
<i>Cribrostomoides jeffreysi</i>											1.12				
standard error (\pm)											0.49				
<i>Cribrostomoides subglobosum</i>	0.02	0.27	0.04												
standard error (\pm)	0.04	0.18	0.07												
<i>Cyclogyra involvens</i>	0.64	0.72	0.45	1.07	1.25	1.06	0.58	0.27	0.83	0.14	0.50	0.50	0.36		
standard error (\pm)	0.23	0.29	0.25	0.36	0.70	0.53	0.38	0.15	0.30	0.20	0.33	0.49	0.41		
<i>Dentalina sp.</i>								0.02	0.03						
standard error (\pm)								0.04	0.05						
<i>Eggerella advena</i>	0.89	0.36	0.45	0.39	0.62	0.21		0.27	0.33	0.43	0.22	0.50			
standard error (\pm)	0.27	0.20	0.25	0.22	0.50	0.24		0.15	0.19	0.34	0.22	0.49			

Sample	118-0.5	118-2.5	118-4.5	118-6.5	118-8.5	118-10.5	118-12.5	118-14.5	118-16.5	118-18.5	118-20.5	118-22.5	118-24.5	118-26.5	118-28.5
Interval (cm)	0-1	2-3	4-5	6-7	8-9	10-11	12-13	14-15	16-17	18-19	20-21	22-23	24-25	26-27	28-29
Midpoint (cm)	0.50	2.50	4.50	6.50	8.50	10.50	12.50	14.50	16.50	18.50	20.50	22.50	24.50	26.50	28.50
Species/10cc	43	27	26	26	22	27	28	37	37	26	37	25	20	16	25
Specimens/10cc	4700	3324	2676	3091	961	1413	1552	4424	3618	1400	1783	798	824	256	678
Tintinnids (counts/10cc)	120	60	75	84	19.5	39	66	66	21	22	18	10	9	0	0
<i>Elphidiella groenlandica</i>															
standard error (±)															
<i>Elphidium exc. F. clavata</i>	0.15					0.07	0.10	0.29	0.28	0.21	0.28				0.44
standard error (±)	0.11					0.14	0.15	0.16	0.17	0.24	0.25				0.50
<i>Elphidium subarcticum</i>							0.10	0.18	0.08		0.28	0.25			0.15
standard error (±)							0.15	0.13	0.09		0.25	0.35			0.29
<i>Epistominella takayanagii</i>	0.13							0.02	0.08		0.17		0.36		
standard error (±)	0.10							0.04	0.09		0.19		0.41		
<i>Fissurina sp.</i>									0.08						0.15
standard error (±)									0.09						0.29
<i>Fursenkoina fusiformis</i>	0.13							0.27	0.17		0.39			0.39	0.44
standard error (±)	0.10							0.15	0.13		0.29			0.76	0.50
<i>Glomospira gordialis</i>	1.17	1.44	1.05	0.87	0.78	0.32	0.64	0.54	0.66	0.14					
standard error (±)	0.31	0.41	0.39	0.33	0.56	0.29	0.40	0.22	0.26	0.20					
<i>Haynesina orbiculare</i>												0.22			
standard error (±)												0.22			
<i>Hemisphaerammina bradyi</i>	0.13														
standard error (±)	0.10														
<i>Hyperammina spp.</i>															
standard error (±)															
<i>Islandiella narcrossi</i>	0.85							0.63	0.41	0.21	1.01	0.25			1.33
standard error (±)	0.26							0.23	0.21	0.24	0.46	0.35			0.86
<i>Islandiella teretis</i>	0.68			0.13		0.07	0.26	1.06	2.05	0.79	3.59	0.75		0.39	0.29
standard error (±)	0.24			0.13		0.14	0.25	0.30	0.46	0.46	0.86	0.60		0.76	0.41
<i>Lagena sp.</i>	0.04						0.10	0.09			0.22			0.39	
standard error (±)	0.06						0.15	0.09			0.22			0.76	
<i>Miliolids</i>									0.17						
standard error (±)									0.13						

Sample	118-0.5	118-2.5	118-4.5	118-6.5	118-8.5	118-10.5	118-12.5	118-14.5	118-16.5	118-18.5	118-20.5	118-22.5	118-24.5	118-26.5	118-28.5
Interval (cm)	0-1	2-3	4-5	6-7	8-9	10-11	12-13	14-15	16-17	18-19	20-21	22-23	24-25	26-27	28-29
Midpoint (cm)	0.50	2.50	4.50	6.50	8.50	10.50	12.50	14.50	16.50	18.50	20.50	22.50	24.50	26.50	28.50
Species/10cc	43	27	26	26	22	27	28	37	37	26	37	25	20	16	25
Specimens/10cc	4700	3324	2676	3091	961	1413	1552	4424	3618	1400	1783	798	824	256	678
Tintinnids (counts/10cc)	120	60	75	84	19.5	39	66	66	21	22	18	10	9	0	0
<i>Neogloboquadrina pachyderma</i>	0.02					0.11	0.23	1.31	4.01	1.86	12.28	1.13			14.16
standard error (±)	0.04					0.17	0.24	0.34	0.64	0.71	1.52	0.73			2.62
<i>Nonion barleeianum</i>	0.47							0.02		0.07	0.06	0.13			0.44
standard error (±)	0.20							0.04		0.14	0.11	0.25			0.50
<i>Nonionellina labradorica</i>												0.34			
standard error (±)												0.27			
<i>Ordisalis umbonatus</i>															
standard error (±)															
<i>Psammosphaera fusca</i>	0.02					0.07					0.06				
standard error (±)	0.04					0.14					0.11				
<i>Quinqueloculina agglutinans</i>															
standard error (±)															
<i>Quinqueloculina lamarckiana</i>	0.13														
standard error (±)	0.10														
<i>Quinqueloculina seminulum</i>															
standard error (±)															
<i>Recurvoides turbinatus</i>	4.21	4.33	3.59	2.52	1.25	0.96	1.55	1.02	0.91	1.07	1.07	0.50	0.73		0.15
standard error (±)	0.57	0.69	0.70	0.55	0.70	0.51	0.61	0.30	0.31	0.54	0.48	0.49	0.58		0.29
<i>Reophax arctica</i>	0.13	0.18		0.39		0.53							0.36		
standard error (±)	0.10	0.14		0.22		0.38							0.41		
<i>Reophax bilocularis</i>	0.26					0.39	1.03	0.32	0.36				0.49	0.39	
standard error (±)	0.14					0.32	0.50	0.17	0.19				0.47	0.76	
<i>Reophax dentaliniformis</i>		0.09	0.04												
standard error (±)		0.10	0.07												
<i>Reophax fusiformis</i>	0.94	0.06	0.07	0.19	0.10	0.35	0.52	0.05	0.14						
standard error (±)	0.28	0.08	0.10	0.16	0.20	0.31	0.36	0.06	0.12						

Sample	118- 0.5	118- 2.5	118- 4.5	118- 6.5	118- 8.5	118- 10.5	118- 12.5	118- 14.5	118- 16.5	118- 18.5	118- 20.5	118- 22.5	118- 24.5	118- 26.5	118- 28.5
Interval (cm)	0-1	2-3	4-5	6-7	8-9	10-11	12-13	14-15	16-17	18-19	20-21	22-23	24-25	26-27	28-29
Midpoint (cm)	0.50	2.50	4.50	6.50	8.50	10.50	12.50	14.50	16.50	18.50	20.50	22.50	24.50	26.50	28.50
Species/10cc	43	27	26	26	22	27	28	37	37	26	37	25	20	16	25
Specimens/10cc	4700	3324	2676	3091	961	1413	1552	4424	3618	1400	1783	798	824	256	678
Tintinnids (counts/10cc)	120	60	75	84	19.5	39	66	66	21	22	18	10	9	0	0
<i>Reophax guttifer</i>	4.43	3.19	2.58	0.68	0.16		0.16	0.07	0.08						
standard error (±)	0.59	0.60	0.60	0.29	0.25		0.20	0.08	0.09						
<i>Reophax nodulosa</i>	0.15	0.30	0.34	0.03											
standard error (±)	0.11	0.19	0.22	0.06											
<i>Reophax ovicula</i>	0.38	1.08	0.34	0.10			0.19				0.17				
standard error (±)	0.18	0.35	0.22	0.11			0.22				0.19				
<i>Reophax pilulifer</i>															
standard error (±)															
<i>Reophax scorpiurus</i>	0.15	0.45	0.07	0.06	0.10	0.14	0.58	0.07	0.55	0.29	0.34	0.88	0.24		
standard error (±)	0.11	0.23	0.10	0.09	0.20	0.20	0.38	0.08	0.24	0.28	0.27	0.65	0.34		
<i>Reophax scottii</i>				0.19											
standard error (±)				0.16											
<i>Rhizammina algaeformis</i>	3.38	2.71	1.46	0.13											
standard error (±)	0.52	0.55	0.45	0.13											
<i>Robertinoides charlottensis</i>															
standard error (±)															
<i>Saccammina difflugiformis</i>	5.19	2.98	4.04	1.29	0.94	1.27	3.16	0.86	1.82	2.86	3.93	3.76	1.21	1.95	0.88
standard error (±)	0.63	0.58	0.75	0.40	0.61	0.58	0.87	0.27	0.44	0.87	0.90	1.32	0.75	1.70	0.70
<i>Saccammina sphaerica</i>											0.90	0.25			
standard error (±)											0.44	0.35			
<i>Sorosphaera confusa</i>	0.21	0.21	0.07		0.21				0.03						
standard error (±)	0.13	0.16	0.10		0.29				0.05						
<i>Spiroplectammina biformis</i>	0.13	0.27	0.45	0.58	0.31	0.32	0.39	0.14	0.17	0.64	0.73		0.61		
standard error (±)	0.10	0.18	0.25	0.27	0.35	0.29	0.31	0.11	0.13	0.42	0.39		0.53		
<i>Stetsonia arctica</i>	1.53			0.58	0.62	0.21	1.26	9.97	8.79	3.21	3.48	0.75	2.18	5.08	3.83
standard error (±)	0.35			0.27	0.50	0.24	0.55	0.88	0.92	0.92	0.85	0.60	1.00	2.69	1.45

Sample	118-0.5	118-2.5	118-4.5	118-6.5	118-8.5	118-10.5	118-12.5	118-14.5	118-16.5	118-18.5	118-20.5	118-22.5	118-24.5	118-26.5	118-28.5
Interval (cm)	0-1	2-3	4-5	6-7	8-9	10-11	12-13	14-15	16-17	18-19	20-21	22-23	24-25	26-27	28-29
Midpoint (cm)	0.50	2.50	4.50	6.50	8.50	10.50	12.50	14.50	16.50	18.50	20.50	22.50	24.50	26.50	28.50
Species/10cc	43	27	26	26	22	27	28	37	37	26	37	25	20	16	25
Specimens/10cc	4700	3324	2676	3091	961	1413	1552	4424	3618	1400	1783	798	824	256	678
Tintinnids (counts/10cc)	120	60	75	84	19.5	39	66	66	21	22	18	10	9	0	0
<i>Textularia earlandi</i>	10.21	21.93	22.31	26.30	18.43	23.46	19.81	8.95	9.54	5.07	4.88	9.52	4.73	4.69	1.03
standard error (±)	0.87	1.41	1.58	1.55	2.45	2.21	1.98	0.84	0.96	1.15	1.00	2.04	1.45	2.59	0.76
<i>Textularia torquata</i>	1.66	1.99	2.13	3.01	2.65	2.97	2.22	2.24	2.32	2.07	1.29	1.50	0.73		1.03
standard error (±)	0.37	0.47	0.55	0.60	1.02	0.89	0.73	0.44	0.49	0.75	0.52	0.84	0.58		0.76
<i>Thurammia papillata</i>															
standard error (±)															
<i>Trifarina fluens</i>								0.02				0.25			0.15
standard error (±)								0.04				0.35			0.29
<i>Triloculina carinata</i>	0.13							0.02	0.33		0.28				
standard error (±)	0.10							0.04	0.19		0.25				
<i>Trochammina globigeriniformis</i>	11.30	16.76	23.88	20.38	15.30	14.79	17.94	8.07	8.96	20.57	10.04	9.77	5.95	6.64	4.13
standard error (±)	0.91	1.27	1.62	1.42	2.28	1.85	1.91	0.80	0.93	2.12	1.39	2.06	1.61	3.05	1.50
<i>Trochammina nana</i>	6.77	10.53	10.43	9.32	8.54	13.84	5.67	6.35	10.45	15.00	8.08	7.14	6.67	6.25	2.36
standard error (±)	0.72	1.04	1.16	1.02	1.77	1.80	1.15	0.72	1.00	1.87	1.26	1.79	1.70	2.97	1.14
<i>Trochammina nitida</i>	7.40	11.73	10.99	9.71	12.49	9.45	11.60	5.76	6.97	16.07	10.71	17.04	17.96	8.20	9.14
standard error (±)	0.75	1.09	1.18	1.04	2.09	1.53	1.59	0.69	0.83	1.92	1.44	2.61	2.62	3.36	2.17
<i>Trochammina pseudoinflata</i>	0.26	0.90	0.67	1.33	1.72	1.17	0.58	0.07	0.33	3.50	1.68	2.26	0.73	2.73	0.74
standard error (±)	0.14	0.32	0.31	0.40	0.82	0.56	0.38	0.08	0.19	0.96	0.60	1.03	0.58	2.00	0.64
<i>Uvigerina canariensis</i>															
standard error (±)															
<i>Valvulinaria artica</i>	0.38								0.33		0.50				0.15
standard error (±)	0.18								0.19		0.33				0.29

Table B5. Data summary from Amundsen Gulf Core 124. Rows below tintinnid counts are 32 species-specific percentages (\pm SE).

Sample	124-0.5	124-2.5	124-4.5	124-6.5	124-8.5	124-10.5	124-12.5	124-14.5	124-16.5	124-18.5	124-20.5	124-22.5	124-24.5	124-26.5	124-28.5	124-30.5	124-32.5
Interval (cm)	0-1	2-3	4-5	6-7	8-9	10-11	12-13	14-15	16-17	18-19	20-21	22-23	24-25	26-27	28-29	30-31	32-33
Midpoint (cm)	0.50	2.50	4.50	6.50	8.50	10.50	12.50	14.50	16.50	18.50	20.50	22.50	24.50	26.50	28.50	30.50	32.50
Species/10cc	29	25	25	29	37	34	33	32	32	34	31	32	35	34	32	36	34
Specimens/10cc	2590	2315	3065	3537	5761	4513	4308	2798	2699	2072	2631	2865	3350	3730	3884	4206	3637
Tintinnids (counts/10cc)	60	87	84	102	135	126	48	81	72	36	37	54	51	84	54	102	78
<i>Adercotryma glomerata</i>	3.13	2.51	0.39		0.21	0.27				0.19		0.10	0.09	0.05		0.07	0.16
standard error (\pm)	0.67	0.64	0.22							0.19		0.12	0.10	0.07		0.08	0.13
<i>Bathysiphon rufus</i>	2.86	6.52	18.96	13.18	6.35	6.40	3.34	12.33	11.23	8.20	7.41	13.44	9.22	11.98	3.60	3.85	10.50
standard error (\pm)	0.64	1.01	1.39	1.11	0.63	0.71	0.54	1.22	1.19	1.18	1.00	1.25	0.98	1.04	0.59	0.58	1.00
<i>Bolivina arctica</i>	4.63	3.63	4.11	2.21	2.29	2.13	2.51	2.25	3.33	3.38	2.96	3.35	1.61	4.18	1.54	1.64	1.48
standard error (\pm)	0.81	0.76	0.70	0.48	0.39	0.42	0.47	0.55	0.68	0.78	0.65	0.66	0.43	0.64	0.39	0.38	0.39
<i>Buccella frigida</i>	0.23	0.13		0.17	0.89	0.89	0.77	0.25	0.48	0.72	1.37	0.56	1.07	0.97	1.57	1.47	0.96
standard error (\pm)	0.19	0.15		0.14	0.24	0.27	0.26	0.19	0.26	0.37	0.44	0.27	0.35	0.31	0.39	0.36	0.32
<i>Bulinimella hensoni</i>	5.79	0.91	1.96	5.94	20.10	14.62	22.01	10.29	14.23	16.51	10.49	15.29	14.87	20.59	16.07	22.04	11.71
standard error (\pm)	0.90	0.39	0.49	0.78	1.03	1.03	1.24	1.13	1.32	1.60	1.17	1.32	1.20	1.30	1.15	1.25	1.05
<i>Cassidulina reniforme</i>		0.13		1.02	1.67	5.58	5.50	4.07	2.22	4.44	8.32	4.96	6.72	3.65	6.80	4.23	4.84
standard error (\pm)		0.15		0.33	0.33	0.67	0.68	0.73	0.56	0.89	1.06	0.79	0.85	0.60	0.79	0.61	0.70
<i>Cibicides lobatus</i>					0.12								0.14	0.03	0.03	0.26	0.05
standard error (\pm)					0.09								0.14	0.06	0.05	0.16	0.07
<i>Cribr stomoides crassimargo</i>	0.04		0.03	0.03	0.10				0.07	0.05	0.04	0.03	0.06	0.13	0.21	0.02	0.30
standard error (\pm)	0.08		0.06	0.06	0.08				0.10	0.09	0.07	0.07	0.08	0.12	0.14	0.05	0.18
<i>Cribr stomoides jeffreysi</i>												0.03				0.14	
standard error (\pm)												0.07				0.11	
<i>Cribr stomoides subglobosum</i>	0.69	0.26	0.03		0.10	0.02	0.09		0.22	0.05		0.10	0.06	0.11	0.08	0.07	0.22
standard error (\pm)	0.32	0.21	0.06		0.08	0.04	0.09		0.18	0.09		0.12	0.08	0.11	0.09	0.08	0.15
<i>Cyclogyra involvens</i>	0.46	1.56	1.76	0.85	0.52	0.93	0.56	0.21	0.89	0.48	1.14	0.42	0.45	0.64	0.93	0.64	0.66
standard error (\pm)	0.26	0.50	0.47	0.30	0.19	0.28	0.22	0.17	0.35	0.30	0.41	0.24	0.23	0.26	0.30	0.24	0.26
<i>Dentalina sp.</i>																	
standard error (\pm)																	
<i>Eggerella advena</i>	0.69	1.43	0.78	0.68	1.35	1.60	0.70	0.75	0.44		0.11		0.36	0.80	0.46	0.43	0.41
standard error (\pm)	0.32	0.48	0.31	0.27	0.30	0.37	0.25	0.32	0.25		0.13		0.20	0.29	0.21	0.20	0.21

Sample	124- 0.5	124- 2.5	124- 4.5	124- 6.5	124- 8.5	124- 10.5	124- 12.5	124- 14.5	124- 16.5	124- 18.5	124- 20.5	124- 22.5	124- 24.5	124- 26.5	124- 28.5	124- 30.5	124- 32.5
Interval (cm)	0-1	2-3	4-5	6-7	8-9	10-11	12-13	14-15	16-17	18-19	20-21	22-23	24-25	26-27	28-29	30-31	32-33
Midpoint (cm)	0.50	2.50	4.50	6.50	8.50	10.50	12.50	14.50	16.50	18.50	20.50	22.50	24.50	26.50	28.50	30.50	32.50
Species/10cc	29	25	25	29	37	34	33	32	32	34	31	32	35	34	32	36	34
Specimens/10cc	2590	2315	3065	3537	5761	4513	4308	2798	2699	2072	2631	2865	3350	3730	3884	4206	3637
Tintinnids (counts/10cc)	60	87	84	102	135	126	48	81	72	36	37	54	51	84	54	102	78
<i>Elphidiella groenlandica</i>																	
standard error (±)																	
<i>Elphidium exc. F. clavata</i>					0.02		0.02	0.14	0.15	1.06	0.91	0.98	1.19	0.43	0.49	0.24	0.33
standard error (±)					0.03		0.05	0.14	0.15	0.44	0.36	0.36	0.37	0.21	0.22	0.15	0.19
<i>Elphidium subarcticum</i>					0.02					0.19	0.08				0.08		
standard error (±)					0.03					0.19	0.11				0.09		
<i>Epistominella takayanagii</i>							0.28		0.07	0.10	0.57	0.10	0.27	0.21		0.07	0.44
standard error (±)							0.16		0.10	0.13	0.29	0.12	0.18	0.15		0.08	0.22
<i>Fissurina sp.</i>				0.03	0.14	0.07	0.14	0.11			0.34	0.21		0.27	0.15	0.21	
standard error (±)				0.06	0.10	0.08	0.11	0.12			0.22	0.17		0.17	0.12	0.14	
<i>Fursenkoina fusiformis</i>	0.58	0.13		0.34	0.31	0.13	0.42	0.32	0.15	0.19		0.94	0.18	0.21		1.00	
standard error (±)	0.29	0.15		0.19	0.14	0.11	0.19	0.21	0.15	0.19		0.35	0.14	0.15		0.30	
<i>Glomospira gordialis</i>	0.73	2.38	1.21	1.22	0.82	1.06	1.28	1.97	0.82	1.16	0.34	0.31	0.72	0.91	0.31	0.57	0.66
standard error (±)	0.33	0.62	0.39	0.36	0.23	0.30	0.34	0.51	0.34	0.46	0.22	0.20	0.29	0.30	0.17	0.23	0.26
<i>Haynesina orbiculare</i>						0.04	0.02			0.43	0.30	0.03	0.75		0.18		0.08
standard error (±)						0.06	0.05			0.28	0.21	0.07	0.29		0.13		0.09
<i>Hemisphaerammina bradyi</i>																	
standard error (±)																	
<i>Hyperammina spp.</i>							0.02										
standard error (±)							0.05										
<i>Islandiella narcrossi</i>																	
standard error (±)																	
<i>Islandiella teretis</i>	0.23			0.34	1.15	2.42	1.18	1.50	0.89	0.77	0.27	1.50	1.16	0.64	2.21	2.33	1.59
standard error (±)	0.19			0.19	0.27	0.45	0.32	0.45	0.35	0.38	0.20	0.45	0.36	0.26	0.46	0.46	0.41
<i>Lagena sp.</i>				0.03	0.14			0.14		0.14			0.06	0.13	0.05	0.21	
standard error (±)				0.06	0.10			0.14		0.16			0.08	0.12	0.07	0.14	
<i>Miliolids</i>									0.10	0.04			0.06		0.05	0.07	0.03
standard error (±)									0.13	0.07			0.08		0.07	0.08	0.05

Sample	124- 0.5	124- 2.5	124- 4.5	124- 6.5	124- 8.5	124- 10.5	124- 12.5	124- 14.5	124- 16.5	124- 18.5	124- 20.5	124- 22.5	124- 24.5	124- 26.5	124- 28.5	124- 30.5	124- 32.5
Interval (cm)	0-1	2-3	4-5	6-7	8-9	10-11	12-13	14-15	16-17	18-19	20-21	22-23	24-25	26-27	28-29	30-31	32-33
Midpoint (cm)	0.50	2.50	4.50	6.50	8.50	10.50	12.50	14.50	16.50	18.50	20.50	22.50	24.50	26.50	28.50	30.50	32.50
Species/10cc	29	25	25	29	37	34	33	32	32	34	31	32	35	34	32	36	34
Specimens/10cc	2590	2315	3065	3537	5761	4513	4308	2798	2699	2072	2631	2865	3350	3730	3884	4206	3637
Tintinnids (counts/10cc)	60	87	84	102	135	126	48	81	72	36	37	54	51	84	54	102	78
<i>Neogloboquadrina pachyderma</i>				0.37	2.10	4.19	4.60	3.93	3.15	1.50	7.22	3.18	7.37	3.83	11.74	14.03	8.55
standard error (±)				0.20	0.37	0.58	0.63	0.72	0.66	0.52	0.99	0.64	0.88	0.62	1.01	1.05	0.91
<i>Nonion barleeianum</i>	0.35	0.09				0.07	0.14		0.07	0.10	0.04		0.03				
standard error (±)	0.23	0.12				0.08	0.11		0.10	0.13	0.07		0.06				
<i>Nonionellina labradorica</i>																	
standard error (±)																	
<i>Ordisalis umbonatus</i>																	0.08
standard error (±)																	0.09
<i>Psammosphaera fusca</i>																	
standard error (±)																	
<i>Quinqueloculina agglutinans</i>																	
standard error (±)																	
<i>Quinqueloculina lamarckiana</i>																	
standard error (±)																	
<i>Quinqueloculina seminulum</i>							0.05										
standard error (±)							0.06										
<i>Recurvoides turbinatus</i>	5.44	3.93	1.99	1.53	2.08	1.60	0.70	2.36	1.70	1.16	0.80	0.63	0.63	0.91	0.31	0.64	0.99
standard error (±)	0.87	0.79	0.49	0.40	0.37	0.37	0.25	0.56	0.49	0.46	0.34	0.29	0.27	0.30	0.17	0.24	0.32
<i>Reophax arctica</i>			0.20	0.34					0.22					0.16		0.14	
standard error (±)			0.16	0.19					0.18					0.13		0.11	
<i>Reophax bilocularis</i>	0.23		0.20		0.02			0.11	0.07	0.05			0.12	0.05	0.08	0.02	0.16
standard error (±)	0.19		0.16		0.03			0.12	0.10	0.09			0.12	0.07	0.09	0.05	0.13
<i>Reophax dentaliniformis</i>																	
standard error (±)																	
<i>Reophax fusiformis</i>								0.11		0.05							
standard error (±)								0.12		0.09							

Sample	124- 0.5	124- 2.5	124- 4.5	124- 6.5	124- 8.5	124- 10.5	124- 12.5	124- 14.5	124- 16.5	124- 18.5	124- 20.5	124- 22.5	124- 24.5	124- 26.5	124- 28.5	124- 30.5	124- 32.5
Interval (cm)	0-1	2-3	4-5	6-7	8-9	10-11	12-13	14-15	16-17	18-19	20-21	22-23	24-25	26-27	28-29	30-31	32-33
Midpoint (cm)	0.50	2.50	4.50	6.50	8.50	10.50	12.50	14.50	16.50	18.50	20.50	22.50	24.50	26.50	28.50	30.50	32.50
Species/10cc	29	25	25	29	37	34	33	32	32	34	31	32	35	34	32	36	34
Specimens/10cc	2590	2315	3065	3537	5761	4513	4308	2798	2699	2072	2631	2865	3350	3730	3884	4206	3637
Tintinnids (counts/10cc)	60	87	84	102	135	126	48	81	72	36	37	54	51	84	54	102	78
<i>Reophax guttifer</i>	7.68	6.65	5.09	3.36	1.53	0.58	0.84	0.04	0.22	0.10	0.27		0.09	0.24		0.10	0.08
standard error (±)	1.03	1.02	0.78	0.59	0.32	0.22	0.27	0.07	0.18	0.13	0.20		0.10	0.16		0.09	0.09
<i>Reophax nodulosa</i>	0.04	0.13	0.07	0.08				0.04									
standard error (±)	0.08	0.15	0.09	0.10				0.07									
<i>Reophax ovicula</i>	0.12	0.52				0.13											
standard error (±)	0.13	0.29				0.11											
<i>Reophax pilulifer</i>																	
standard error (±)																	
<i>Reophax scorpiurus</i>	0.85		0.03		0.02	0.02	0.02	0.11	0.07	0.14	0.08	0.10	0.03	0.11	0.05		0.27
standard error (±)	0.35		0.06		0.03	0.04	0.05	0.12	0.10	0.16	0.11	0.12	0.06	0.11	0.07		
<i>Reophax scottii</i>																	
standard error (±)																	
<i>Rhizammina algaeformis</i>	4.63	3.33	2.74	2.29	0.83	0.58	0.56	1.39	0.33	0.05							
standard error (±)	0.81	0.73	0.58	0.49	0.23	0.22	0.22	0.43	0.22	0.09							
<i>Robertinoides charlottensis</i>																	0.10
standard error (±)																	0.09
<i>Saccammina difflugiformis</i>	15.56	7.73	10.90	8.88	5.73	5.07	3.09	6.79	4.26	3.28	1.33	2.41	2.24	2.06	1.03	0.76	1.84
standard error (±)	1.40	1.09	1.10	0.94	0.60	0.64	0.52	0.93	0.76	0.77	0.44	0.56	0.50	0.46	0.32	0.26	0.44
<i>Saccammina sphaerica</i>				0.03	0.10												
standard error (±)				0.06	0.08												
<i>Sorosphaera confusa</i>	0.12		0.03			0.02											
standard error (±)	0.13		0.06			0.04											
<i>Spiroplectammina biformis</i>		0.26	0.39	0.34	0.21	0.40	0.42	0.64	0.07			0.21	0.18	0.16			0.49
standard error (±)		0.21	0.22	0.19	0.12	0.18	0.19	0.30	0.10			0.17	0.14	0.13			0.23
<i>Stetsonia arctica</i>	0.35			1.70	14.89	11.30	16.02	8.79	9.63	12.45	21.21	17.07	13.25	11.42	17.61	11.84	14.60
standard error (±)	0.23			0.43	0.92	0.92	1.10	1.05	1.11	1.42	1.56	1.38	1.15	1.02	1.20	0.98	1.15

Sample	124-0.5	124-2.5	124-4.5	124-6.5	124-8.5	124-10.5	124-12.5	124-14.5	124-16.5	124-18.5	124-20.5	124-22.5	124-24.5	124-26.5	124-28.5	124-30.5	124-32.5
Interval (cm)	0-1	2-3	4-5	6-7	8-9	10-11	12-13	14-15	16-17	18-19	20-21	22-23	24-25	26-27	28-29	30-31	32-33
Midpoint (cm)	0.50	2.50	4.50	6.50	8.50	10.50	12.50	14.50	16.50	18.50	20.50	22.50	24.50	26.50	28.50	30.50	32.50
Species/10cc	29	25	25	29	37	34	33	32	32	34	31	32	35	34	32	36	34
Specimens/10cc	2590	2315	3065	3537	5761	4513	4308	2798	2699	2072	2631	2865	3350	3730	3884	4206	3637
Tintinnids (counts/10cc)	60	87	84	102	135	126	48	81	72	36	37	54	51	84	54	102	78
<i>Textularia earlandi</i>	10.19	17.02	16.05	17.81	12.91	13.56	9.75	11.08	13.26	12.45	7.75	8.27	10.93	11.42	6.95	12.70	7.59
standard error (±)	1.17	1.53	1.30	1.26	0.87	1.00	0.89	1.16	1.28	1.42	1.02	1.01	1.06	1.02	0.80	1.01	0.86
<i>Textularia torquata</i>	0.46	1.04	0.59	1.19	0.94	0.93	1.39	1.39	1.04	2.51	1.25	1.68	0.36	1.29	0.46	0.64	0.58
standard error (±)	0.26	0.41	0.27	0.36	0.25	0.28	0.35	0.43	0.38	0.67	0.43	0.47	0.20	0.36	0.21	0.24	0.25
<i>Thurammina papillata</i>			0.03														
standard error (±)			0.06														
<i>Trifarina fluens</i>					0.02	0.13											
standard error (±)					0.03	0.11											
<i>Triloculina carinata</i>					0.31	0.16		0.18			0.11	0.10			0.05	0.21	0.33
standard error (±)					0.14	0.11		0.16			0.13	0.12			0.07	0.14	0.19
<i>Trochammina globigeriniformis</i>	15.71	23.71	17.88	24.40	12.25	12.50	11.10	14.15	14.97	13.18	11.29	12.08	13.70	10.59	8.86	7.23	13.28
standard error (±)	1.40	1.73	1.36	1.42	0.85	0.96	0.94	1.29	1.35	1.46	1.21	1.19	1.16	0.99	0.89	0.78	1.10
<i>Trochammina nana</i>	6.68	6.44	8.52	7.61	5.05	7.29	7.50	7.22	8.74	8.25	5.06	5.06	4.81	4.16	4.99	5.02	8.22
standard error (±)	0.96	1.00	0.99	0.87	0.57	0.76	0.79	0.96	1.07	1.18	0.84	0.80	0.72	0.64	0.69	0.66	0.89
<i>Trochammina nitida</i>	10.89	8.81	6.07	3.90	3.54	4.65	3.62	6.65	6.52	5.69	7.30	5.86	6.09	7.08	8.50	4.64	6.19
standard error (±)	1.20	1.15	0.85	0.64	0.48	0.61	0.56	0.92	0.93	1.00	0.99	0.86	0.81	0.82	0.88	0.64	0.78
<i>Trochammina pseudoinflata</i>	0.62	0.78		0.17	0.23	0.27	0.28	0.43	0.30	0.87	0.34	0.31	0.90	0.24	2.47	0.86	1.57
standard error (±)	0.30	0.36		0.14	0.12	0.15	0.16	0.24	0.21	0.40	0.22	0.20	0.32	0.16	0.49	0.28	0.40
<i>Uvigerina canariensis</i>																	
standard error (±)																	
<i>Valvulinaria artica</i>					0.62	0.13	0.70	0.21	0.15		1.03	0.52	0.36	0.32	1.85	1.71	0.66
standard error (±)					0.20	0.11	0.25	0.17	0.15		0.39	0.26	0.20	0.18	0.42	0.39	0.26

Appendix C - Abundance Data – Viscount Melville Sound

Depth-specific data summaries from the single Viscount Melville Sound boxcore sample.

The following three pages divide the species list into three parts, each indicating the percentage contribution of $n = 21$ foraminiferal species and their standard errors in the row immediately beneath. Species per 10 cc, specimens per 10 cc and tintinnid counts are presented above the species-specific percentages.

Data summary from Viscount Melville Sound core. Rows below tintinnid counts are 21 species-specific percentages (\pm SE).

Interval (cm)	0-1	2-3	4-5	6-7	8-9	10-11	12-13	14-15	16-17	18-19	20-21
Midpoint (cm)	0.5	2.5	4.5	6.5	8.5	10.5	12.5	14.5	16.5	18.5	20.5
Species/10cc	30	36	33	32	32	29	30	30	27	25	16
Specimens/10cc	2930	3689	3697	2993	3959	5187	4106	4324	2013	778	239
Tintinnids (counts/10cc)	270	252	264	252	192	246	84	78	30	6	0
<i>Adercotryma glomerata</i>	6.18	11.85	10.39	9.59	13.44	13.92	14.27	8.44	9.74	7.46	5.44
standard error (\pm)	0.87	1.04	0.98	1.05	1.06	0.94	1.07	0.83	1.30	1.85	2.88
<i>Bathysiphon rufus</i>	0.58	0.22	0.22	0.10	0.30	0.12					
standard error (\pm)	0.28	0.15	0.15	0.11	0.17	0.09					
<i>Bolivina arctica</i>	2.66	4.72	2.76	3.01	4.09	5.44	4.68	5.41	4.17	12.60	13.39
standard error (\pm)	0.58	0.68	0.53	0.61	0.62	0.62	0.65	0.67	0.87	2.33	4.32
<i>Buccella frigida</i>	0.20	0.65	0.16		0.30	0.69	0.58	0.56	0.45	0.26	
standard error (\pm)	0.16	0.26	0.13		0.17	0.23	0.23	0.22	0.29	0.36	
<i>Bulinimella hensoni</i>	9.62	12.69	10.22	9.42	4.85	8.21	8.62	4.58	15.50	8.48	25.10
standard error (\pm)	1.07	1.07	0.98	1.05	0.67	0.75	0.86	0.62	1.58	1.96	5.50
<i>Cassidulina reniforme</i>		0.16		0.20		0.12	0.15			0.26	
standard error (\pm)		0.13		0.16		0.09	0.12			0.36	
<i>Cribr stomoides crassimargo</i>		0.03	0.05	0.13	0.10	0.04	0.07	0.05	0.35	0.64	1.67
standard error (\pm)		0.05	0.07	0.13	0.10	0.05	0.08	0.06	0.26	0.56	1.63
<i>Cribr stomoides jeffreysi</i>	0.07	0.35	0.16	0.27	0.68	0.83	1.22	1.39	1.99	2.06	1.26
standard error (\pm)	0.09	0.19	0.13	0.18	0.26	0.25	0.34	0.35	0.61	1.00	1.41
<i>Cyclogyra involvens</i>	1.84	0.65	0.32	0.60	0.45	0.58	0.15	0.14	1.19		
standard error (\pm)	0.49	0.26	0.18	0.28	0.21	0.21	0.12	0.11	0.47		
<i>Eggerella advena</i>	0.41	0.65	0.32	0.40	0.45	0.93	0.73	0.69	1.04	3.08	2.51
standard error (\pm)	0.23	0.26	0.18	0.23	0.21	0.26	0.26	0.25	0.44	1.22	1.98
<i>Elphidium exc. F. clavata</i>		0.16									
standard error (\pm)		0.13									
<i>Eoeponides pulchella</i>				0.20	0.45	0.46	0.29	0.42	0.60		
standard error (\pm)				0.16	0.21	0.18	0.17	0.19	0.34		
<i>Fursenkoina fusiformis</i>	0.82	0.98	0.65	0.20	0.15	0.58	0.58	0.28			0.84
standard error (\pm)	0.33	0.32	0.26	0.16	0.12	0.21	0.23	0.16			1.15
<i>Glomospira gordialis</i>	1.13	1.55	0.97	1.04	1.24	0.12	0.29	0.58	1.19	0.26	
standard error (\pm)	0.38	0.40	0.32	0.36	0.34	0.09	0.17	0.23	0.47	0.36	

Interval (cm)	0-1	2-3	4-5	6-7	8-9	10-11	12-13	14-15	16-17	18-19	20-21
Midpoint (cm)	0.5	2.5	4.5	6.5	8.5	10.5	12.5	14.5	16.5	18.5	20.5
Species/10cc	30	36	33	32	32	29	30	30	27	25	16
Specimens/10cc	2930	3689	3697	2993	3959	5187	4106	4324	2013	778	239
Tintinnids (counts/10cc)	270	252	264	252	192	246	84	78	30	6	0
<i>Hemisphaerammina bradyi</i>		0.65	0.19	0.60	0.61	0.37	0.58	0.76	1.04	1.03	
standard error (±)		0.26	0.14	0.28	0.24	0.16	0.23	0.26	0.44	0.71	
<i>Hyperammina spp.</i>		0.03	0.22								
standard error (±)		0.05	0.15								
<i>Islandiella teretis</i>			0.16	0.23	0.18				0.20		0.42
standard error (±)			0.13	0.17	0.13				0.19		0.82
<i>Neogloboquadrina pachyderma</i>							0.29				
standard error (±)							0.17				
<i>Nonion barleeianum</i>	0.07	0.03	0.11	0.17	0.05				0.05	0.13	
standard error (±)	0.09	0.05	0.11	0.15	0.07				0.10	0.25	
<i>Psammospaera fusca</i>	1.06	1.14	0.62	0.37	0.18	0.08	0.15	0.14	0.15		2.09
standard error (±)	0.37	0.34	0.25	0.22	0.13	0.08	0.12	0.11	0.17		1.81
<i>Quinqueloculina agglutinans</i>	0.07	0.08	0.19	0.03	0.15						
standard error (±)	0.09	0.09	0.14	0.07	0.12						
<i>Recurvoides turbinatus</i>	0.20	1.00	0.97	0.20	0.05	1.39	0.15	0.42	0.15	0.51	0.84
standard error (±)	0.16	0.32	0.32	0.16	0.07	0.32	0.12	0.19	0.17	0.50	1.15
<i>Reophax arctica</i>	3.89	3.74	2.95	4.81	3.81	4.76	3.95	2.08	2.09	0.77	
standard error (±)	0.70	0.61	0.55	0.77	0.60	0.58	0.60	0.43	0.62	0.61	
<i>Reophax bilocularis</i>	0.17			0.07							
standard error (±)	0.15			0.09							
<i>Reophax dentaliniformis</i>	0.20										
standard error (±)	0.16										
<i>Reophax fusiformis</i>			0.35								
standard error (±)			0.19								
<i>Reophax ovicula</i>		0.16									
standard error (±)		0.13									
<i>Reophax scoriurus</i>	0.78	1.11	0.51	0.50	0.56	0.10	0.05	0.05	0.15	0.64	
standard error (±)	0.32	0.34	0.23	0.25	0.23	0.08	0.07	0.06	0.17	0.56	

Interval (cm)	0-1	2-3	4-5	6-7	8-9	10-11	12-13	14-15	16-17	18-19	20-21
Midpoint (cm)	0.5	2.5	4.5	6.5	8.5	10.5	12.5	14.5	16.5	18.5	20.5
Species/10cc	30	36	33	32	32	29	30	30	27	25	16
Specimens/10cc	2930	3689	3697	2993	3959	5187	4106	4324	2013	778	239
Tintinnids (counts/10cc)	270	252	264	252	192	246	84	78	30	6	0
<i>Reophax scottii</i>	1.23	0.81	0.81	1.00	2.27	2.31	0.73	0.69	0.30	2.31	
standard error (±)	0.40	0.29	0.29	0.36	0.46	0.41	0.26	0.25	0.24	1.06	
<i>Rhizammina algaeformis</i>	0.61	0.57	0.03		0.03						
standard error (±)	0.28	0.24	0.05		0.05						
<i>Saccamina difflugiformis</i>	6.59	1.27	3.84	6.41	4.93	3.03	2.14	2.20	2.24	4.37	8.37
standard error (±)	0.90	0.36	0.62	0.88	0.67	0.47	0.44	0.44	0.65	1.44	3.51
<i>Saccamina sphaerica</i>	1.88	1.79	1.68	0.63	0.35	0.87	0.88	0.30			
standard error (±)	0.49	0.43	0.41	0.28	0.18	0.25	0.29	0.16			
<i>Spiroplectammina biformis</i>	2.25	1.30	3.60	2.21	1.97	3.93	1.61	1.94	1.94	1.03	
standard error (±)	0.54	0.37	0.60	0.53	0.43	0.53	0.38	0.41	0.60	0.71	
<i>Stetsonia arctica</i>		0.33	0.32	0.20	0.30	0.81	0.29	0.28	0.30	0.77	
standard error (±)		0.18	0.18	0.16	0.17	0.24	0.17	0.16	0.24	0.61	
<i>Textularia earlandi</i>	1.02	1.30	0.65	1.00	1.36	1.16	0.73	0.56	0.45	0.77	
standard error (±)	0.36	0.37	0.26	0.36	0.36	0.29	0.26	0.22	0.29	0.61	
<i>Textularia torquata</i>	35.63	33.04	35.87	35.08	35.46	35.40	39.45	33.88	30.25	28.28	19.25
standard error (±)	1.73	1.52	1.55	1.71	1.49	1.30	1.49	1.41	2.01	3.16	5.00
<i>Thurammina papillata</i>	1.47										
standard error (±)	0.44										
<i>Trifarina fluens</i>								0.14			0.42
standard error (±)								0.11			0.82
<i>Trochammina globigeriniformis</i>	2.49	2.01	2.62	1.84	2.48	1.58	2.95	6.17	4.97	5.14	5.86
standard error (±)	0.56	0.45	0.52	0.48	0.48	0.34	0.52	0.72	0.95	1.55	2.98
<i>Trochammina nana</i>	8.63	7.26	5.87	8.85	5.81	6.30	5.48	12.00	9.84	10.67	6.69
standard error (±)	1.02	0.84	0.76	1.02	0.73	0.66	0.70	0.97	1.30	2.17	3.17
<i>Trochammina nitida</i>	7.58	6.99	12.01	9.82	12.28	5.78	8.48	14.99	8.49	6.17	5.02
standard error (±)	0.96	0.82	1.05	1.07	1.02	0.64	0.85	1.06	1.22	1.69	2.77
<i>Trochammina pseudoinflata</i>	0.44	0.68		0.80	0.66	0.12	0.44	0.83	1.19	2.06	
standard error (±)	0.24	0.26		0.32	0.25	0.09	0.20	0.27	0.47	1.00	

Cribrostomoides crassimargo (Norman)*Haplophragmium crassimargo* Norman, 1892, p. 17;*Cribrostomoides crassimargo* (Norman). Schafer and Cole, 1978, p. 27, pl. 4, figs. 20a-b.*Cribrostomoides jeffreysi* (Williamson)*Nonionina jeffreysi* Williamson, 1858, p. 34, figs. 72-73;*Cribrostomoides jeffreysi* (Williamson) Vilks, 1969, p. 45, pl. 1, figs. 17a-b.*Cribrostomoides subglobosum* (Sars)*Lituola subglobosus* Sars, 1872, p. 252;*Cribrostomoides subglobosum* (Sars) Herb, 1971, pl. 11, figs. 2a-c, 3a-c.*Cyclogyra involvens* (Reuss)*Operculina involvens* Reuss, 1850, p. 370, pl. 46, fig. 20;*Cornuspira involvens* (Reuss) Loeblich and Tappan, 1953, p. 49, pl. 7, figs. 4-5;*Cyclogyra involvens* (Reuss) Scott, 1987, p. 327.*Dentalina* sp. D'Orbigny, 1826.*Eggerella advena* (Cushman)*Verneuilina advena* Cushman, 1922, p. 141;*Eggerella advena* (Cushman), 1937, p. 51, pl. 5, figs. 12-15.*Elphidiella groenlandica* (Cushman)*Elphidium groenlandica* Cushman, 1933;*Elphidiella groenlandica* (Cushman) Loeblich and Tappan, 1953, p. 106, pl. 19, figs. 13-14.*Elphidium excavatum* (Terquem) forma *clavatum**Polystomella excavata* Terquem, 1876, p. 429, pl. 2, fig. 2;*Elphidium excavatum* (Terquem) forma *clavata* Miller et al., 1982, p. 124, pl. 1, figs. 9-12; pl. 2, figs., 3-8; pl. 4, figs. 1-7.*Elphidium subarcticum* Cushman, 1944, p. 27, pl. 3, figs. 34-35.*Eoeponides pulchella* (Parker)*Pninaella pulchella* Parker, 1952, p. 420, pl. 6, figs. 18-20;*Asterellina pulchella* (Parker) Anderson, 1963, p. 314, pl. 1, figs. 5-7;*Eoeponides pulchella* (Parker) Scott, 1987, p. 327.*Epistominella takayanagii* Iwasa, 1955, p. 16-17, text figs. 4a-c.*Fissurina* sp. Reuss, 1850.

Fursenkoina fusiformis (Williamson)

Bulimina pupoides d'Orbigny var. *fusiformis* Williamson, 1858, p. 64, pl. 5, figs. 129-130;

Fursenkoina fusiformis (Williamson). Gregory, 1970, p. 232

Glomospira gordialis (Parker and Jones)

Trochammina squamata var. *gordialis* Parker and Jones, 1860, p. 304;

Glomospira gordialis (Parker and Jones) Barker, 1960, pl. 38, figs. 10-16.

Haynesina orbiculare (Brady)

Nonionina orbiculare Brady, 1881a, p. 415, pl. 21, fig. 5;

Elphidium orbiculare (Brady). Hessland, 1943, p. 262;

Protelphidium orbiculare (Brady). Todd and Low, 1961, p. 20, pl. 2, fig. 11;

Haynesina orbiculare (Brady). Scott et al., 1980, p. 226.

Hemisphaerammina bradyi Loeblich et al., 1957, p. 224, pl. 72, fig. 2.

Hyperammina sp. Brady, 1878, p. 433, pl. 20, fig. 2a-b.

Islandiella teretis (Tappan)

Cassidulina teretis Tappan, 1951, p. 7, pl. 1, figs. 30a-c;

Islandiella teretis (Tappan) Scott, 1987, p. 328, pl. 2, fig. 13;

Islandiella helenae Feyling-Hanssen and Buzas, 1976, p. 155-157, text figures 1;

Islandiella teretis (Tappan) Scott, 2008, p. 248, pl. 4, fig. 9; pl. 6, figs. 1-14.

Islandiella narcrossi (Cushman)

Cassidulina narcrossi Cushman, 1933, p. 7, pl. 2, fig. 7;

Islandiella narcrossi (Cushman) Vilks, 1969, p. 49, pl. 3, figs. 4a-b.

Lagena sp. Walker and Boys, 1784.

Miliolina sp. Delage and Hérouard, 1896.

Neogloboquadrina pachyderma (Ehrenberg)

Aristospira pachyderma Ehrenberg, 1861, p. 276-277, 303;

Globerigerina pachyderma (Ehrenberg) Bé, 1960, p. 66, text fig. 1;

Globorotalia pachyderma (Ehrenberg) Vilks, 1973, pl. 1-4;

Neogloboquadrina pachyderma (Ehrenberg) Rogl and Bolli, 1973, p. 571, pl. 11, figs. 2-6, pl. 16, fig. 12.

Nonion barleeanaum (Williamson)

Nonionina barleeanaum Williamson, 1858, p. 32, pl. 4, figs. 68-69;

Nonion barleeanaum (Williamson) Scott, 1987, p. 328.

Nonionellina labradorica (Dawson)*Nonionina labradorica* Dawson, 1860, p. 191, fig. 4;*Nonionellina labradorica* (Dawson). Williamson et al., 1984, p. 224, pl. 1, fig. 11.*Oridorsalis umbonatus* (Reuss)*Rotalina umbonata* Reuss, 1851, p. 75, pl. 5, figs. 35a-c;*Oridorsalis umbonatus* (Reuss). Todd, 1965, p. 23, pl. 6, fig. 2.*Psammosphaera fusca* Schulze, 1875, p. 113, pl. 2, figs. 8a-f.*Quinqueloculina agglutinata* Cushman, 1917, p. 43, pl. 9, fig. 2,a-c; p. 168, pl. 12, figs. 11-13.*Quinqueloculina lamarckiana* d'Orbigny, 1839a, p. 189, pl. 11, figs. 14-15.*Quinqueloculina seminulum* (Linné)*Serpula seminulum* Linné, 1758, p. 786;*Quinqueloculina seminulum* (Linné), d'Orbigny, 1826, p. 301.*Recurvoides turbinatus* (Brady)*Haplophragmium turbinatum* Brady, 1881b, p. 50;*Recurvoides turbinatus* (Brady) Parker, 1952, p. 402, pl. 2, figs. 23-24.*Reophax arctica* Brady, 1881a, p. 405, pl. 21, fig. 2.*Reophax bilocularis* Flint, 1899, p. 273, pl. 17, fig. 2.*Reophax dentaliniformis* Brady, 1881b, p. 49, pl. 30, figs. 21,22.*Reophax fusiformis* (Williamson)*Proteonina fusiformis* Williamson, 1858, p. 1, pl. 1, fig. 1;*Reophax curtus* Cushman, 1920, p. 8, pl. 2, figs. 2-3;*Reophax fusiformis* (Williamson) Vilks, 1969, p. 44, pl. 1, fig. 8a-b.*Reophax guttifer* Brady, 1881b, p. 49; Barker, 1960, pl. 31, figs. 10-15.*Reophax nana* Rhumbler, 1911, p. 182, pl. 8, figs. 6-12.*Reophax nodulosa* Brady, 1879, p. 52, pl. 4, figs. 7-8.*Reophax ovicula* (Brady)*Hormosina ovicula* Brady, 1879, p. 61, pl. 4, figs. 3-4;*Reophax ovicula* (Brady) Milam and Anderson, 1981, pl. 1, fig. 8.*Reophax pilulifer* Brady, 1884, p. 292, pl. 30, figs. 18-20.

Reophax scorpiurus de Montfort, 1808, p. 331, text fig.

Reophax scottii Chaster, 1892, p. 57, pl. 1, fig. 1.

Rhizammina algaeformis Brady, 1879, p. 39, pl. 4, fig. 16-17.

Robertinoides charlottensis (Cushman)

Cassidulina charlottensis Cushman, 1925, p. 41, pl. 6, figs. 6-7;

Robertinoides charlottensis (Cushman) Loeblich and Tappan, 1953, p. 108, pl. 20, figs. 6-7.

Saccammina difflugiformis (Brady)

Reophax difflugiformis Brady, 1879, p. 51, pl. 4, fig. 3a-b;

Proteonina atlantica Cushman, 1944, p. 5, pl. 1, fig. 4;

Saccammina atlantica Vilks, 1969, p. 43, pl. 1, fig. 13;

Saccammina difflugiformis (Brady) Thomas et al., 1990, p. 234, pl. 2, figs. 10-12.

Saccammina sphaerica Brady, 1871, p. 183.

Sorosphaera confusa Brady, 1879

Sorosphaera confusa Brady, 1879, pl. 18, figs. 9, 10.

Spiroplectammina biformis (Parker and Jones)

Textularia agglutinans d'Orbigny var. *biformis* Parker and Jones, 1865, p. 370, pl. 15, figs. 23-24;

Spiroplectammina biformis (Parker and Jones) Cushman, 1927b, p. 23, pl. 5.

Stetsonia arctica (Green)

Epistominella arctica Green, 1960, p. 71, pl. 1, figs. 4a-b;

Stetsonia horvathi Green, 1960, p. 72, pl. 1, figs. 6a-b;

Epistominella sp. Lagoe, 1977, p. 126, pl. 4, figs. 19-21;

Stetsonia arctica (Green). Scott and Vilks, 1991, p. 35, pl. 3, figs. 5-15, pl. 4, figs. 19-21.

Textularia earlandi Parker, 1952, p. 458, pl. 2, fig. 4.

Textularia torquata Parker, 1952, p. 403, pl. 3, figs. 9-11.

Thurammina papillata Brady, 1879, p. 45, pl. 5, figs. 4-8.

Trifarina fluens (Todd)

Anglogerina fluens Todd, In Cushman and Todd, 1947, p. 67, pl. 16, figs. 6-7.

Trifarina fluens (Todd) Scott et al., 1980, p. 231, pl. 4, figs. 12-13

Triloculina tricarinata d'Orbigny, 1826, p. 299, no. 7, mod. no. 94.

Trochammina globigeriniformis (Parker and Jones)

Lituloa nautiloidea Lamarck var. *globigeriniformis* Parker and Jones, 1865, p. 407, pl. 17, fig. 96;

Trochammina globigeriniformis (Parker and Jones) Cushman, 1910, p. 124, text figs. 193-195.

Trochammina nana (Brady)

Haplophragmium nana Brady, 1881b, p. 50;

Trochammina nana (Brady). Loeblich and Tappan, 1953, p. 50, pl. 8, fig. 5a-c.

Trochammina nitida Brady, 1879, pl. 41, figs. 5-6.*Trochammina pseudoinflata* Scott and Vilks, 1991

Trochammina inflata Brady. Schröder et al., 1990, p. 36, pl. 3, figs. 9-10 pl. 9, figs. 24-26;

Trochammina pseudoinflata Scott and Vilks, 1991, p. 35, pl. 2, figs. 3-6.

Uvigerina canariensis d'Orbigny 1839a

Uvigerina canariensis d'Orbigny. Barker 1960, p. 154, pl. 74, fig. 3.

Valvulinaria arctica Green, 1960, p. 71, pl. 1, figs. 3a-c.Tintinnids*Tintinnopsis rioplatensis* Souto

Tintinnopsis rioplatensis Souto, 1973, p. 251, figs. 5-8.

Diffugia elegans Pénard, 1890. Scott and Martini, 1982, listed in tables 1 and 2;

Diffugia bacillariarum Perty, 1849. Medioli and Scott, 1983, p. 20, pl. 5, figs. 16-19, pl. 6, figs. 1-4.